DETERMINATION OF THE INCIDENCE OF FUNGAL SPORES FOR IMPORTANT WHEAT PATHOGENS IN WESTERN CANADA

GABRIELA TOSCANO DE ARAUJO
Bachelor of Science, Universidade Estácio de Sá, 2011

A Thesis
Submitted to the School of Graduate Studies
of the University of Lethbridge
in Partial Fulfilment of the
Requirements for the Degree

MASTER OF SCIENCE

Biological Sciences
University of Lethbridge
LETHBRIDGE, ALBERTA – CANADA

DETERMINATION OF THE INCIDENCE OF FUNGAL SPORES FOR IMPORTANT WHEAT PATHOGENS IN WESTERN CANADA

GABRIELA TOSCANO DE ARAUJO

Date of Defence: August 7th, 2018

Dr. André Laroche Co-Supervisor	Research Scientist	Ph.D.
Dr. Brent Selinger Co-Supervisor	Professor	Ph.D.
Dr. Denis Gaudet Thesis Examination Committee Member	Research Scientist	Ph.D.
Dr. James Thomas Thesis Examination Committee Member	Professor	Ph.D.
Dr. Syama Chatterton External Examiner Lethbridge Research and Development Centre Lethbridge, AB	Research Scientist	Ph.D.
Dr. Igor Kovalchuk Chair, Thesis Examination Committee	Professor	Ph.D.

Dedication

To my mother and my stepdad, Denise and Natan, thank you for your extraordinary support, encouragement, and unconditional love during every step of my life. Leaving home and my family back in Brazil to search for higher education was emotionally and financially challenging.

To my husband Antonio Keller, thank you for being this amazing partner and friend, and for being supportive in this whole new adventure and challenge of living abroad.

To my sisters, Daniella and Jade, thank you for all the emotional support, all the long talks about life challenges, and all the love.

To my nephew and niece, João Vitor and Ana Clara, who I miss so much. Thank you for the love.

Abstract

Wheat (*Triticum aestivum* L.) is affected by widespread fungal diseases that can severely decrease yield and grain quality. Threshold concentrations of stripe rust and powdery mildew spores required for disease development in both controlled growth chamber and field conditions were established. Air samples were collected in eight areas of Southern Alberta to investigate the presence of airborne spores of six important fungal wheat pathogens. Identification and quantification of the collected spores were conducted using qPCR assays and light microscopy. Results showed that the threshold concentrations of spores necessary to cause significant disease development under controlled conditions for *Pst* and *Bgt* were 10^6 spores/ml. Threshold values for *Pst* under field conditions were different in 2016 and 2017. Analyses of air samples showed that all six wheat pathogens are present in Southern Alberta, *Fg* being the most predominant among them while *Pst* was the most predominant species among the three rusts.

Acknowledgements

I would like to express my deepest appreciation to my supervisors Dr. André Laroche and Dr. Brent Selinger for their extraordinary support and guidance during this whole new journey. Their impressive patience and understanding of the challenges of this new journey, and most important, the challenges of the tongue for an international student were extremely important for my success.

I would like to thank my supervisory committee members, Dr. Denis Gaudet and Dr. James Thomas; their suggestions and arguments in our meetings were of extreme relevance. I also would like to thank Eric Amundsen and Michele Frick for the daily support with the experiments, all the talking about science and sharing knowledge, and, also, for all the funny moments of Christmas door decorations and Halloween costumes creations. To Dr. Nora Foroud, Dr. Reem Aboukhaddour, Dr. Syama Chatterton and Dr. Harpinder Randhawa, I would like to thank for the knowledge shared and samples provided. Thank you to Dr. Gaganpeet Dhariwal and Dr. Raman Dhariwal for sharing knowledge and life experiences, for all the great time and funny moments during lunch time and coffee breaks, and most important, thank you for the friendship.

I would like to thank the collaborators and growers who participated to the spore collection effort.

Thank you to Christofer Lee Sehn, Gabrielle Jensen, Marie Schussler, Michelle Cradduck, and all summer students for the helpful discussions, encouragement, support, and friendship during my time working at Laroche's Lab.

Lastly, I would like to thank my family and Antonio Keller for the unconditional love, support, and patience while dealing with all the challenges, fears, and stresses.

Table of Contents

List of Tables

List of Figures

List of Abbreviations

Bgt - Blumeria graminis f. sp. tritici
DON - Deoxynivalenol
Fg - Fusarium graminearum
F.spp – Fusarium species
FHB – Fusarium head blight
HSTs – Host-selective toxins
ITS – Internal transcribed spacer
LeRDC – Lethbridge Research and Development Centre
Log10 – Logarithm base 10 transformation
Lr – Leaf rust gene
PCR – Polymerase chain reaction
Pgt - Puccinia graminis f. sp. tritici
Pn - Parastagonospora nodorum
Psh - Puccinia striiformis f. sp hordei
Pst - Puccinia striiformis f. sp. tritici
Pt - Puccinia triticina f. sp. tritici
Ptr - Pyrenophora tritici-repentis
qPCR – Quantitative polymerase chain reaction
SLR – Simple linear regression
Sr – Stem rust gene
Tox A – Toxin type A
Yr – Yellow rust (stripe rust) gene

Epigraph

"It is possible to fail in many ways...while to succeed is possible only in one way."

–Aristotle

"Nobody said that it'd be easy, they just promised it would be worth it."

–Anonymous

CHAPTER ONE: IMPORTANT WHEAT PATHOGENS IN WESTERN CANADA

1.1 Literature review

1.1.1 Wheat importance

The period between 1896 to 1913 has been called the "Wheat Boom Era", which rapidly transformed the Canadian economy (McInnis 2015). Since then, wheat (*Triticum aestivum* L.) has become one of the most important grain crops for the Canadian economy, worth an average of more than CAD$5 billion dollars annually for the period between 2012 and 2016 (AAFC 2016). In Canada, the regions of highest agriculture importance are the Prairie provinces (Alberta, Saskatchewan, and Manitoba) where wheat production is a very important activity, having large wheat farms with an average of 600 hectares in size (Geo 2016). In 2017, wheat harvested areas were lower than in 2016 because of drought on the Prairie provinces. The total wheat harvested area for Alberta, Saskatchewan, and Manitoba was 23.9 million acres in 2017 and was worth $3.8 billion (Statistics Canada 2017 A). Beside drought, pests are another important cause for wheat production losses. It is estimated that 29% of the global wheat production is lost due to pests (Oerke 2006). Due to the great importance of wheat, scientists, food agencies, and producers work together to minimize crop losses and increase productivity.

1.1.2 Host-pathogen interaction

The interaction between pathogen and plant host is highly related to the plant's immune system and health. Plant health is an important component against pathogens because a healthier plant has a better chance to resist pathogen infections. In many cases, even while under pathogen attack, plants can find a balance to keep growing and

producing seeds (Pandey et al. 2017). Moreover, not every host-pathogen interaction is successful because not all pathogenic organisms are able to cause disease in all hosts (Chisholm et al. 2006). There are pathogens that only attack certain hosts, perhaps because they have evolved together with their hosts or because of certain nutrients provided only by these specific hosts (Agrios 2005).

Environmental conditions are also very important factors in host-pathogen interactions because both components can be influenced by the environment. Environmental conditions, such as temperature, humidity, drought, and wind can exert an advantageous or disadvantageous influence on both host and pathogen (Scholthof 2007). In 1960s, George Lee McNew, a plant pathologist, implemented the "Disease Triangle Concept", which can be used to understand the relationship between the three factors (host, pathogen, and environment) on the development of plant disease (Scholthof 2007). The concept states that for plant disease establishment, it is fundamental to have favorable environmental conditions for pathogen development, a susceptible host, and a virulent pathogen (Agrios 2005; Scholthof 2007). There are six sub-factors influencing disease development, and they are environmental characteristics (temperature, moisture, and wind), duration of infection, pathogen virulence level, pathogen inoculum size, maturity of host, and susceptibility level of host (Agrios 2005; Scholthof 2007) (Figure 1.1).

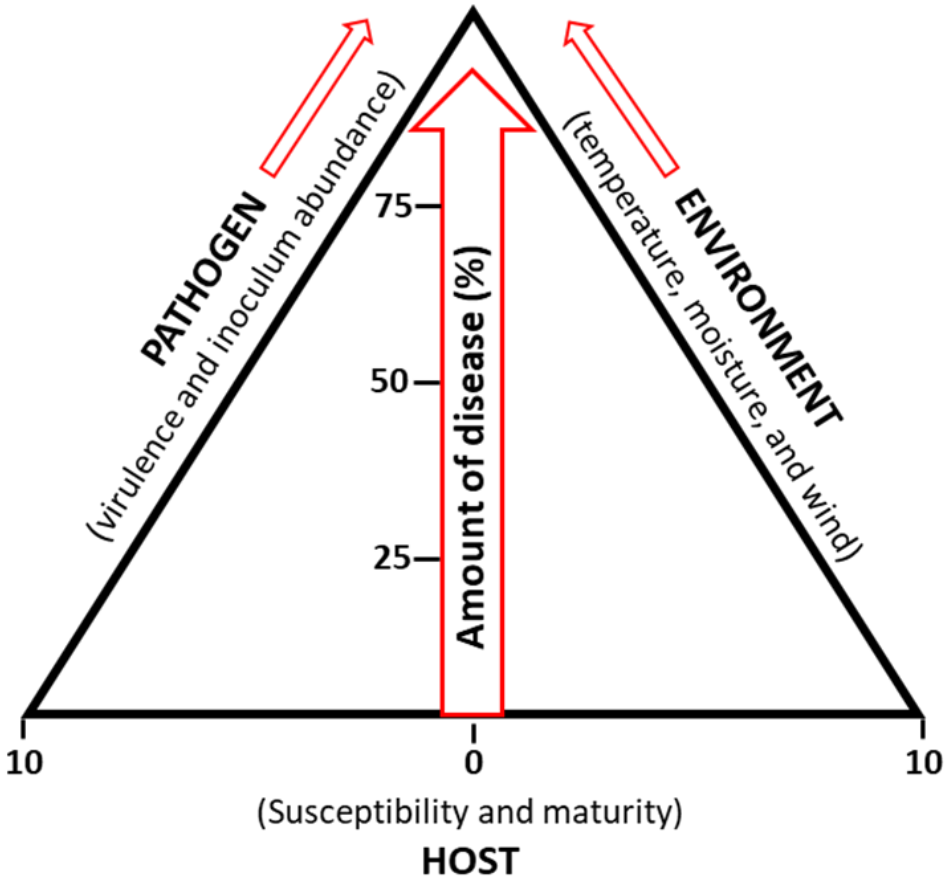

Figure 1.1 – Disease Triangle model for explaining interactions among the three main factors at the beginning of infection. Susceptibility and maturity are measured in levels from 0 (highly susceptible and young seedling) to 10 (resistant and mature host) (adapted from Scholthof 2007)

1.1.3 Six important wheat pathogens in Western Canada

Wheat yield can be affected by biotic and abiotic stressors. Six important wheat fungal diseases encountered in Western Canada are stripe rust (*Puccinia striiformis f. sp. tritici* Westend. (*Pst*)), leaf rust (*Puccinia triticina f. sp. tritici* Erikss. (*Pt*)), stem rust (*Puccinia graminis f. sp. tritici* Pers. (*Pgt*)), powdery mildew (*Blumeria graminis* (DC.) Speer *f. sp. tritici* Em. Marchal (*Bgt*)), tan spot (*Pyrenophora tritici-repentis* (Died.) Drechs. (*Ptr*)), and Fusarium head blight (FHB) caused predominantly by *Fusarium graminearum* (Schwein.) Petch. (*Fg*) (Regional Plant Disease Diagnostic Labs 2010; Marone et al. 2013; Tittlemier et al. 2013) (Figure 1.2).

1.1.3.1 Rusts

Rusts affect wheat crops worldwide and are considered one of the most important wheat fungal diseases. They are considered a great threat to wheat crops because of their ability to develop new races and overcome resistant wheat varieties, and their capacity to travel long distances on wind currents (Wegulo & Byamukama 2012). The three types of wheat rust: stripe, leaf, and stem rusts, are found in all wheat growing areas around the world (Wegulo & Byamukama 2012; Beddow et al. 2015). In Canada, most wheat cultivars carry resistance against leaf and stem rusts thus limiting the impact of these pathogens as long as sources of resistance remain effective. Rusts are basidiomycete fungi that only survive and develop on green tissues of plants (obligate biotroph) (Agrios 2005). Their sexual life cycle is complex, with five different spore stages (Figure 1.3). Urediniospores are the asexual spores, which can be produced several times during a wheat growing season (Agrios 2005; Wegulo & Byamukama 2012; Chen et al. 2014).

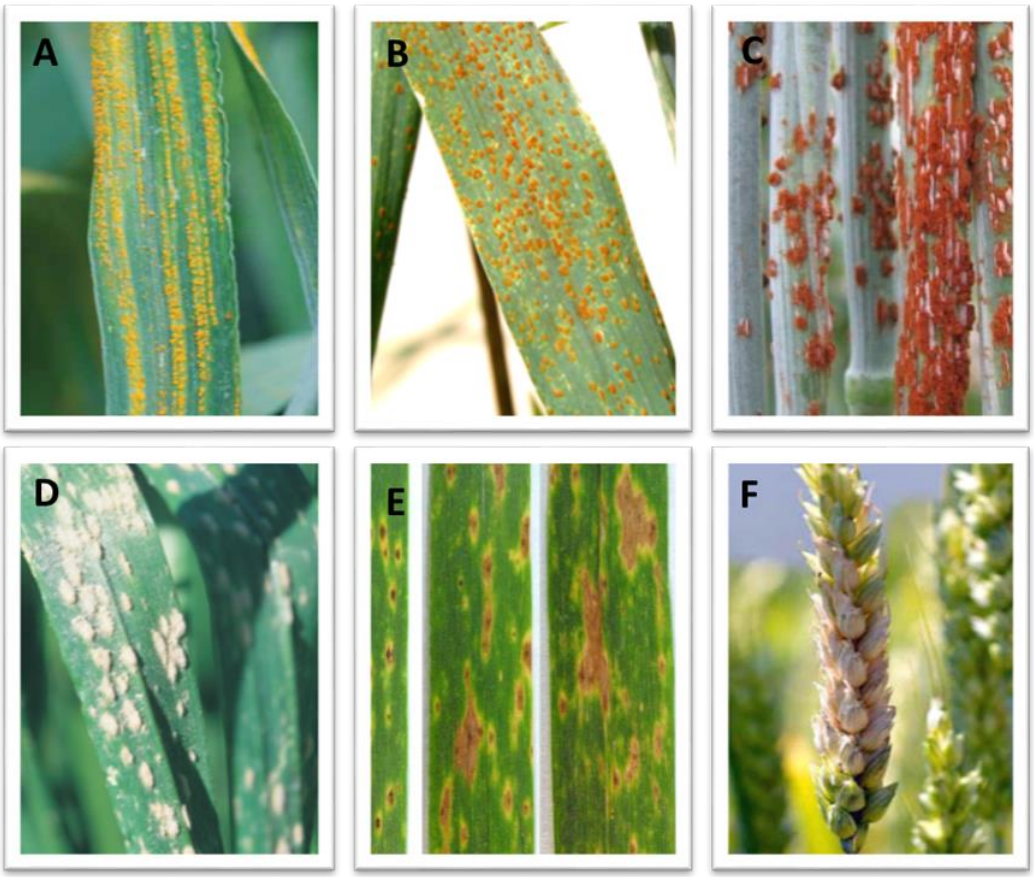

Figure 1.2 – Disease signs of the six important wheat pathogens. **A)** *Puccinia striiformis f. sp. tritici* (Kelly 2016), **B)** *Puccinia triticina f. sp. tritici* (DPIRD 2016), **C)** *Puccinia graminis f. sp. tritici* (Lagudah & Pretorius 2013), **D)** *Blumeria graminis f. sp. tritici* (DPIRD 2017), **E)** *Pyrenophora tritici-repentis* (Simpfendorfer 2015), and **F)** *Fusarium graminearum* (Wharton 2011).

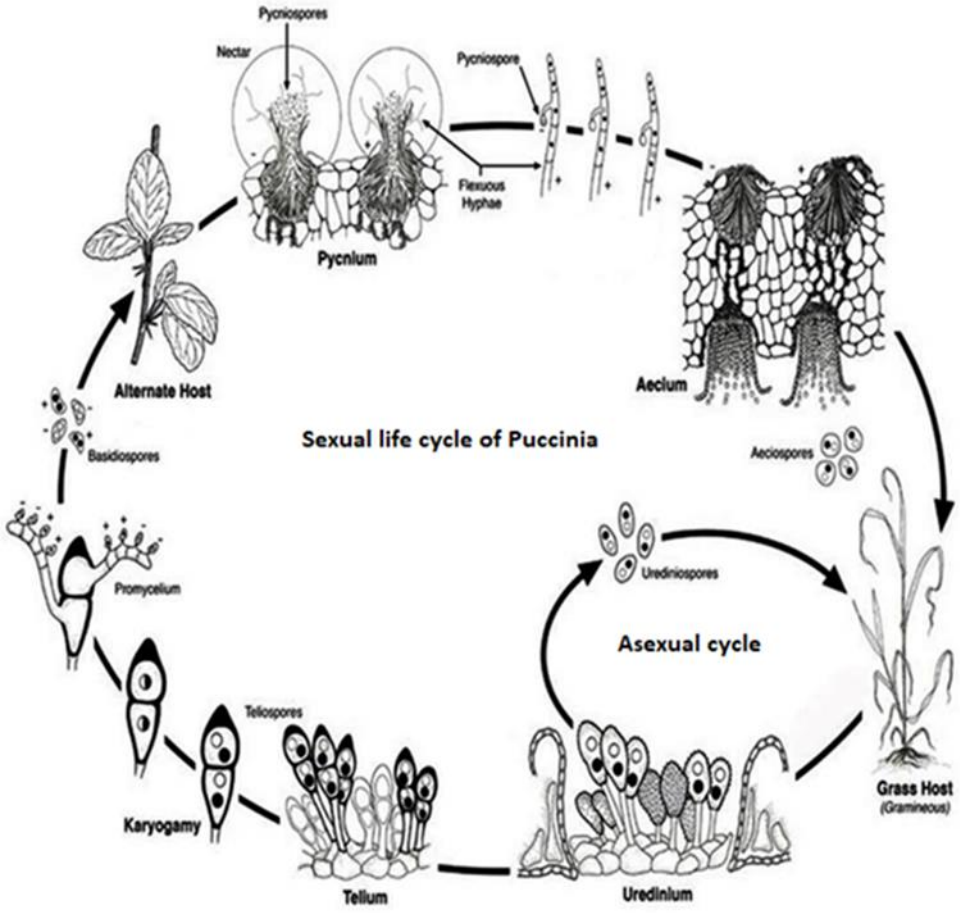

Figure 1.3 – *Puccinia* life cycle (adapted from USDA 2017).

The sexual stage of the rust life cycle requires an alternate host, which is infected by basidiospores. Rusts weaken wheat plants by reducing photosynthesis rates, reducing carbohydrate translocation through the whole plant (moving only to the infection site) and increasing moisture loss. All these modifications cause reduced root growth, foliage, and yield (Agrios 2005; Dubin & Brennan 2009). Rust has been the focus of many research projects for identification and selection of plant resistance genes for the development of markers and resistant wheat varieties, genome comparison, and effector genes (Randhawa et al. 2013; McCallum et al. 2016; Cuomo et al. 2017).

1.1.3.1.1 Stripe rust

In Canada, stripe rust has become the most important of the three rusts because its epidemics are fairly recent; consequently, most Canadian wheat varieties lack stripe rust resistance genes (all-stage and adult resistance genes), and its capacity to overwinter (Conner et al. 1988; Brar et al. 2017). The stripe rust life cycle was believed to be similar to the other rusts, which have several spore stages and an alternate host. However, the identity of the alternate host of *Pst* was unknown for close to a century because a number of attempts to identify the alternate host had failed. In 2010, Jin et al. identified *Berberis* species as the alternate host of *Puccinia striiformis* life cycle.

Stripe rust can infect plants at any stage of development, but only the leaves are affected. Disease signs appear differently on seedlings and adult plants. Seedling signs are yellow blotches, while on adult plants, the presence of yellow stripes appear on the leaves (Chen 2005). The stripes are formed by a few to many uredium pustules aligned on the leaf surface, where each uredium produces thousands of yellow to orangish

urediniospores (Chen 2005; Agrios 2005). First signs of sporulation appear about 14 days after infection (Chen 2005). Under favorable environmental conditions, stripe rust can become a destructive disease, causing yield losses typically between 10 to 70%, achieving 100% yield losses if the infection starts early in the season and if the host is highly susceptible (Chen 2005; McCallum et al. 2006; Chen et al. 2014; Xi et al. 2015). Prior to 2000, stripe rust of wheat was not believed to be a global threat because it was associated with cooler and higher elevation areas. Currently, *Pst* races seem to be evolving and thriving in warmer and drier areas (Beddow et al. 2015; Brar & Kutcher 2016). Favorable environmental conditions for spore germination are cool temperatures (7° to 15°C) and light moisture (relative humidity or dew formation) (Roelfs et al. 1992; Chen 2005; Chen et al. 2014). Optimum temperature range for disease development depends on the *Pst* race because new and more adaptable races are emerging in different US and Canada regions (Chen 2005; Chen et al. 2014; Beddow et al. 2015; Brar & Kutcher 2016). High humidity is essential for spore germination; though, prolonged periods under high moisture can cause a reduction in spore viability (Chen 2005).

There are two pathways for *Pst* inocula to arrive in Canada; one is the Pacific Northwest (California, Oregon, Washington, and Idaho), which is the inocula path to British Columbia, Alberta, and Northwest Saskatchewan. The other pathway is through the US Great Plains, which delivers *Pst* of inocula to Eastern Saskatchewan, Manitoba, and Ontario (Brar & Kutcher 2016; Aboukhadour 2017) (Figure 1.4).

Pst management can be done by fungicide application, crop rotation to prevent a green bridge between winter and spring wheat, seed treatments to prevent early infections on seedling; however, the most effective and preferred option is development and cultivation of resistant wheat varieties (Xi et al. 2015; Brar et al. 2017).

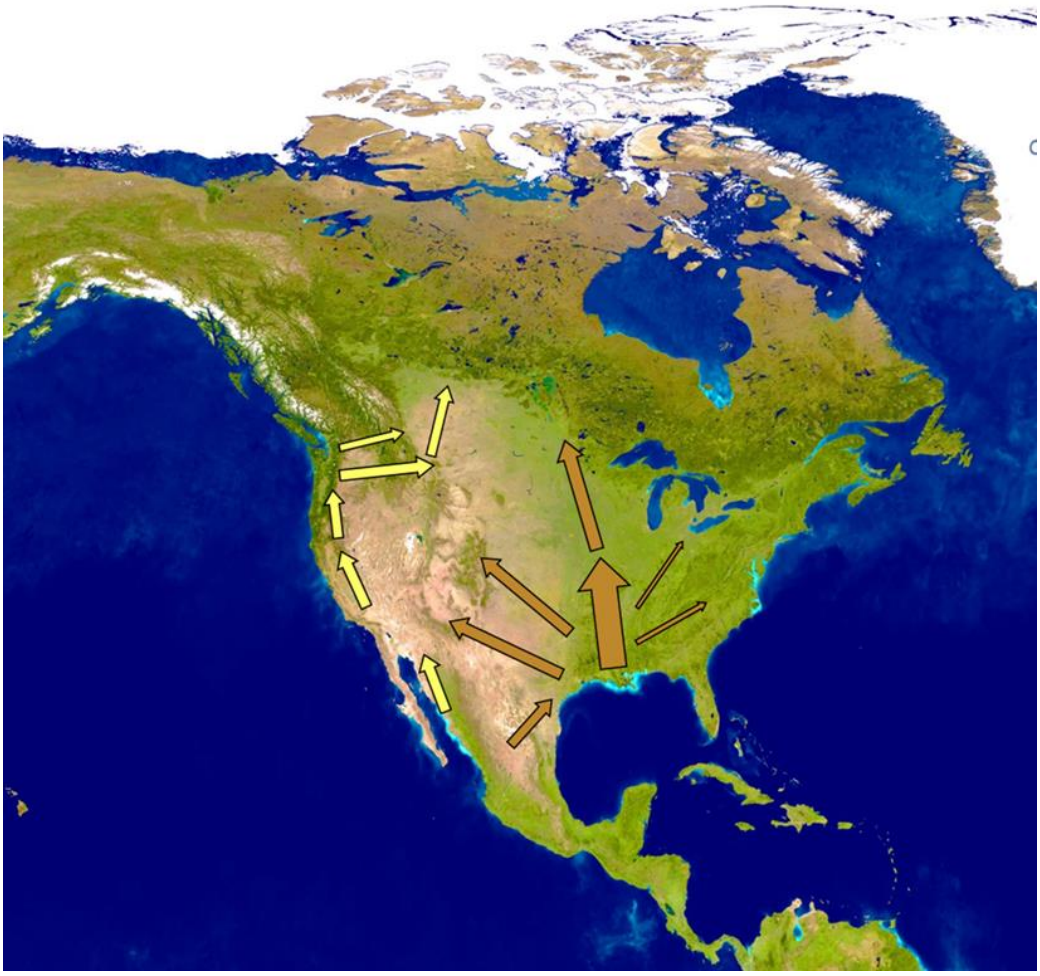

Figure 1.4 – *Puccinia* pathways from Mexico to United States and Canada. Yellow arrows represent the Pacific Northwest pathway and brown arrows represent the Great Plains pathway (Dr. Denis Gaudet, used with permission).

1.1.3.1.2 Leaf rust

In Canada, leaf rust of wheat is found mostly in Saskatchewan and Manitoba. The inoculum comes to Canada through the Great Plains pathway, where leaf rust is the most abundant among the three rusts (Wegulo & Byamukama 2012). Leaf rust can infect plants at any stage of growth. The upper side of leaves are typically affected, but it can also be found on the leaf sheath (Hershman 1985). The disease signs are brown to reddish, round to oval pustules that are mostly scattered on the plant leaf surface. Pustules contain thousands of urediniospores, which are wind dispersed (Hershman 1985; Agrios 2005; Baka & Rabei 2013).

Pt's alternate host is *Thalictrum spp*, from the Ranuculaceae family, but in the Mediterranean regions, *Pt*'s alternate host was identified as *Anchusa italica* (Boraginaceae family) (Ezzahiri et al. 1992; Huerta-Espino et al. 2011; Wegulo & Byamukama 2012).

The optimum environmental conditions for spore germination are temperatures ranging from 15° to 20°C and high humidity (Wegulo & Byamukama 2012).

In the 1920s to 1930s, *Pt* infections in wheat plants were moderate to severe, causing millions of dollars in annual losses in Western Canada (McCallum et al. 2016). Yield losses caused by *Pt* can range from 7 to 50%, depending on the plant stage at the time of infection, the host susceptibility level, and weather conditions (Huerta-Espino et al. 2011). Damages caused by *Pt* are not as great as those caused by stripe or stem rust. Losses frequently result in reduction of yield, protein content, and seed weight (Huerta-Espino et al. 2011; McCallum et al. 2016). The most efficient methods of controlling *Pt* are by foliar fungicide application and use of resistant wheat varieties that carry resistance

genes like *Lr16*, *Lr21*, *Lr34*, which are effective in Canada (Fetch et al. 2011; Randhawa et al. 2013).

1.1.3.1.3 Stem rust

Historically, stem rust of wheat was one of the most important wheat diseases because of several outbreaks around the world. For example, in 1946/1947 in India, yield losses were about 20% of the total wheat production; in 1951, in Chile losses represented 40% of total wheat production; in 1953-1954, in US, it was estimated that 4.5 million tonnes of total wheat production were lost (35% for spring wheat and 80% for durum) (Dubin & Brennan 2009).

The sexual stage of the *Pgt* life cycle is completed when it encounters barberry bush, where it produces aecia on the under side of the leaves, and new virulent races can be developed (Wegulo & Byamukama 2012; Peterson 2013). An effective way to protect wheat plants is to interrupt the life cycle of the pathogen. In 1918, a campaign in US to eliminate barberry plants (*Berberis* sp.), which was called the "Barberry Eradication Program", led to an important decrease in stem rust infection.

Over 40 years ago, a stem rust resistant gene (*Sr31*) was incorporated into winter wheat varieties in the US and provided efficient resistance to the disease. This gene has been used alone or combined with other *Sr* gene(s) in many wheat varieties worldwide (Milus et al. 2010). In 1998/99, a very aggressive race of *Pgt* (Ug99 or TTKSK) was detected in Uganda, which, surprisingly, overcame the wheat resistant gene *Sr31* when it first infected wheat crops (Singh et al. 2008; FAO 2010). Since then, it has overcome more resistance genes and infected wheat crops in Kenya in 2001, Ethiopia in 2003,

Sudan and Yemen in 2006, and Iran in 2007 (FAO 2010). Losses up to 80% have been reported in Uganda and Kenya (McKie & Rice 2007). Ug99 presence has not been detected in North America, but it might arrive on this continent because of its ability to travel long distances on wind currents or due to accidental introduction by travelers. Thus, scientists are working to develop wheat varieties that are resistant to Ug99. In Canada, Dr. Tom Fetch and a team of scientists were able to identify three new genes that are producing high resistance levels when combined (AAFC 2015 A).

Signs of stem rust disease on wheat appear as elongated red to brownish pustules, which are filled with thousands of urediniospores. Pustules can be formed on almost all plant parts, but the most common locations are stems, leaves and leaf sheaths (Agrios 2005; Wegulo & Byamukama 2012; Baka & Rabei 2013). The optimum environmental conditions for germination of spores are temperatures between 15° to 24°C and high humidity; however, disease development is favored between 24° to 30°C (Milus et al. 2010; Wegulo & Byamukama 2012). Presently, yield losses, caused by *Pgt* in susceptible varieties, are around 70%, under optimum conditions for disease development (FAO 2010). Cultivation of resistant wheat varieties is the preferred and most efficient method of controlling stem rust.

1.1.3.2 Powdery mildew

Bgt is a formae speciales of the *Blumeria graminis* family, which infects common wheat crops worldwide. *Bgt* is an Ascomycete, obligate biotroph fungus (Agrios 2005; Parks et al. 2011; Jankovics et al. 2015). The *Bgt* life cycle is composed of asexual and sexual stages (Figure 1.5). Asexual spores, called conidia, are capable of numerous

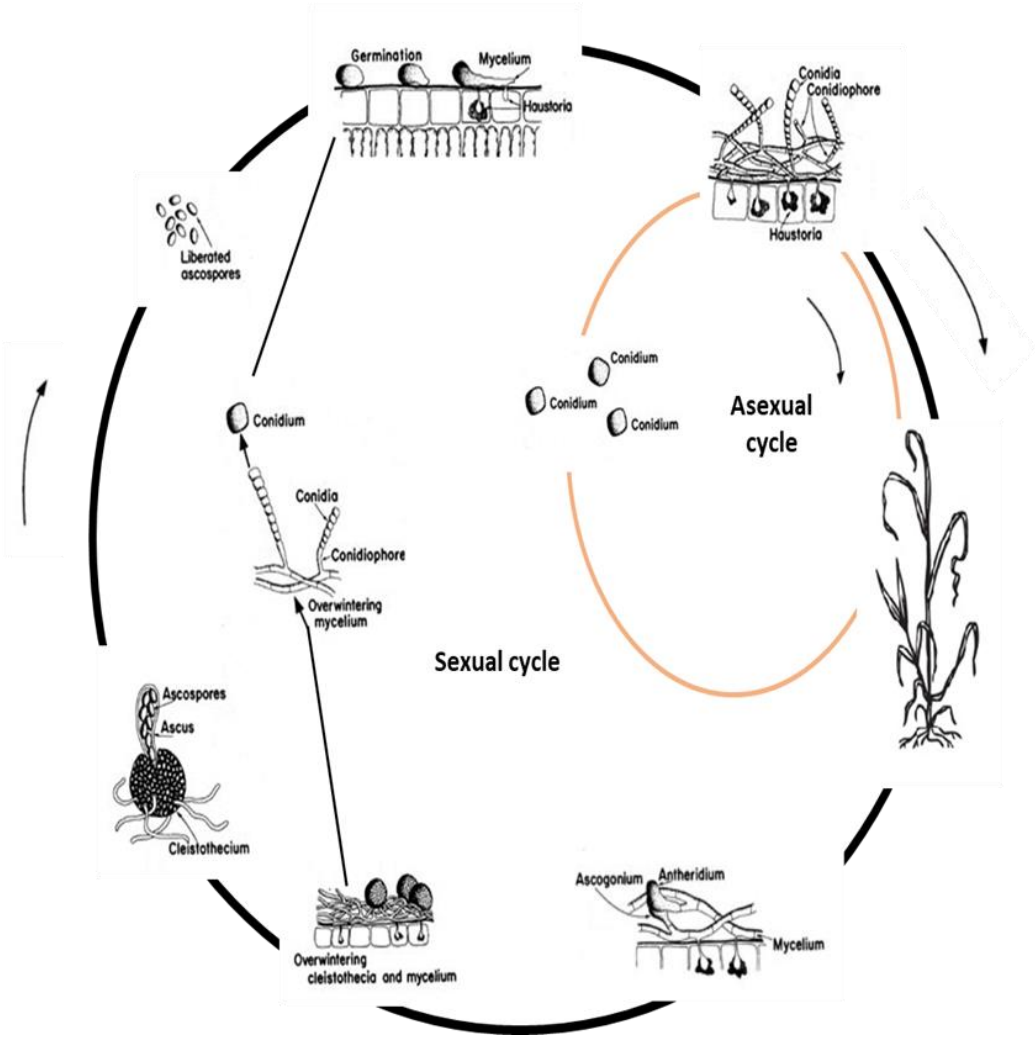

Figure 1.5 – *Blumeria graminis f. sp. tritici* life cycle (adapted from Agrios 2005).

reproduction cycles that occur during the wheat cultivation season. Ascospores (sexual spores) might be produced toward the end of the wheat growth cycle, but only if moisture is present for at least a few days (Wicker et al. 2013; Jankovics et al. 2015). Both types of spores can be spread over long distances by wind currents. Close to the end of summer, *Bgt* can produce chasmothecium (or cleistothecium), which allow it to overwinter. Alternatively, it can overwinter as mycelia on wheat plants (Heffer et al. 2006; Wicker et al. 2013).

Disease signs are cottony white to brownish mass(es), which can spread and infect almost all plant parts (leaves, stem, and head) (Agrios 2005; Parks et al. 2011). Powdery mildew grows epiphytically on host surfaces (Heffer et al. 2006). *Bgt* spore germination is facilitated under high humidity and cool weather, with an optimum temperature between 15 to 22°C (Parks et al. 2011; Duveiller et al. 2012; Marone et al. 2013; Cao et al. 2016). According to Ghemawat (1979), an increase of nitrogen fertilizer applications can favor powdery mildew disease development. The need for durable powdery mildew resistant wheat varieties is increasing because, according to some studies, *Bgt* is becoming insensitive to some classes of fungicides (Rong et al. 2000; Marone et al. 2013; Orton & Brown 2016). Powdery mildew damage to wheat crops is due to a reduction in the rate of photosynthesis, which decreases grain quality and yield (Rabbinge et al. 1985). Yield losses caused by *Bgt* can be higher than 35% depending on favorable environmental conditions and host susceptibility level (University of Saskatchewan 2018). *Bgt* disease management methods are using resistant wheat varieties, fungicide applications, elimination of crop residues to prevent a green bridge between the previous crop and the new one, balanced fertilizer applications, and crop rotation (University of Saskatchewan 2018).

1.1.3.3 Tan spot

Ptr is an Ascomycete, necrotrophic, foliar fungus, which affects common wheat and other grasses (Strelkov & Lamari 2003). It causes tan spot disease, also called yellow leaf spot, worldwide. First described in Europe in the 1850s, and it was found in US, Canada, and Japan in the 1900s (Abdullah et al. 2017). It is a stubble-borne pathogen, which can cause substantial damage on wheat leaves, leading to yield losses up to 50% under optimal environmental conditions, depending on cultivar susceptibility, and pathogen virulence/race (Abdullah et al. 2017). The tan spot life cycle is composed of sexual and asexual cycles. During the sexual cycle, ascospores are produced by fruiting bodies (pseudothecia), while in the asexual cycle, large septate conidia are produced by conidiophores (Agrios 2005) (Figure 1.6). Signs show up as an association of necrotic lesions with a chlorotic halo, or as necrotic or chlorotic lesions (Faris et al. 2013; Moffat et al. 2014). *Ptr* produces mycotoxins, host-selective toxins (HSTs), which cause different lesions. Different lesion characteristics can be used to identify the different toxins. Three HSTs (Ptr Tox A, Ptr Tox B, and Ptr Tox C) are known to be produced by eight different *Ptr* races (Martinez et al. 2001; Strelkov & Lamari 2003). In Western Canada, Ptr Tox A is the only HSTs found on wheat crop samples. This mycotoxin is produced by races 1 and 2 of *Ptr* (Aboukhaddour et al. 2013). Mild to warmer temperatures (20 to 27°C) and high humidity are optimal conditions for *Ptr* spore development (De Wolf 2008; Fernandez et. al. 2010). The most efficient methods for controlling *Ptr* are removal of infected plant debris, fungicide application, crop rotation, and use of resistant wheat varieties (Agrios 2005).

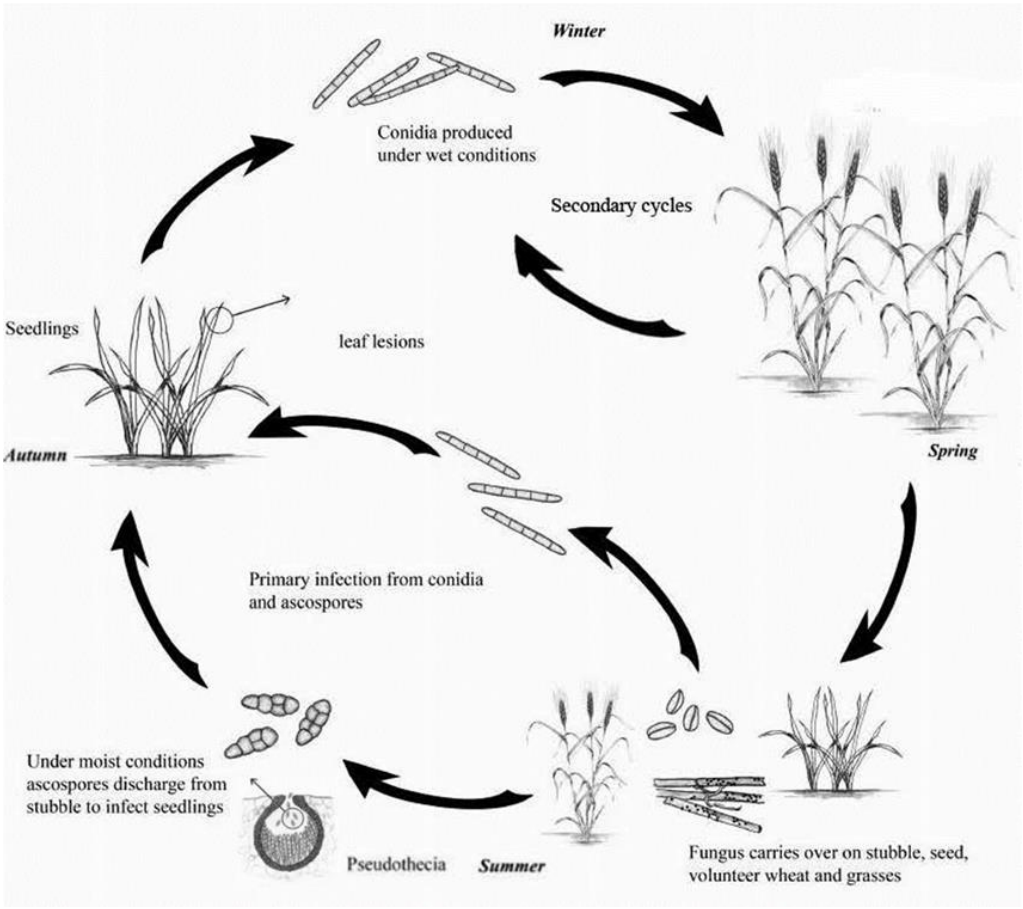

Figure 1.6 – *Pyrenophora tritici-repentis* life cycle. From season to season the fungus survives on stubble, seed, and volunteer grasses and wheat, so the infection time changes according to the wheat planting time (winter or spring). This cycle represents infection of winter wheat (Fowler 2014).

1.1.3.4 Fusarium head blight

In Western Canada, FHB is mainly caused by *Fusarium graminearum* (teleomorph - *Gibberella zeae* [Schwein] Petch). However, it can also be caused by many different species of the *Fusarium* genus (Leslie & Summerell 2006; Gräfenhan et al. 2013). *Fusarium* species are facultative saprophytic Ascomycota. They are present on wheat, corn, and other small grains produced around the world (Ireta & Gilchrist 1994; Agrios 2005). The life cycle is monocyclic, composed of a sexual cycle, where perithecia produce ascospores, and an asexual cycle, where macroconidia are produced after ascospore infection occurs (Beyer et al. 2004) (Figure 1.7). Different from many *Fusarium* species, *Fusarium graminearum* does not produce microconidia during its asexual cycle (Leslie & Summerell 2006). Ascospores are considered to be the primary inoculum of wheat heads because of their dispersal mechanism, which consists of spores being forcefully expelled from perithecia by water splashes. Macroconidia can also be transported by water splashes and wind; alternatively, insect such as midges can transport the spores (Fernando et al. 2000; Mongrain et al. 2000; Beyer et al. 2004). Macroconidia are much less frequent at the height of wheat heads, likely because of their size and spreading mechanism (Fernando et al. 2000). FHB frequently infects wheat heads, but other parts of the plant can also be infected. Signs associated with FHB infection are pinkish mycelial mass(es) and orange sporodochia, asexual fruiting bodies bearing conidiophores (and producing conidia), on plant surfaces (Fernando et al. 2000). FHB is economically important because it can affect wheat crops worldwide, causing yield losses of 30 to 70%. Despite yield losses, the biggest concern is mycotoxin accumulation on grains (Waalwijk et al. 2004). Optimal conditions for spore germination are a

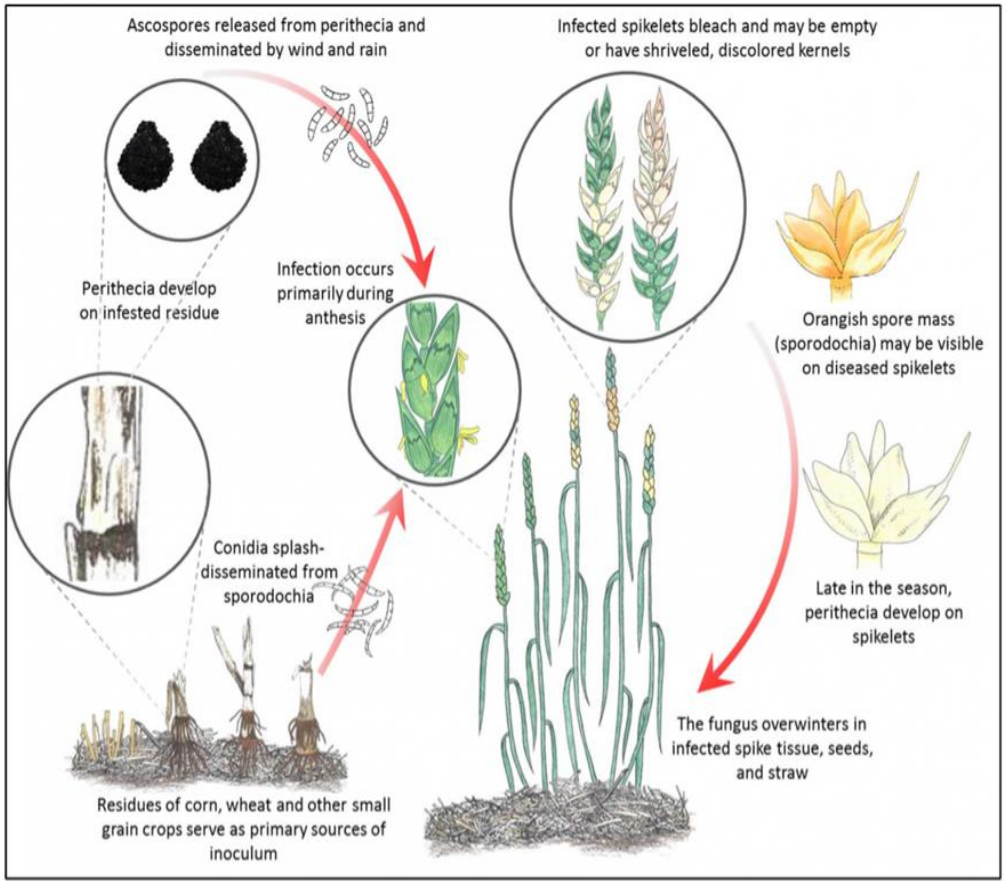

Figure 1.7 – Fusarium head blight life cycle (Mills et al. 2016).

humid/semi-humid climate and warm temperatures (16° to 30°C), and the optimum range for *Fusarium graminearum* development is between 25° to 28°C (Kikot et al. 2011; Gautam & Dill-Macky 2012; Government of Saskatchewan 2018). High humidity is very important for disease development, principally during and/or just after anthesis development, which can be linked with high disease severity and mycotoxin accumulation (Fernando et al. 2000; Kikot et al. 2011; Gautam & Dill-Macky 2012).

Fusarium species produce different mycotoxins on wheat grains which can affect grain quality by making it unsuitable for consumption because mycotoxins can be harmful to both humans and animals (Gautam & Dill-Macky 2012). These toxins include deoxynivalenol (DON), 15-acetyldeoxynivalenol (15-AcDON), and nivalenol (NIV) (Gautam & Dill-Macky 2012). Among FHB toxins, DON is the principal mycotoxin produced in wheat. In Canada, DON concentration of ≤ 2 mg/kg in uncleaned wheat grain destined for human consumption is allowed (Charmley & Trenholm 2017). If ingested in higher concentrations, DON toxin can cause food refusal, vomiting, and fertility reduction in humans and animals (Charmley & Trenholm 2017). FHB disease management options include proper levels of nitrogen and potassium fertilizer, crop rotation, and use of resistant cultivars (Agrios 2005).

1.1.4 Control of plant diseases

1.1.4.1 Genetic resistance

Deploying effective plant host resistance genes against pathogens using breeding techniques is the most effective and environmentally friendly method of controlling diseases of wheat (Bailey et al. 2009). Modern breeding techniques that use molecular genetic markers linked to known wheat resistance genes is referred to as Marker-Assisted Breeding (MAB) (Randhawa et al. 2013). This approach permits breeders to select desired genotypes based on presence or absence of a marker rather than selecting for the resistant phenotype that may be difficult to select for directly. MAB is assisting with the development of varieties with more durable disease resistance with resistance genes such as *Sr2* against stem rust races in North America, *Lr34* and *Lr16* against leaf rust races in Canada, and *Yr17* and *Yr29* and many more against stripe rust races in Canada (Randhawa et al. 2013). MAB enables breeders to work with multiple resistant genes of interest in a single line to develop wheat varieties that might be more durable (Randhawa et al. 2013; Djian-Caporalino et al. 2014; Pilet-Nayel et al. 2017). Pathogens can evolve and overcome host resistance with time, but this usually occurs by overcoming one gene at a time. To solve this issue scientists and breeders are working to develop a more stable and durable resistance by combining multiple resistance genes against each one of the different wheat pathogens (AAFC 2015 A).

1.1.4.2 Fungicides

Fungicides are a commonly used method for disease control of crops. Fungicides are effective when applied correctly according to the disease type aimed to control. They

need to be applied at specific plant growth stages, which can help to protect yield potential (Hutcheon & Jordan 1992; Ransom & McMullen 2007). A study by Ransom & McMullen (2007) showed that yield productivity was increased by 5.5 to 44% when foliar fungicides were applied on wheat plants to control leaf diseases and FHB. Examples of commercially available fungicides used to protect wheat are Twinline and Folicur EW. Both fungicides can be used to control a variety of wheat and small cereal diseases, including stripe rust, Fusarium head blight, and tan spot. Fungicides should be only used when really needed because some chemicals used in fungicides have the potential of causing environmental contamination. Studies have shown that fungicides can contaminate estuarine waters, bee-collected pollen, soil, and terrestrial and aquatic species (Wightwick et al. 2012; David et al. 2016). Fungicides are not always the best method because their effectiveness can be altered by environmental factors, so a combination of different cultural controls is the ideal approach (Termorshuizen 2002; Ransom & McMullen 2007). Pathogens are known to become resistant to certain chemicals (Agrios 2005). The loss of sensitivity of *Bgt* populations against some types of fungicides has been reported during the last few years, so this fact increases the need for durable resistant wheat varieties (Rong et al. 2000; Marone et al. 2013; Orton & Brown 2016).

1.1.4.3 Cultural control

Cultural control are field methods applied to prevent disease build-up without using chemicals, breeding techniques, or biological control (Termorshuizen 2002). Examples of cultural control methods are crop rotation, fertilization level, and timing of

seeding. Crop rotation is frequently used to control soil-borne pathogens. This method is based on rotation of different crops that are non-host to the targeted pathogen (Termorshuizen 2002). Fertilization can be used to increase plant health, which helps with resistance and tolerance againts pathogen effects (Termorshuizen 2002; Bailey et al. 2009). However, the use of fertilizers needs to be well balanced because the effect can be adverse. For example, increase of nitrogen levels stimulate plant growth hence increasing canopy density which can lead to more disease (Bailey et al. 2009). Furthermore, an increase of nitrogen can decrease silicon content in the leaves, which makes plants more susceptible to disease (Termorshuizen 2002). Seeding timing methods prevent green bridge formation between crops, which decreases the survival of obligate biotroph pathogens. These methods can also prevent the whole crop from flowering at the same time hence decreasing the build-up of pathogens that infect wheat heads, such as FHB (Bailey et al 2009). However, on the Canadian Prairies, there is always the risk of frost at the end of August, which limits the time of maturation of most crops, so if spring wheat grains are not fully mature before the frost period arrives, the risk of losing the crop is high.

1.1.5 Importance of disease assessment

Assessment of pathogen presence and incidence is important for development of disease management strategies, which help with prevention of yield losses and reduction of excessive application of environmentally harmful fungicides (Agrios 2005). Evaluation of fungal spore incidence in air currents is an important factor to predict possible pathogen infestations before the first signs appear on crop plants (Cao et al. 2016). Several studies worldwide have monitored the incidence of fungal spores in wind

currents, including FHB in Eastern Canada by Fernando et al. (2000), soybean rust in North America by Isard et al. (2011), powdery mildew of wheat in China by Cao et al. (2016). Passive and active methods can be used for fungal monitoring, such as spore trapping using wax-coated film, double-sided adhesive tape, white petroleum jelly, or air-sampling instruments (Galán & Domínguez-Vilches 1997; Fernando et al. 2000; Cao et al. 2016). These methods have different applications, efficiency, and analysis approaches. The efficiency may vary according to weather conditions because higher temperatures can alter spore adherence (increasing or decreasing) and rainfall can wash off the sampling surface (Galán & Domínguez-Vilches 1997; Alcázar et al. 2003). The materials used to cover or coat passive spore trapping systems are mostly commercially available, which makes them easier to obtain and reduces possible inconsistencies with results (Alcázar et al. 2003).

1.1.6 Methods of identification and quantification of fungal spores

Air samples collected by spore traps can be analysed by different approaches, including microscopy and PCR-based methods. It is essential for disease monitoring and management that fast and reliable methods for identification and quantification of airborne fungal pathogens are available (Tsui et al. 2011; Cao et al. 2016). PCR-based methods are considered the most reliable when pathogen-specific PCR primers are available and used to identify pathogen spores based on their DNA. Depending on the specificity of primers, pathogens can be identified to genus, species, or even specific race (Lubeck & Lubeck 1996). PCR-based methods are considered as one of the most reliable because these methods allow amplification of a specific DNA target of the pathogen of interest, by multiplying the initial target piece of DNA by millions of copies (Lubeck &

Lubeck 1996). It is necessary to go through three very important steps for a more specific, reliable, and consistent PCR result. The first step is optimization of the DNA extraction method to ensure adequate cell disruption and DNA release. Second step, it is extremely important to design/acquire highly pathogen-specific primers for a highly specific target amplification (Tsui et al. 2011). The third step is optimization of primers, PCR material (or kit), and methods (master mix concentration and thermocycler set up) that will be utilized for sample analyses (Reischer et al. 2004; Nicolaisen et al. 2009; Cao et al. 2016). After method optimization, the PCR process can be automated, reducing the process time, human error, and possible inconsistency of results.

Microscopic analyses of airborne pathogen spores collected in air currents is commonly used because it is an inexpensive and relatively fast analysis. However, for a confident identification of pathogen spores it is essential to have extensive training in spore morphology and/or taxonomy because spore morphology can be very similar among different species (Cao et al. 2016). Identification under a microscope is frequently carried out to the family or genus levels, but in some cases, taxonomists are able to identify different species when using microscopes with higher resolution and magnification, such as SEM (scanning electron microscope). This is an efficient method; however, it requires training and more time for preparation of samples, which makes this method unfit for routine and repetitive tasks. Rust asexual spores are an example of species with similar spore morphologies, which require more taxonomic knowledge and specialized microscopy to differentiate them (Baka & Rabei 2013).

1.1.7 Objectives

Globally, wheat is a commercially and economically very important crop because it is the largest single crop to provide >20% calories and >25% protein in human intake. However, fungal pathogens cause numerous yield losses, which leads to important economic losses. Among the best approaches to protect wheat are disease monitoring and management, understanding pathogen infection mechanisms, identification and quantification of pathogens, awareness of environmental conditions and fertilizer influence on disease development, and development of durable resistance against many different pathogens in new wheat varieties. Consequently, plant pathologist, agronomists, breeders, farmers and producers organizations are working very hard to protect and increase yield of this very important cereal crop.

In this research project, four experiments were conducted, two related to plant pathology and two related to monitoring pathogen prevalence using morphological identification of fungal spores and qPCR-based method. For the plant pathology experiments, stripe rust of wheat was rated under field natural conditions and controlled growth chamber conditions, after a susceptible wheat variety was inoculated with six different concentrations of pathogen spores. A similar study was conducted with powdery mildew of wheat, under controlled growth chamber conditions. These experiments were performed to establish the minimum threshold concentration of spores from these two wheat pathogens to cause significant infection.

For morphological identification, microscope slides were coated with double-sided adhesive tape and placed in or near wheat fields. Slides were analysed under light microscopy for detection of prevalent asexual fungal spores using morphological

characteristics of important airborne wheat pathogens (*Pst*, *Pt*, *Pgt*, *Bgt*, *Ptr*, and *Fg*) for the identification.

For qPCR-based identification, six important wheat pathogens (*Pst*, *Pt*, *Pgt*, *Bgt*, *Ptr*, and *Fg*) were characterized in air samples collected in Southern Alberta areas. Samples were collected using Burkard Cyclone instruments. Pathogen-specific PCR primers were optimized for highly specific identification and quantification of each pathogen.

CHAPTER TWO: DOSE-RESPONSE RELATIONSHIPS BETWEEN STRIPE RUST AND POWDERY MILDEW PATHOGENS AND SUSCEPTIBLE WHEAT

2.1 Introduction

2.1.1 Importance of wheat crop

In Western Canada, wheat cultivations started between 1812 and 1813 in Winnipeg, Manitoba (Martens et al. 2014; AAFC 2015 B). Wheat (*Triticum aestivum* L.) has become an important crop since the "Wheat Boom Era" from 1896 to 1913, which transformed the Canadian economy (McInnis 2015). This period was marked by the success of breeding wheat in Canada, the Marquis cultivar, which had a higher bread-making quality, higher yield, and earlier maturity (Martens et al. 2014). Since then, common wheat is one of the most produced crop in Canada, and worth approximately CAD$5.1 billion dollars annually (AAFC 2016). The annual, Western Canada wheat production average was approximately 28.8 million tonnes for the last five years (2013 to 2017) (Statistics Canada 2016 & 2017 B). In Canada, wheat production is economically very important; approximately 75% of the total annual production is exported (CAFTA 2018). It is also important for the daily human and livestock consumption.

2.1.2 Role of plant disease

Plant diseases might be caused by bacteria, fungi, viruses, nematodes, and insects. Plants can also be affected by abiotic factors, such as lack of nutrients, moisture, or light. A sick plant has its development and yield reduced, or it can even lead to death in some cases (Agrios 2005). It is estimated that every year, millions of tonnes of wheat are lost worldwide due to all pathogen infections, adding up to a loss of US$979 million per year

(Beddow et al. 2015), representing approximately 20% of the total value of wheat annually (AAFC 2016). There are many diseases of wheat in Canada, including stem rust, leaf rust, stripe rust, powdery mildew, common bunt, loose-smut, fusarium head blight, mosaic virus, tan spot, and common root rot (Bailey et al. 2009).

2.1.3 Two important diseases of wheat in Alberta

2.1.3.1 Stripe rust

In the Western regions of the Canadian Prairies, stripe rust caused by *Puccinia striiformis f. sp. tritici* Westend. *(Pst*) is one of the most important fungal diseases of wheat, causing severe yield losses in some years (Chen 2005; Xi et al. 2015). Stripe rust can cause up to 100% of yield losses depending on host susceptibility levels, weather conditions for disease development, and initial infection period (Chen 2005; McCallum et al. 2006). Stripe rust is reported in most years because prevailing mild winter conditions and persistent winter snow cover enable the pathogen to survive on overwintering winter wheat plants and volunteer grasses; these conditions permit early re-infection and spread the following spring (Chen 2005; Kumar et al. 2013). Stripe rust is a leaf disease caused by an obligate biotrophic fungi (Chen et al. 2014). As the name 'obligate biotrophic' suggests, the pathogen only develops in living plant tissues, absorbing water and nutrients from the plant (Agrios 2005). A fine balance on the amount of water and nutrients that are withdrawn from the host by the pathogen must exist to keep both pathogen and host alive and growing. The most common stripe rust disease sign is presence of yellow stripes-like pustules (uredia – singular uredium) on leaves of mature plants. Each uredium produces thousands of yellow to orange urediniospores that are wind-dispersed over long distances

(Agrios 2005; Chen 2005; Chen et al. 2014). The optimum weather conditions for most *Pst* races are cool temperatures, between 7 to 18ºC, and high humidity. However, new and more aggressive *Pst* races are emerging in US regions; they tend to be more resistant to higher temperatures than the older races, so the optimum temperature for disease development will depend on the *Pst* race (Chen 2005; Chen et al. 2014; Brar & Kutcher 2016). Even though high moisture content is required for germination of spores, it can also cause adverse effects on spore survival because prolonged periods under high moisture can reduce spore viability (Chen 2005). Under optimum weather conditions, stripe rust can cause severe damage to susceptible wheat crops, leading to high yield losses (Chen 2007; Chen et al. 2010; Chen 2013).

In addition to originating from overwintering in winter wheat, *Puccinia* inocula come from Mexico to the US and Canada through two different pathways, Pacific Northwest and Great Plains. In Alberta, inoculum of stripe rust comes from the Pacific Northwest (Oregon, Washington, and Idaho), principally from areas were the fungal spores overwinter. *Puccinia* spores travel through the Pacific coast regions of US, (i.e., Pacific Northwest pathway) arriving in British Columbia, Alberta, and Northwest Saskatchewan provinces of Western Canada. The Great Plains pathway transports spores from areas of the Great Plains in US to Manitoba and Saskatchewan and regions of Eastern Canada (Brar & Kutcher 2016; Aboukhadour 2017). According to Su et al. (2003) and Chen et al. (2010), there are a total of 115 races of *P. striiformis f. sp. tritici* in the US, and 39 races in Western Canada.

2.1.3.2 Powdery mildew

Powdery mildew caused by *Blumeria graminis f. sp. tritici* (*Bgt*) is also widespread in Western Canada and can cause yield losses of up to 20% in some areas of Alberta, particularly in wheat grown under irrigation (Conner et al. 2003). *Bgt* is an obligate biotrophic fungus that can infect wheat crops, causing considerable destruction to susceptible wheat when the weather conditions are favorable for spore development (Parks et al. 2011). *Bgt* spore germination is favored in maritime areas (i.e., high humidity and cool to warm temperatures) and semi-continental climates (i.e., cool winter) (Marone et al. 2013; Cao et al. 2016; Orton & Brown 2016). The optimum temperature for *Bgt* spore germination is between 15 to 22°C (Duveiller et al. 2012). It is a host-specific pathogen, having at least eight different *formae speciales* where each *formae speciales* infects one specific host (Wicker et al. 2013). *Bgt* produces asexual spores, known as conidia, and sexual ascospores close to the end of the season. Powdery mildew overwinters in sexual structures (chasmothecia) in stubble and ascospores can be released during warm, humid conditions during spring and summer (Wicker et al. 2013). Conidia are the primary inoculum because they are produced numerous times during the wheat growing season, and easily detached from older lesions by wind or rain. Conidia and ascospores can travel long distances suspended in air currents (Costamilan 2005; Cao et al. 2016). The disease infection signs are fluffy white to brownish masses that can be found on all plant surfaces (leaves, stem, and head) (Agrios 2005; Parks et al. 2011).

2.1.4 Control of plant disease

Disease management and assessment are essential for controlling crop diseases, and among all the methods and techniques the use of resistant wheat varieties and disease monitoring systems are among the most effective tools (Termorshuizen 2002; Xi et al. 2015; Cao et al. 2016). However, fungicides are still one of the most used methods among growers because of its easy access and because wheat resistant varieties to all diseases are not yet widely available in Canada. Fungicide applications should only be applied after pathogen identification and disease assessment are done because not all fungi can be properly controlled by fungicides, such as vascular pathogens (McGrath 2004). Also, fungicides should be carefully used because of their potential of causing environmental harm and increasing growing costs (Hollomon 2002). Inoculum monitoring is an important prophylactic method, which also contributes to development of forecasting systems for early detection of potential epidemics (Xi et al. 2015; Cao et al. 2016). Increasing plant host resistance against the pathogen through breeding techniques is the most effective method of controlling stripe rust of wheat. Recent developments in maker-assisted breeding enable breeders to select resistant genotypes that are difficult to select through conventional phenotype-based approaches (Randhawa et al. 2013).

2.1.5 Disease severity assessment

In general, the earlier the infection starts, the greater the disease severity; frequently, resulting in higher yield losses (Conner et al. 1988; Wan et al. 2004; Gaudet et al. 2015). For this reason, disease severity rating and monitoring are considered of great importance to understand pathogen spread pathways and capability to cause crop damage,

and to reduce disease spread by applying effective management methods (Martinelli 2015). The reasons for conducting a disease severity assessment depends on the scientific objectives. It might be for plant breeding programs (e.g., to establish minimum levels of resistance of crops), for crop protection and determination of pesticide application, for effective decisions on the best disease management method, for estimation of yield losses, or for understanding pathogen infection and its different levels of pathogenicity (Bock et al. 2015; Martinelli et al. 2015). Methods for disease severity assessment may vary according to the project approach and material availability, and they can be visual recognition and rating scales, serology, or DNA-based methods (Bock et al. 2015; Martinelli et al. 2015; Cao et al. 2016). Visual estimates of disease severity are considered subjective because they are a judgment call based on a pre-established rating scale; however, this method is the most widely used approach because of its convenience and rapidity (Bock et al. 2015; Cao et al. 2016).

2.1.6 Minimum inoculum concentration to enable disease establishment

Airborne fungal spores may cause diseases when in contact with an adequate host and favorable environment conditions. The Disease Triangle Concept states that three main factors must be present for disease development: a susceptible host, a virulent pathogen, and a favorable environment (Francl 2001). The host-pathogen interaction is affected by variables associated within each of the three factors. For example, under a favorable environment, a virulent pathogen encounters a host that has some level of resistance, but it is not fully immune, this interaction will probably result in a lower level of disease (Francl 2001). Other variables that can interact with this host-pathogen

relationship are plant health status, plant location, and concentration of pathogen inoculum (Scholthof 2007). However, the minimum inoculum size necessary to enable disease development is not known for *Pst* and *Bgt*.

Disease forecast models currently rely primarily on environmental data on susceptible crops to predict disease progression as a key component of the Disease Triangle Concept. The presence and quantity of a virulent pathogen is missing from forecast models. Current molecular technologies that permit real-time identification and quantification of crop pathogens are rapid and highly sensitive. They are so sensitive that they can potentially detect spore numbers at really low levels, which may be lower than inoculum thresholds for wheat diseases. Therefore, it is important to determine the inoculum threshold spore numbers for important wheat diseases. In the present study, we establish inoculum threshold levels for stripe rust and powdery mildew under controlled environment conditions and in the field in Southern Alberta.

2.2 Objective and hypothesis

2.2.1 Approach

I investigated and assessed the dose-response relationship between stripe rust and powdery mildew in susceptible wheat. Also, the results from this project might increase the understanding of how some of the Disease Triangle Concept factors contribute to disease rating. This concept is a paradigm to phytopathology because of the unique relationship between host and pathogen, which is influenced by the environment in numerous ways.

2.2.2 Objectives

To establish the minimum concentration of spores required to cause an infestation of stripe rust and powdery mildew in a susceptible wheat variety under controlled growth chamber and under natural field conditions for the rust.

2.2.3 Hypothesis

There is a threshold concentration of spores required for causing an infestation of stripe rust and powdery mildew in susceptible wheat under different environmental conditions.

2.3 Materials and methods

2.3.1 Potting mix preparation

The soil mix used was prepared, by the Lethbridge Research and Development Centre (LeRDC) greenhouse staff. It is a soilless peat-base mix for all plants species (Boodly & Sheldrake 1972, with modifications made by the greenhouse staff – addition of zinc and Turface to the mix). The materials used for the peat-based mix are sphagnum peat moss (one bale of 108 liter), vermiculite (2 bags of 18.6 kg), Turface MVP (22.7 kg), fertilizers mix (1000 g of calcium carbonate powder, 1500 g of 18-6-12 Osmocote, 1200g of monocalcium-dicalcium phosphate, 15 g of 13.2% chelated iron, and 7 g of 14% chelated zinc), and water (between 9 to 23 litres, depending on the end use of the mix).

2.3.2 Plant material and seeding set up

2.3.2.1 Growth chamber experiment

Seeds of Avocet, a susceptible spring wheat variety to stripe rust and powdery mildew, were used for growth chamber experiments. Seeds were planted in 32-well (4 x 8) rootrainers (size 36 cm x 20 cm x 9 cm) (Rootrainers^{TM} by Haxnicks^{TM}) whereby only 24 wells were seeded to reduce density in between the plants and facilitate disease rating. Two seeds were planted per well to ensure an adequate number of plants were available for the experiments. Aproximately, one week after seeding, extra seedlings were culled from the experimental rootrainers, leaving only one healthy looking seedling in each well. A total of 18 rootrainers were used, with 3 rootrainers per treatment for a total of 72 plants per treatment. For stripe rust experiment, rootrainers were seeded on March 3, 2016 for the first trial and on Aug. 18, 2016 for the second trial. For powdery mildew

experiment, rootrainers were seeded on April 24, 2017 for the first trial and on Aug. 28, 2017 for the second trial. Rootrainers were organized in three rows, going from the lowest to the highest spore concentration treatments.

2.3.2.2 Field experiment

The field experiment was seeded with a different susceptible spring wheat variety, Barrie rather than Avocet, because it is better adapted to Western Canada growth conditions. The field was divided in three equal sized sections for the growing season 2016 (approximately 15 m x 27 m for each section) and two equal sized sections for the growing season 2017 (approximately 15 m x 27 m for each section), with each section representing one trial. Each trial was surrounded by the stripe rust resistant triticale variety Sunray in order to create a barrier between the trials. Also, each side of the treatments with the Barrie plants (approximately 1 m x 2 m) were separated by triticale plants and an access corridor (Figure 2.1). The barriers between the treatments were created to minimize possible cross-contamination between treatments. The trials were seeded on two different dates for the growing season 2016 (April 22, 2016 for trial one and May 3, 2016 for trials two and three), and on May 11, 2017 for both trials of the growing season 2017.

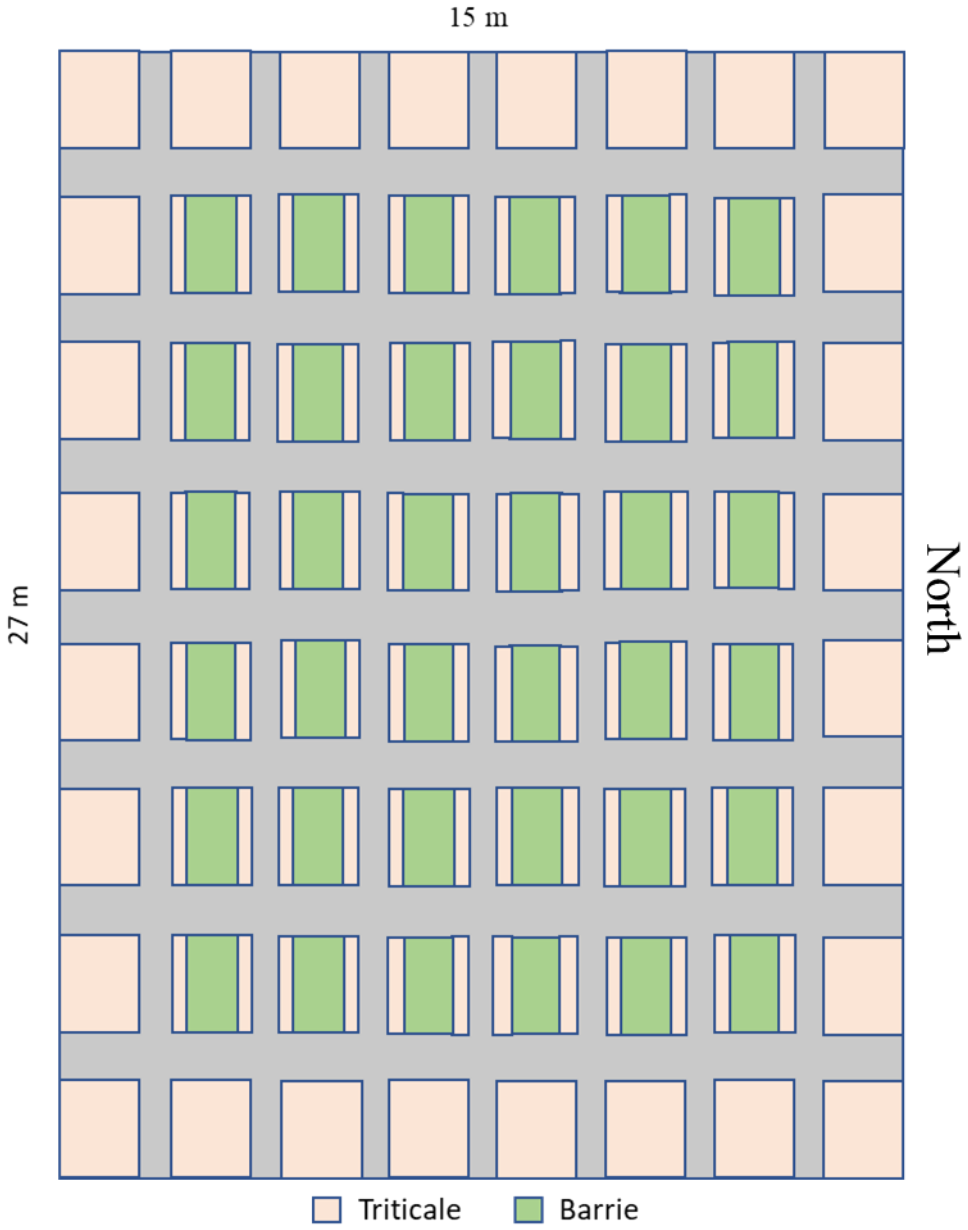

Figure 2.1 – Diagram of one field trial (same design for all trials): Barrie plants (6x6 design) surrounded by triticale plants.

2.3.3 Inoculum of fungal spores

2.3.3.1 Inoculation of growth chamber plants

Prior to starting experiments, growth chambers were vacuumed, thoroughly washed with 20% bleach solution, heated at 30°C for 5 days to kill possible remaining spores, and then cleaned with ethanol 70% in order to reduce spurious contamination. Wheat seedlings were inoculated at Zadoks stage 12 for *Pst* and stage Z14 for *Bgt* (Zadoks et al. 1974). Five different concentrations (10^3, 10^4, 10^5, 10^6, and 10^7 spores/ml and a negative control) of the virulent stripe rust isolate SRC484-1997 spores and virulent powdery mildew spores (uncharacterized isolate) were used for inoculation. Frozen (trial one) and fresh (trial two) *Pst* spores were suspended in Soltrol® 170 Isoparaffin (Chevron Phillips Chemical) in 15 ml spray glass vials from which the dilutions were made (Appendix 1). *Pst* frozen spores were prepared as follows before dilutions were made: spores were removed from storage at -80°C in 2 ml tubes and heat shocked at 42°C for 2 min (modified from McIntosh et al. 1995). *Pst* first trial's inoculation date was on March 17, 2016, and second trial's inoculation was on September 2, 2016. Fresh *Bgt* spores (uncharacterized isolate) were collected at the LeRDC greenhouses on May 16, 2017 for first trial and September 25, 2017 for second trial. *Bgt* spores were suspended in Novec™ 7100 Engineered Fluid (Sigma-Aldrich) in 15 ml spray glass vials from which the dilutions were made. The Novec 7100 Engineered Fluid is a colourless volatile liquid, so it dries out very rapidly from the leaf surface. *Bgt* spores were diluted in a different fluid because it seemed that Soltrol 170 oil was disturbing germination of powdery mildew spores. The final volume of all dilutions used to spray the plants was 1 ml. The plants were sprayed using a sprayer atomizer (built at the University of Minnesota) attached to a

compressor, set up at 20 psi (Appendix 2). All the six replicates of each concentration were sprayed at the same time, so 1 ml of the dilution was used for the six replicates (72 plants in total). After inoculation, the plants were besprinkled with a diluted solution of Tween 20 (polyoxyethylene sorbitol monolaurate - 2 drops in 600 ml of water) to simulate dew formation on the top of the leaf surface, and they were covered with black plastic bags for 24 hours to simulate darkness. Plants inoculated with stripe rust were placed inside a cold room, set up at 5°C, for 24 hours. *Pst* needs a cool temperature and darkness for its spores to germinate. Then, they were placed inside a controlled growth chamber, which had the temperature set at 15°C for the *Pst* experiment with a photoperiod of 18 hours. Plants inoculated with powdery mildew, after being bagged, were placed directly inside the growth chamber at 20°C, but with the lights off for 24 hours. For *Bgt* experiment, the temperature was maintained at 20°C with a photoperiod of 18 hours. The humidity inside the chamber was maintained around 50% for the *Pst* experiment by filling up the pot trays with water every two days and, at 60 to 65% for the *Bgt* experiment by filling up the bottom of the chamber and the rootrainer trays with water every two days. Each spore concentration was replicated six times, and two trials of the entire block of experiment was done to ensure reproducibility. The stripe rust and powdery mildew trials were done one at the time in order to have independent biological trials for more representative results. In between each trial, the chamber was vacuumed and thoroughly cleaned as described above.

2.3.3.2 Inoculation of field plants

The field experiment was repeated during two consecutive years during the cropping season in 2016 and 2017, and the protocol used was the same for both years and for all trials (three trials in 2016 and two trials in 2017). Plants were inoculated on two different dates for the growing season 2016, June 24, 2016 for trials one and two, and June 30, 2016 for trial three, and for growing season 2017 both trials were inoculated on July 6, 2017. Field plants where inoculated with five different concentrations of spores (10^3, 10^4, 10^5, 10^6, and 10^7 spores/ml and a negative control) of the virulent stripe rust isolate SRC484-1997. Field plant growth stages were between Z18 to Z21 (Zadoks et al. 1974). In the field, plants were inoculated from the lowest to the highest concentration taking the wind direction into consideration. This strategy was used to minimize cross-contamination between the different treatments at the time of inoculation. Frozen spores were used and treated as described above. The solutions with different spore concentrations were prepared by diluting the spore stock suspension in Soltrol® 170 Isoparaffin (Chevron Phillips Chemical); total final volume of each solution was 1.2 ml. Plants were sprayed as described above.

2.3.4 Disease rating

To evaluate overall disease severity, three parameters were recorded, including infection incidence, disease severity, and infection type. For the first trial of the stripe rust growth chamber experiment, the rating dates were March 31, April 7, and April 14, 2016. Ratings for the second trial were performed on September 15, September 22, and September 29, 2016. For the stripe rust field experiments conducted in 2016 and 2017,

plants were rated once at 14 days after inoculation (dai). For the first trial of the powdery mildew growth chamber experiment, ratings dates were May 25, June 1, and June 6, 2017. Ratings for the second trial were on October 4, October 11, and October 16, 2017. Infection incidence measurement, reported as a percentage, was based on the number of inoculated leaves (two and four leaves for *Pst* and *Bgt*, respectively) that had signs of infection. The disease severity rating was conducted by visual evaluation during a period of two weeks. The disease severity rating was assessed by estimating percentage of the total surface area of the leaf that presented stripe rust (Figure 2.2) or powdery mildew infection signs. In the field, stripe rust ratings were measured as a percentage of the average of random 100 leaves of each treatment.

Stripe rust infection type evaluation was recorded according to McNeal et al. (1971) using a 0 to 9 scale where 0 = no visible signs or symptoms, 1 = necrotic and/or chlorotic flecks; no sporulation, 2 = necrotic and/or chlorotic blotches or stripes; no sporulation, 3 = necrotic and/or chlorotic blotches or stripes; trace sporulation, 4 = necrotic and/or chlorotic blotches or stripes; light sporulation, 5 = necrotic and/or chlorotic blotches or stripes; intermediate sporulation, 6 = necrotic and/or chlorotic blotches or stripes; moderate sporulation, 7 = necrotic and/or chlorotic blotches or stripes; abundant sporulation, 8 = chlorosis behind sporulation area; abundant sporulation, and 9 = no necrosis or chlorosis; abundant sporulation (McNeal et al. 1971; WSU 2015). Disease severity percentage and infection type ratings were used for both stripe rust studies (growth chamber and field); however, for the growth chamber experiment, the inoculated leaves were marked to be evaluated again on the three rating dates (every seven days), so the evaluations were made on each individual leaf. For the field

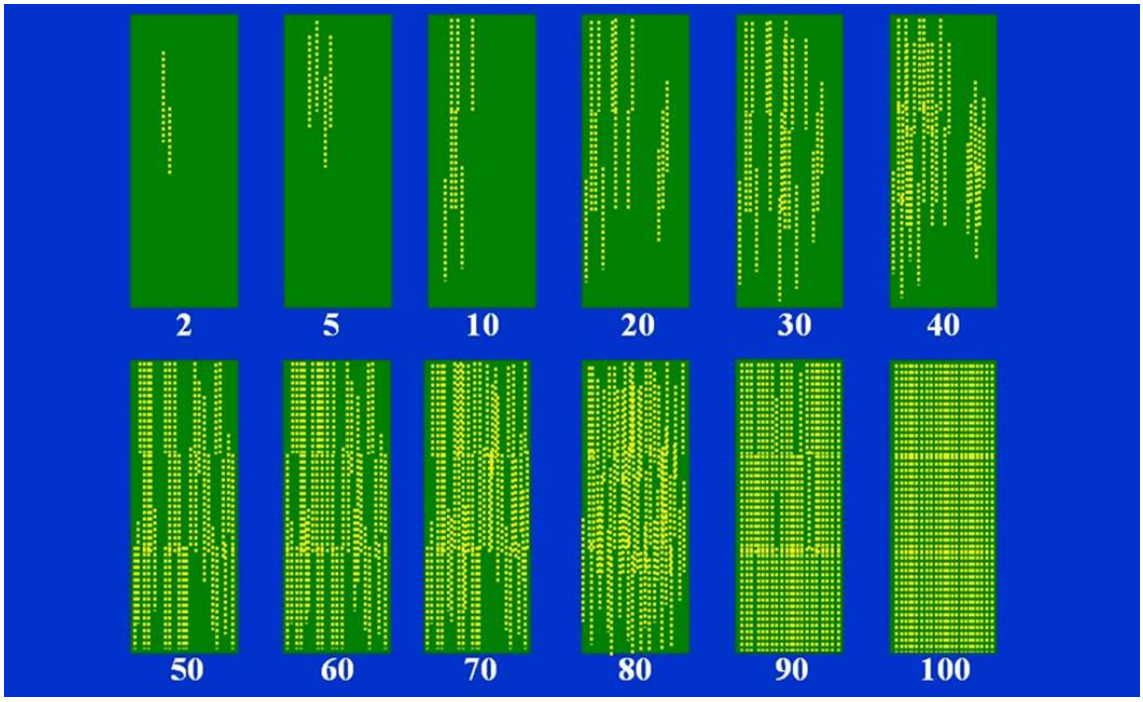

Figure 2.2 – Illustration of stripe rust disease severity rating scale as a percentage of the leaf surface covered in rust pustules (WSU 2018) where 2 to 5% = low severity, 6 to 20% = moderate severity, and > 20% = high severity.

experiment, the leaves of each concentration (of each trial and each replicate) were evaluated per group of 100 leaves (average evaluation).

Powdery mildew infection type evaluation used the scale developed for powdery mildew of grape by Riaz et al. (2011) with modifications for wheat. The scale ranged from 0 to 6 where; 0 = no disease signs or symptoms, 1 = trace of the disease sings or symptoms; one or two white tiny spots, 2 = many tiny spots, 3 = small spot(s) with light sporulation, 4 = patch(es) with intermediate sporulation, 5 = patch(es) with moderate sporulation and/or mycelial growth, and 6 = tissue covered with numerous patches; abundant sporulation. Two out of four of the inoculated leaves were randomly marked to be individually evaluated again on the three rating dates (9, 16, and 21days after inoculation).

2.3.5 Statistical analyses

All statistical analyses were performed using SPSS Statistics (IBM Analytics, release 23.0.0.0). Descriptive statistics were used in a preliminary assessment of the data. Mixed design ANOVA (Bonferroni post-hoc test and Mauchly's test for sphericity [Greenhouse-Geisser and Huynh-Feldt correction test for sphericity]) and One-way ANOVA (Dunnett 2-sided post-hoc test) were performed to analyse the data and to correct sphericity violations. Mixed design ANOVA test was conducted to assess whether the different treatments had significant effects on disease severity and, also, whether the disease severity had significantly increased over time. One-way ANOVA test, was conducted to determine which treatments were statistically significant in each rating day. Bonferroni and Dunnett 2-sided post-hoc tests were performed to compare variances

within different groups (rating days) and between variables inside the same group (treatments), respectively. Mauchly's test for sphericity was performed to check if the variances of differences (means) between the groups were equal or not. This test is considered violated if $p < .05$ (variances are not equal) (Laerd Statistics 2013), so to overcome this problem the correction tests (Greenhouse-Geisser and Huynh-Feldt) were performed. Greenhouse-Geisser results were reported when epsilon (ε) results were less than 0.75; whereas, Huynh-Feldt results were reported when epsilon (ε) results were more than 0.75 (Laerd Statistics 2013; personal communication with Dr. Olu Awosoga 2017).

2.4 Results

2.4.1 Stripe rust rating under controlled conditions

2.4.1.1 Stripe rust disease incidence

Before the first rating of trial one, three plants died, so the total number of plants analysed was 71 plants for treatment 10^5, 70 plants for 10^6 and 72 plants for other treatments and controls. In both trials, disease incidence was measured as a percentage of the two inoculated leaves of each plant that became infected (produced one or more pustules). Results of both trials demonstrated that the disease incidence for the negative controls and the two lowest treatments (10^3 and 10^4) were 0%, meaning that there was no sign of stripe rust disease infection. Inoculated leaves of the treatments 10^5 to 10^7 of both trials presented some level of stripe rust infection, where the incidence varied from 0% to 69% for treatment 10^5, from 77% to 98% for treatment 10^6, and from 95% to100% for treatment 10^7 (Table 2.1). These results illustrate the different dose-relationships between the host and pathogen, where higher concentrations of the pathogen inoculum resulted in higher disease incidence.

2.4.1.2 Stripe rust infection type

The negative controls, and treatments 10^3 and 10^4 presented no sign of infection on both trials, so the infection type was 0 (no symptoms). For both trials, treatments 10^5 to 10^7 spores/ml showed a range of infection types varying from no symptoms to trace, trace to moderate sporulation, and light sporulation to moderate sporulation, respectively (Table 2.2). The results showed a distinct development of the infection for the different concentrations of inoculum, where each of the three higher treatments had a different

Table 2.1 – Stripe rust disease incidence under growth chamber conditions.

Dai	Incidence	Trial one (%)			Trial two (%)		
	Number of infected leaves	10^5 spores/ml	10^6 spores/ml	10^7 spores/ml	10^5 spores/ml	10^6 spores/ml	10^7 spores/ml
14	No infection	81.7	21.4	1.4	100	22.2	4.2
	One leaf infected	0	18.6	9.7	0	55.6	45.8
	Two leaves infected	18.3	60.0	88.9	0	22.2	50.0
21	No infection	59.2	1.4	0	75.0	9.7	1.4
	One leaf infected	2.8	2.9	6.9	22.2	65.3	43.1
	Two leaves infected	38.0	95.7	93.1	2.8	25.0	55.5
28	No infection	31.0	2.9	0	54.2	9.7	1.4
	One leaf infected	18.3	2.9	5.6	41.7	65.3	43.1
	Two leaves infected	50.7	94.2	94.4	4.2	25.0	55.5
Total of plants		71	70	72	72	72	72

Dai: Days after inoculation.

Table 2.2 – Stripe rust infection type under growth chamber conditions.

Dai	Infection type	Trial one (%)			Trial two (%)		
	Symptoms	**10^5 spores/ml**	**10^6 spores/ml**	**10^7 spores/ml**	**10^5 spores/ml**	**10^6 spores/ml**	**10^7 spores/ml**
14	No symptoms	81.7	21.4	1.4	100	22.2	4.2
	N/C - no sporulation	0	2.9	0	0	22.2	11.1
	Trace	11.3	41.4	22.2	0	30.6	11.1
	Light sporulation	7.0	32.9	45.8	0	25.0	62.5
	Intermediate sporulation	0	1.4	30.6	0	0	11.1
	Moderate sporulation	0	0	0	0	0	0
	Abundant sporulation	0	0	0	0	0	0
21	No symptoms	59.2	7.1	0	75.0	9.7	1.4
	N/C - no sporulation	0	0	0	0	0	0
	Trace	8.4	1.4	2.8	1.4	23.6	2.8
	Light sporulation	14.1	34.3	20.8	8.3	51.4	48.6
	Intermediate sporulation	14.1	54.3	58.3	15.3	15.3	33.3
	Moderate sporulation	4.2	2.9	18.1	0	0	13.9
	Abundant sporulation	0	0	0	0	0	0
28	No symptoms	31.0	1.4	0	54.2	9.7	1.4
	N/C- no sporulation	0	0	0	0	0	0
	Trace	4.2	0	0	0	0	0
	Light sporulation	25.4	0	1.4	16.7	9.7	4.2
	Intermediate sporulation	22.5	30.0	25.0	19.4	69.5	40.3
	Moderate sporulation	16.9	61.5	44.4	9.7	11.1	48.5
	Abundant sporulation	0	7.1	29.2	0	0	5.6
Total of plants		71	70	72	72	72	72

Dai: Days after inoculation and N/C: Necrotic and/or chlorotic flecks.

initial infection type. Also, there was progress of infection type over time for the treatments 10^5 to 10^7 spores/ml.

2.4.1.3 Stripe rust disease severity

The disease severity data was non-normally distributed and nonhomogeneous because of the high amount of zeros of the treatments 10^3 and 10^4, and the negative controls, which presented no disease signs. Various data transformation methods were tested, but none corrected the lack of data normality. Therefore, a data clean-up, removing the cause of the skewedness (zeros), was performed to evaluate if the issue with the data normality and homogeneity were only the zeros, and it was confirmed to be the case. After confirming that there were no further issues with the data, the ANOVA tests were performed only on the treatments 10^5 and higher.

Descriptive statistics results for both trials showed that the disease severity increased over time, when the overall means of the three rating dates were compared (Appendix 3). For trial one and two, the mixed design ANOVA showed that the rating days statistically violated the Mauchly's test for sphericity ($X^2_{(2)} = 73.18$, $p < .001$ and $X^2_{(2)} = 53.95$, $p < .001$, respectively). Therefore, for trial one, the F-value for the rating days was corrected for violation of sphericity by the Huynh-Feldt correction (F (1.5, 329.3) = 837.5, $p < .001$ and F (1.7, 353.5) = 351.67, $p < .001$, respectively). The different treatments had statistically significant effects on the disease severity results for trial one and two (F (2, 210) = 153.0, $p < .001$ and F (2, 213) = 112.8, $p < .001$, respectively). Bonferroni post-hoc multiple comparisons test showed that all the three rating days were significantly different when compared between them (all $p < .001$) for

both trials. For trial one, the multiple comparisons Dunnett 2-sided post-hoc test revealed that the treatments 10^6 and 10^7 spores/ml were the only significantly different (both $p < .001$) when compared with the negative controls in the rating one, whereas for rating two and three, the treatment 10^5 along with 10^6 and 10^7 were significantly different (all $p < .001$) when compared with the negative controls (Figure 2.3). For trial two, rating one and two, the multiple comparisons Dunnett 2-sided post-hoc test revealed that the treatments 10^6 and 10^7 spores/ml when compared with the negative controls were the only treatments significantly different (all $p < .001$), whereas for rating three, the treatment 10^5 along with 10^6 and 10^7 were significantly different (all $p < .001$) when compared with the negative controls (Figure 2.4). These results illustrate that the different spore concentrations exerted direct influence on the disease severity results, showing that higher concentrations of spore cause higher disease severity under favorable conditions.

2.4.2 Powdery mildew rating under controlled conditions

2.4.2.1 Powdery mildew disease incidence

Disease incidence evaluation was based on percentage of inoculated leaves (four leaves/plant) that had sign of disease infection. For trial one, rating one, the disease incidence for the negative controls and treatments 10^3 to 10^5 were 0%, while treatments 10^6 and 10^7 presented 91.7% and 98.6% of total inoculated leaves infected, respectively. For the following two rating days, all treatments presented some level of disease incidence (Table 2.3). For trial two, rating one, the disease incidence for the negative

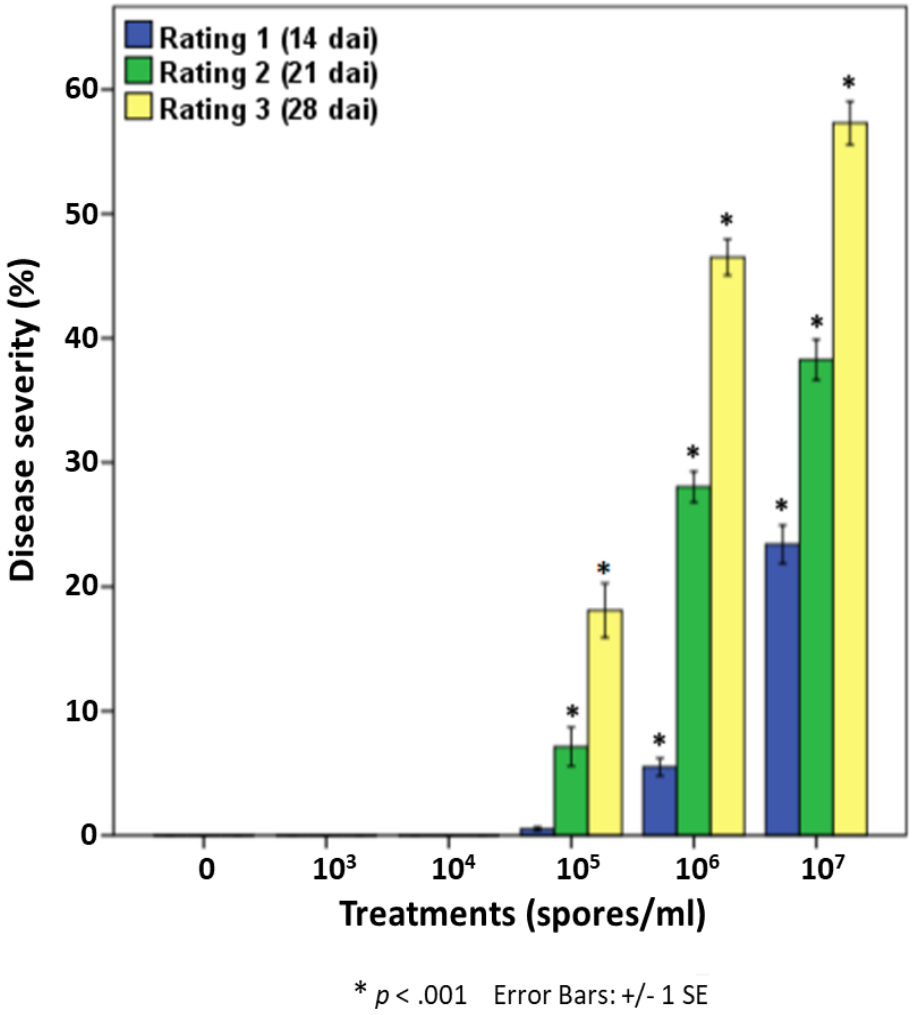

Figure 2.3 – Stripe rust disease severity on Avocet wheat plants after inoculation with different spore concentrations under growth chamber conditions (trial one). Error bars represent +/- 1 standard error. * = probability that mean values are significantly different from the negative controls at $p < .001$. These results are average values from six replicates.

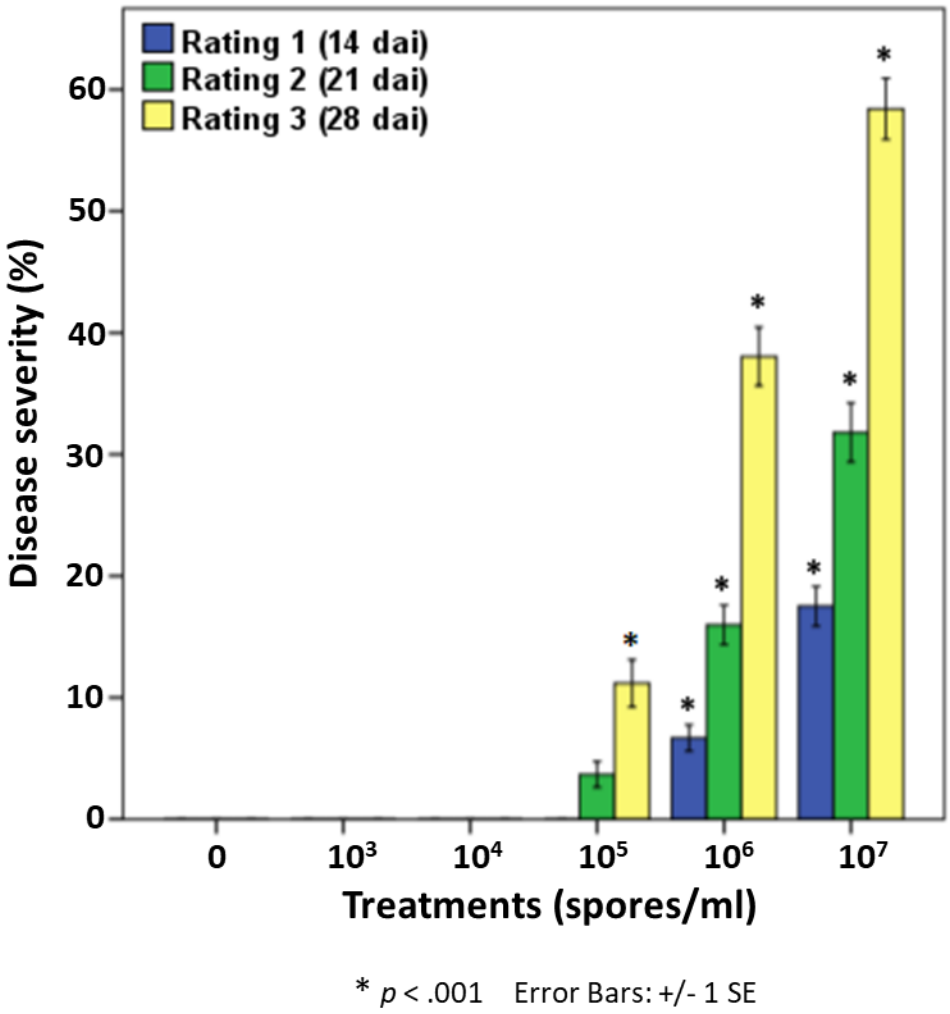

Figure 2.4 – Stripe rust disease severity on Avocet wheat plants after inoculation with different spore concentrations under growth chamber conditions (trial two). Error bars represent +/- 1 standard error. * = probability that mean values are significantly different from the negative controls at $p < .001$. These results are average values from six replicates.

Table 2.3 – Powdery mildew disease incidence under growth chamber conditions (trial one).

Dai	Incidence	Trial one (%)					
	Number of infected leaves	**Control**	**10^3 spores/ml**	**10^4 spores/ml**	**10^5 spores/ml**	**10^6 spores/ml**	**10^7 spores/ml**
9	No infection	100	100	100	100	8.5	1.4
	One leaf infected	0	0	0	0	2.8	0
	Two leaves infected	0	0	0	0	32.4	7.1
	Three leaves infected	0	0	0	0	5.6	7.1
	Four leaves infected	0	0	0	0	50.7	84.4
16	No infection	87.5	63.8	19.4	1.4	0	0
	One leaf infected	5.6	1.4	4.2	1.4	0	0
	Two leaves infected	6.9	13.9	27.8	19.7	10.0	1.4
	Three leaves infected	0	2.8	6.9	7.1	5.7	2.9
	Four leaves infected	0	18.1	41.7	70.4	84.3	95.7
21	No infection	77.8	52.8	6.9	0	0	0
	One leaf infected	5.6	2.8	2.8	2.8	0	0
	Two leaves infected	12.4	13.9	23.6	2.8	0	1.4
	Three leaves infected	1.4	6.9	18.1	5.7	2.9	0
	Four leaves infected	2.8	23.6	48.6	88.7	97.1	98.6
Total of plants		72	72	72	71	70	70

Dai: Days after inoculation.

controls, and treatments 10^3 and 10^4 were 0, while treatments 10^5 to 10^7 presented 5.6%, 84.7% and 94.4% of total inoculated leaves infected, respectively. For rating two and three, all treatments presented some level of disease incidence (Table 2.4). These results illustrate the different dose-relationships between the host and pathogen, where higher concentrations of the pathogen inoculum resulted in higher disease incidence. Also, the disease incidence increased over time for all treatments, including the negative controls, which illustrates cross-contamination between treatments after the first rating.

2.4.2.2 Powdery mildew infection type

For trial one, rating one, the negative controls and treatments 10^3 to 10^5 showed no symptoms, while treatments 10^6 and 10^7 showed predominantly small spots of white mycelia (Table 2.5). The infection developed over time (for ratings two and three) resulting in some sign of infection on negative controls and treatment 10^3, and many tiny to small spots of white mycelia for treatments 10^4 and 10^5, respectively, while for treatment 10^7 varied from intermediate to moderate sporulation. Treatment 10^6 was the only one that presented mainly small spots during all rating dates (Table 2.5). For trial two, rating one, the negative controls and treatments 10^3 and 10^4 showed no symptoms, while treatments 10^5 showed trace of infection in only 5.6% of the inoculated leaves, treatment 10^6 showed predominantly trace of infection, and treatment 10^7 showed predominately many tiny spots of white mycelia (Table 2.6). The infection developed over time (for ratings two and three) resulting in some sign of infection on negative controls, and many tiny spots to small spots of white mycelia for treatments 10^3 to 10^6, while for treatment 10^7 varied mainly from small spots to intermediate sporulation (Table 2.6). The

Table 2.4 – Powdery mildew disease incidence under growth chamber conditions (trial two).

Dai	Incidence	Trial two (%)					
	Number of infected leaves	**Control**	**10^3 spores/ml**	**10^4 spores/ml**	**10^5 spores/ml**	**10^6 spores/ml**	**10^7 spores/ml**
9	No infection	100	100	100	94.4	15.3	5.6
	One leaf infected	0	0	0	2.8	11.1	1.4
	Two leaves infected	0	0	0	2.8	40.3	15.3
	Three leaves infected	0	0	0	0	8.3	6.9
	Four leaves infected	0	0	0	0	25.0	70.8
16	No infection	86.1	25.0	43.1	16.7	1.4	0
	One leaf infected	8.3	11.1	2.8	1.4	0	0
	Two leaves infected	4.2	33.3	6.8	11.1	1.4	0
	Three leaves infected	0	0	4.2	4.2	0	1.4
	Four leaves infected	1.4	30.6	43.1	66.6	97.6	98.6
21	No infection	48.5	23.6	11.1	0	0	0
	One leaf infected	4.2	0	0	0	0	0
	Two leaves infected	12.5	5.6	5.6	0	0	0
	Three leaves infected	4.2	2.7	0	0	0	0
	Four leaves infected	30.6	68.1	83.3	100	100	100
Total of plants		72	72	72	72	72	72

Dai: Days after inoculation.

Table 2.5 – Powdery mildew infection type under growth chamber conditions (trial one).

Dai	Infection type	Trial one (%)					
		Control	10^3 spores/ml	10^4 spores/ml	10^5 spores/ml	10^6 spores/ml	10^7 spores/ml
9	No symptoms	100	100	100	100	8.5	1.4
	Trace	0	0	0	0	21.1	0
	Tiny spots	0	0	0	0	14.1	5.7
	Small spots	0	0	0	0	56.3	90.0
	Intermediate sporulation	0	0	0	0	0	2.9
	Moderate sporulation	0	0	0	0	0	0
	Tissue covered	0	0	0	0	0	0
16	No symptoms	87.5	63.8	19.4	1.4	0	0
	Trace	1.4	2.8	11.1	0	0	0
	Tiny spots	11.1	15.3	40.3	15.5	27.1	0
	Small spots	0	18.1	29.2	83.1	68.6	24.3
	Intermediate sporulation	0	0	0	0	4.3	71.4
	Moderate sporulation	0	0	0	0	0	4.3
	Tissue covered	0	0	0	0	0	0
21	No symptoms	77.8	52.8	11.1	1.4	0	0
	Trace	4.2	11.1	4.2	0	0	0
	Tiny spots	11.1	8.3	30.5	4.2	0	0
	Small spots	6.9	26.4	54.2	74.7	51.5	0
	Intermediate sporulation	0	1.4	0	19.7	47.1	34.3
	Moderate sporulation	0	0	0	0	1.4	57.1
	Tissue covered	0	0	0	0	0	8.6
Total of plants		72	72	72	71	70	70

Dai: Days after inoculation.

Table 2.6 – Powdery mildew infection type under growth chamber conditions (trial two).

Dai	Infection type	Trial two (%)					
		Control	10^3 spores/ml	10^4 spores/ml	10^5 spores/ml	10^6 spores/ml	10^7 spores/ml
9	No symptoms	100	100	100	94.4	15.3	5.6
	Trace	0	0	0	5.6	52.8	0
	Tiny spots	0	0	0	0	25	65.2
	Small spots	0	0	0	0	6.9	29.2
	Intermediate sporulation	0	0	0	0	0	0
	Moderate sporulation	0	0	0	0	0	0
	Tissue covered	0	0	0	0	0	0
16	No symptoms	86.1	25	43.1	16.6	1.4	0
	Trace	9.7	15.3	5.6	5.6	0	0
	Tiny spots	0	50	30.5	51.4	56.9	15.3
	Small spots	4.2	9.7	20.8	26.4	41.7	59.7
	Intermediate sporulation	0	0	0	0	0	15.3
	Moderate sporulation	0	0	0	0	0	9.7
	Tissue covered	0	0	0	0	0	0
21	No symptoms	48.6	23.6	11.1	0	0	0
	Trace	13.9	0	2.8	0	0	0
	Tiny spots	27.8	34.7	18.1	50	8.3	0
	Small spots	9.7	40.3	63.8	50	87.5	34.7
	Intermediate sporulation	0	1.4	4.2	0	4.2	48.6
	Moderate sporulation	0	0	0	0	0	15.3
	Tissue covered	0	0	0	0	0	1.4
Total of plants		72	72	72	72	72	72

Dai: Days after inoculation.

results showed a distinct development of the infection for the different concentrations of inoculum, where each of the three higher treatments had a different initial infection type.

2.4.2.3 Powdery mildew disease severity

The disease severity data was non-normally distributed and nonhomogeneous because of the large amounts of zeros of the treatments 10^3 to 10^5, and the negative controls on the rating one, which presented no disease signs. Various data transformation methods were tested, but none corrected the data normality. No data clean-up, removing the cause of the skewedness (zeros) was performed because for powdery mildew data only rating one of both trials presented large amounts of zeros for the three lowest treatments and the negative controls. Ratings two and three presented some level of infection for all treatments. Therefore, in order to analyse the results of all rating days the same way and be able to compare them, the zeros were kept for data analyses. ANOVA tests were performed for all treatments of both trials. Analyses of variance tests are robust and, when the sample size is moderate or larger, they can be reasonably accurate even when the normality assumption is violated (Glass et al. 1972). It is commonly accepted as a moderate sample size when N is equal 30 subjects (Green & Salkind 2017).

Descriptive statistics results of both trials, showed that disease severity increased over time, when the overall means of the three rating dates were compared (Appendix 4). For trial one and two, the mixed design ANOVA showed that the rating days statistically violated the Mauchly's test for sphericity ($X^2_{(2)} = 404.8$, $p < .001$ and $X^2_{(2)} = 227.5$, $p < .001$, respectively). Therefore, for trial one and two, the F-value for the rating days was corrected for violation of sphericity by the Greenhouse-Geisser correction (*F*

(1.2, 520.2) = 1737.9, $p < .001$ and F (1.4, 602.3) = 2125.6, $p < .001$, respectively). The different treatments had statistically significant effects on the disease severity results for trial one and two (F (5, 421) = 617.9, $p < .001$ and F (5, 426) = 511.5, $p < .001$, respectively). Bonferroni post-hoc multiple comparisons test showed that all the three rating days were significantly different when compared between them (all $p < .001$) for both trials. For trial one, the multiple comparisons Dunnett 2-sided post-hoc test revealed that the treatments 10^6 and 10^7 spores/ml of the rating one, were the only significantly different treatments (both $p < .001$) when compared with the negative controls, whereas for rating two and three, the treatments 10^4 to 10^7 were significantly different (all $p <.001$, except for 10^4 treatments on rating two $p = .004$) when compared with the negative controls (Figure 2.5). For trial two, rating one, the multiple comparisons Dunnett 2-sided post-hoc test revealed that the treatments 10^6 and 10^7 spores/ml when compared with the negative controls were the only treatments significantly different (both $p < .001$); whereas for rating two and three, the treatments 10^3 to 10^7 were significantly different from the negative controls (rating two: $p = .04$ for 10^3 treatments, $p = .03$ for 10^4 treatments, and $p < .001$ for all the others. Rating three: $p = .02$ for 10^3 treatments and $p < .001$ for all the others) (Figure 2.6). These results illustrate that the different spore concentrations exerted direct influence on the disease severity results, showing that higher concentrations of spore cause higher disease severity when under controlled conditions.

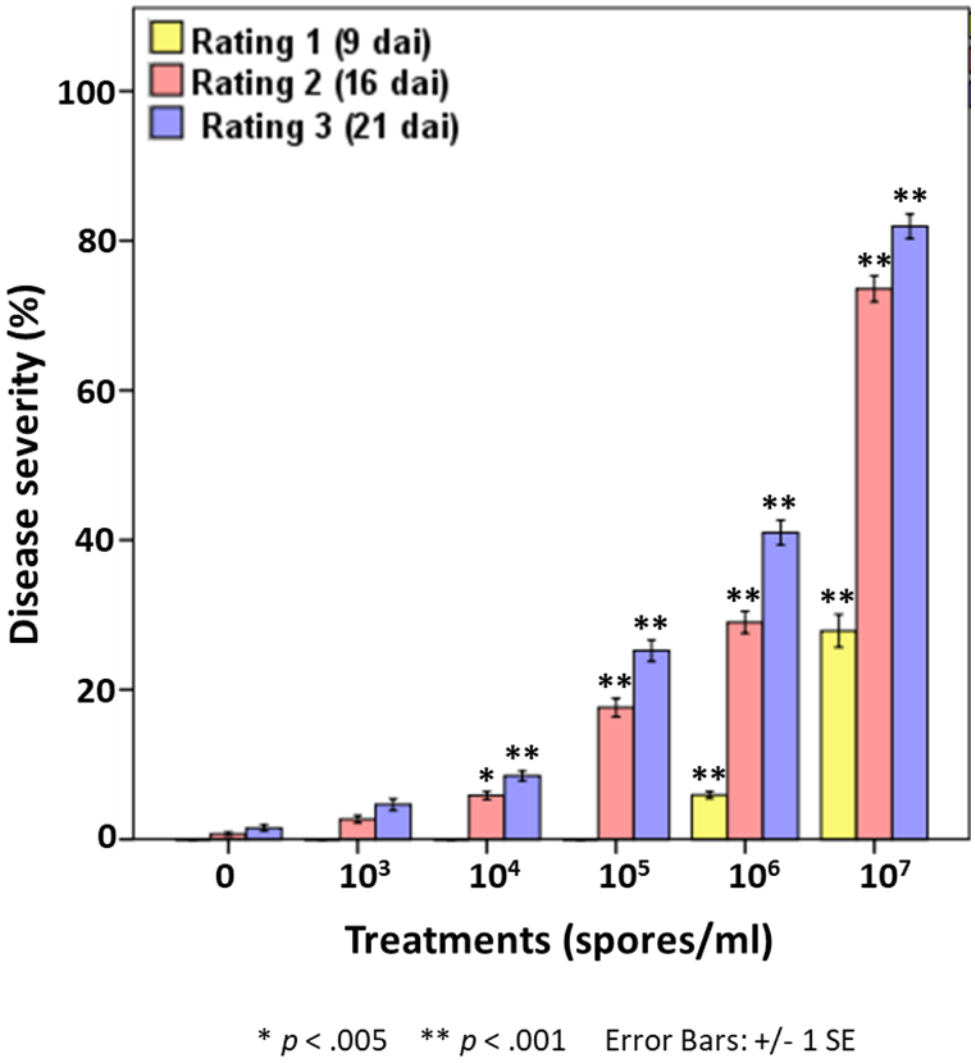

Figure 2.5 – Powdery mildew disease severity on Avocet wheat plants after inoculation with different spore concentrations under growth chamber conditions (trial one). Error bars represent +/- 1 standard error. * = probability that mean value is significantly different from the negative controls at $p < .005$. ** = probability that mean values are significantly different from the negative controls at $p < .001$.

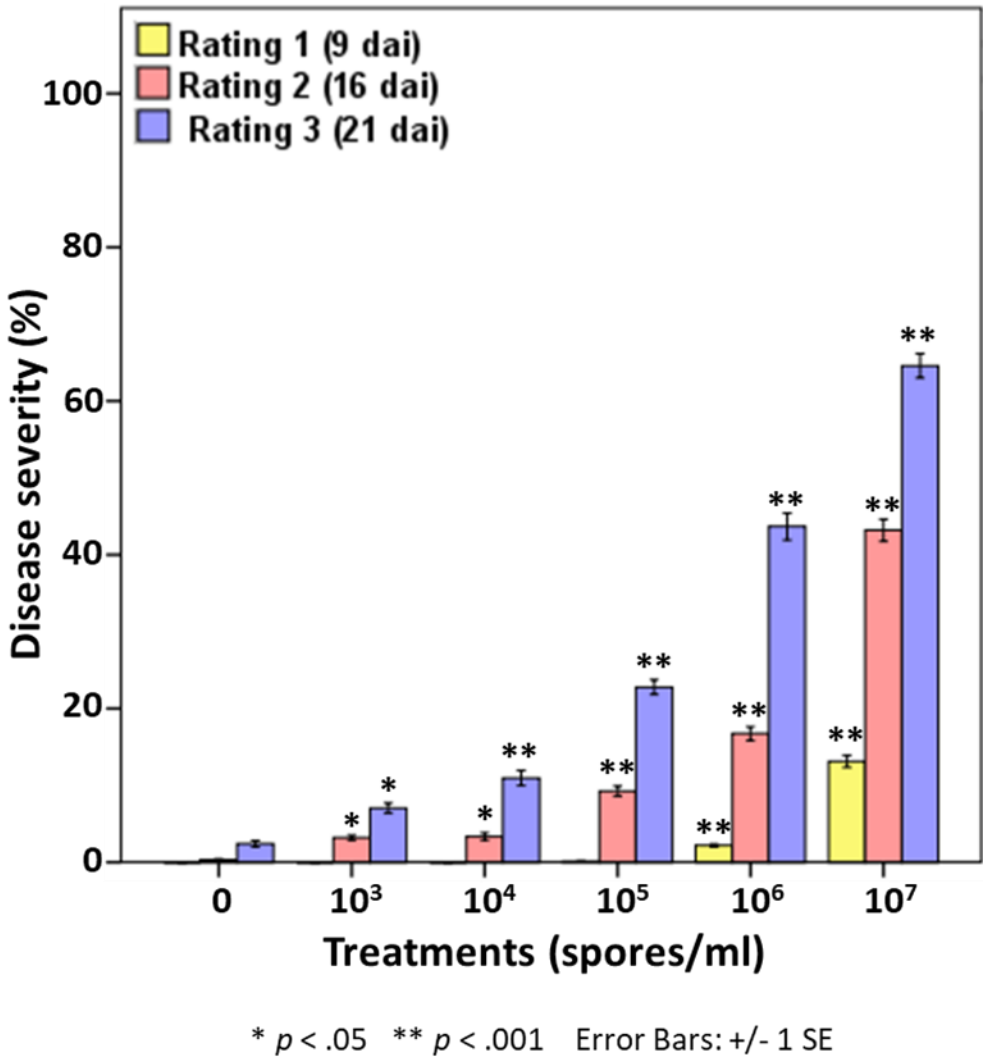

Figure 2.6 – Powdery mildew disease severity on Avocet wheat plants after inoculation with different spore concentrations under growth chamber conditions (trial two). Error bars represent +/- 1 standard error. * = probability that mean values are significantly different from the negative controls at $p < 0.05$. ** = probability that mean values are significantly different from the negative controls at $p < .001$.

2.4.3 Weather conditions during the field experiment

Weather conditions, including air temperature, relative humidity (RH) and dew point were recorded during the field trials in both 2016 and 2017 (Figures 2.7 and 2.8). Despite a wind speed of 40 to 50 km/h (temperature 12°-14°C, 54% RH) on June 24, 2016, we proceeded with inoculation of two of the three field trials because plants were approaching the end of the target development stages Z18/Z21 for inoculation. There was a storm about 2 hours after the inoculation (precipitation of 1.5 mm with strong winds) (AAF 2016 A). For the 3rd inoculation trial on June 30, 2016, weather conditions during inoculation consisted of temperatures of 15° - 16°C, 89% RH, and wind speeds of 10 to 20 km/h. There was a rainfall during the night after the inoculation (precipitation of 7 mm) (AAF 2016 A). Moisture conditions during the growing season were considered normal (approximately 40 mm of rain from June 24 to July 13, 2016) and the dew point formation generally exceeded the ambient temperatures during June following inoculation of the plots (Figure 2.7).

Conversely, growing conditions during 2017 were very dry (precipitation June 6 to July 20, 2017 was approximately 3.30 mm). In order to improve infection conditions in the field, the plots were irrigated with approximately 2 cm of water on July 6, 2017, the morning before inoculation. Weather conditions during inoculation consisted of temperatures of 26°-27°C, 40-60% RH, and wind speeds of 7 to 9 km/h. Weather monitoring showed that meteorological conditions following inoculation were generally favorable for the infection with dew point temperatures exceeding late night time temperatures six out of the fourteen days of experiment. Late night temperature average for the experiment period was 12°C (Figure 2.8).

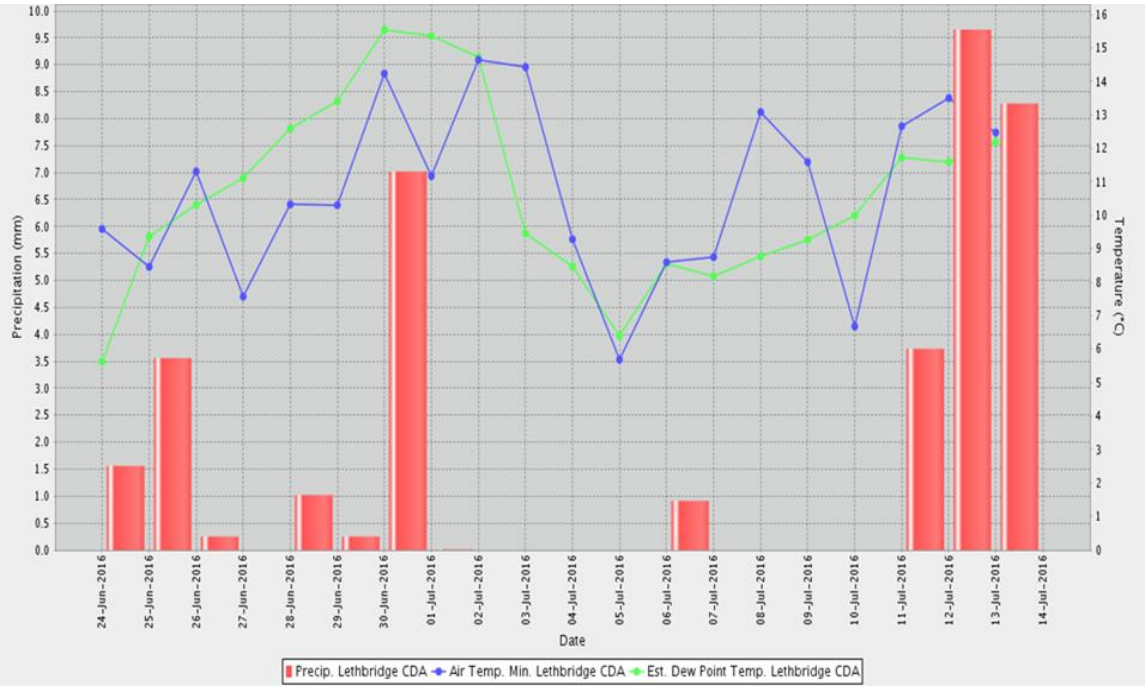

Figure 2.7 – Weather conditions from the day of inoculation until the end of the experiment (Jul. 13, 2016). Trial one and two were inoculated on Jun. 24, 2016 and trial three on Jun. 30, 2016 (AAF 2016 A).

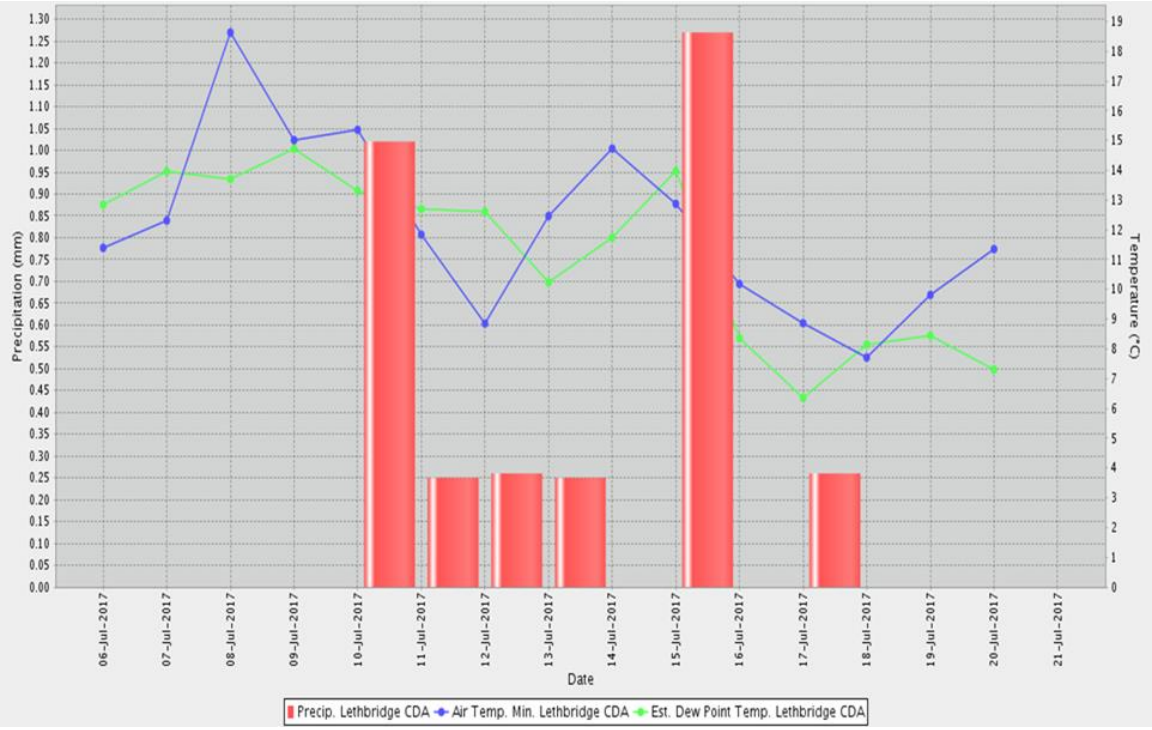

Figure 2.8 – Weather conditions from the day of inoculation until the end of the experiment (Jul. 20, 2017). Trial one and two were inoculated on Jul. 6, 2017 (AAF 2017 A).

2.4.4 Field experiment

2.4.4.1 Stripe rust disease incidence

Statistical analyses of the trials conducted in 2016 showed that the treatments with the highest percentage average of infected leaves for each trial plot were treatments 10^7 spores/ml. However, negative controls of the trial plot one had an average of infection of 68%, which was higher than the treatments 10^3, 10^4, 10^5, and 10^6 (Table 2.7). For the trials conducted in 2017, results showed that the treatments with the highest percentage average of infected leaves were treatments 10^7 spores/ml for both trial plots (Table 2.7). These results illustrate that the different dose-relationships between the host and pathogen are influenced by natural environmental conditions. In some occasions where environmental conditions were more favorable for disease development, it was possible to notice that higher concentrations of the pathogen inoculum resulted in higher disease incidence, which was similar to the results found using a controlled growth chamber.

2.4.4.2 Stripe rust infection type

For the field experiments the infected leaves were evaluated from the average of randomly selected 100 leaves for each treatment. Results of experiment conducted in 2016, showed that the most predominant infection type between the trials was light sporulation for all of them (Table 2.8). For trials conducted in 2017, showed that trace symptoms was the only infection type for all trials and treatments (data not shown). The results showed infection type is influenced no just by the inoculum concentrations, but principally by environmental conditions.

Table 2.7 – Stripe rust disease incidence under field conditions (2016 and 2017). Average results of six replicates per treatment.

Trials 2016	Treatments (%)					
	Control	**10^3 spores/ml**	**10^4 spores/ml**	**10^5 spores/ml**	**10^6 spores/ml**	**10^7 spores/ml**
One	68	54	48	58	65	73
Two	38	42	43	52	62	65
Three	16	13	48	59	80	88
Trials 2017	**Treatments (%)**					
	Control	**10^3 spores/ml**	**10^4 spores/ml**	**10^5 spores/ml**	**10^6 spores/ml**	**10^7 spores/ml**
One	12	56	63	64	71	78
Two	22	69	68	66	75	73

Table 2.8 – Stripe rust infection type under field conditions (2016).

Trials	Infection type	Treatments (%)					
		Control	**10^3 spores/ml**	**10^4 spores/ml**	**10^5 spores/ml**	**10^6 spores/ml**	**10^7 spores/ml**
One	No symptoms	0	0	0	0	0	0
	N/C - no sporulation	0	0	0	0	0	0
	Trace	16.7	0	16.7	0	0	0
	Light sporulation	33.3	33.3	66.6	83.3	33.4	50.0
	Intermediate sporulation	50.0	66.7	16.7	16.7	33.3	33.3
	Moderate sporulation	0	0	0	0	33.3	0
	Abundant sporulation	0	0	0	0	0	16.7
Two	No symptoms	0	0	0	0	0	0
	N/C - no sporulation	0	0	0	0	0	0
	Trace	0	33.3	33.3	33.3	16.7	33.3
	Light sporulation	100	50.0	66.7	66.7	16.7	66.7
	Intermediate sporulation	0	16.7	0	0	49.9	0
	Moderate sporulation	0	0	0	0	16.7	0
	Abundant sporulation	0	0	0	0	0	0
Three	No symptoms	0	0	0	0	0	0
	N/C - no sporulation	0	0	0	0	0	0
	Trace	66.7	16.7	50.0	83.3	0	0
	Light sporulation	33.3	83.3	50.0	16.7	100	0
	Intermediate sporulation	0	0	0	0	0	33.3
	Moderate sporulation	0	0	0	0	0	66.7
	Abundant sporulation	0	0	0	0	0	0

N/C: Necrotic and/or chlorotic flecks.

2.4.4.3 Stripe rust disease severity rating

For the 2016 growing season, substantial levels of infection ranging from 15-40 % were observed in the negative controls across the three trials, indicating that background stripe rust spore levels were high early in the growing season or that cross-contamination occurred during inoculation time (Figure 2.9 A-C). One-way ANOVA results showed no significant differences between treatments for trials one and two by ($F_{(5, 30)} = 1.411$, $p = .294$) and ($F_{(5, 30)} = 2.286$, $p = .071$), respectively. However, for trial three, significant differences were detected between some treatments ($F_{(5, 30)} = 23.664$, $p < .001$). The multiple comparisons Dunnett 2-sided post-hoc test revealed that the disease severity levels for the treatments 10^6 and 10^7 spores/ml for the trial three were higher than the negative controls ($p = .009$ and $p < .001$, respectively) and approached 70% in the highest spore concentration treatment (Figure 2.9 C).

For the 2017growing season, disease severity levels up to 20% were observed in the negative controls (Figures 2.10 A-B). Trials one and two presented significant differences between treatments according to the results of one-way ANOVA tests ($F_{(5, 29)} = 54.135$, $p < .001$) and ($F_{(5, 30)} = 53.274$, $p < .001$), respectively. Therefore, there was variability in disease severity ratings among spore concentration treatments in both trials, with severity levels reaching close to 80% in the highest spore concentration (Figure 2.10 A-B). The multiple comparisons Dunnett 2-sided post-hoc test revealed that the disease severity levels varied significantly for treatments 10^4 to 10^7 spores/ml for trial one and for treatments 10^3 to 10^7 spores/ml of trial two when compared with the negative controls ($p = $ or $< .001$) (Figure 2.10 A-B). These results illustrate that the different spore concentrations exerted influence on the disease severity results, showing in most of the

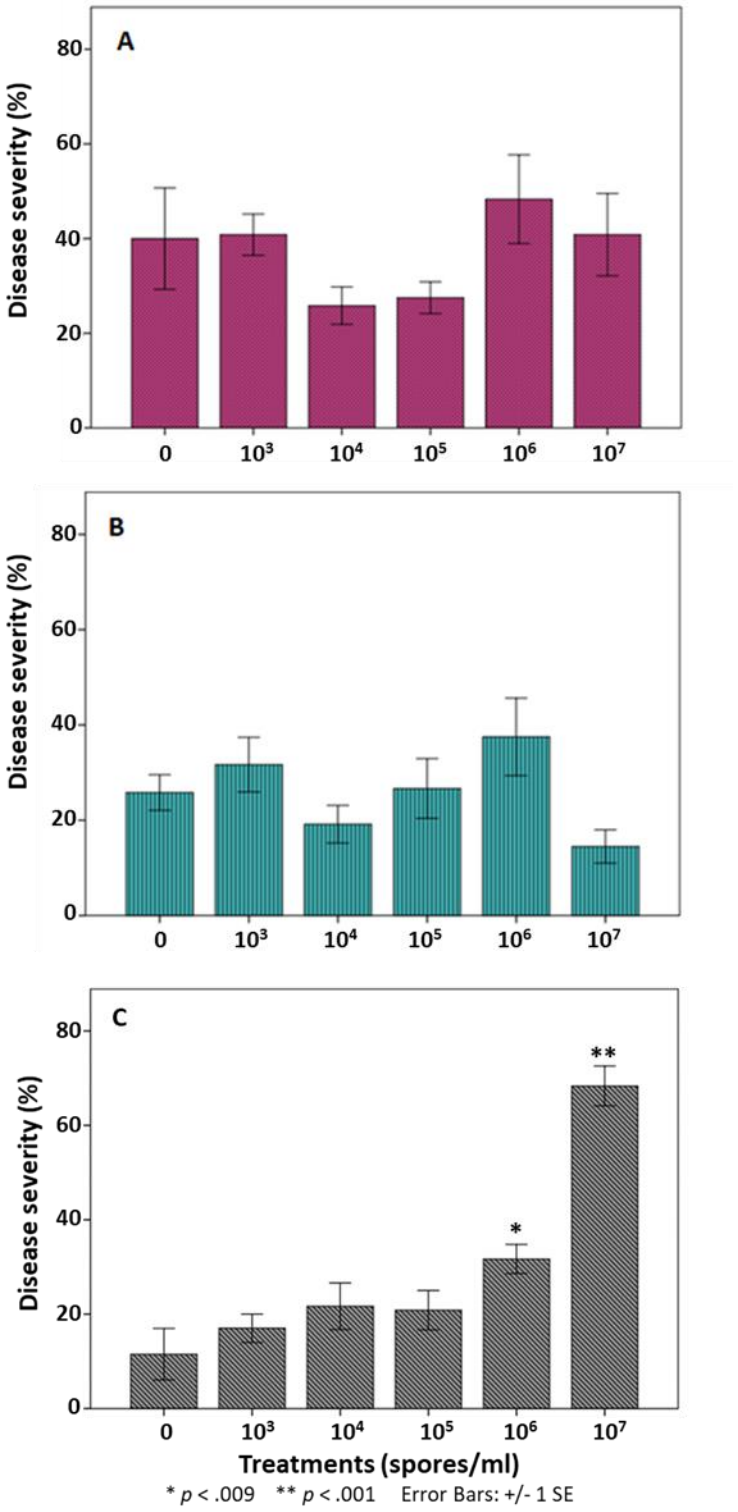

Figure 2.9 – Field experiment 2016: stripe rust disease severity rating (14 dai) under field conditions; trials one (A), two (B), and three (C).

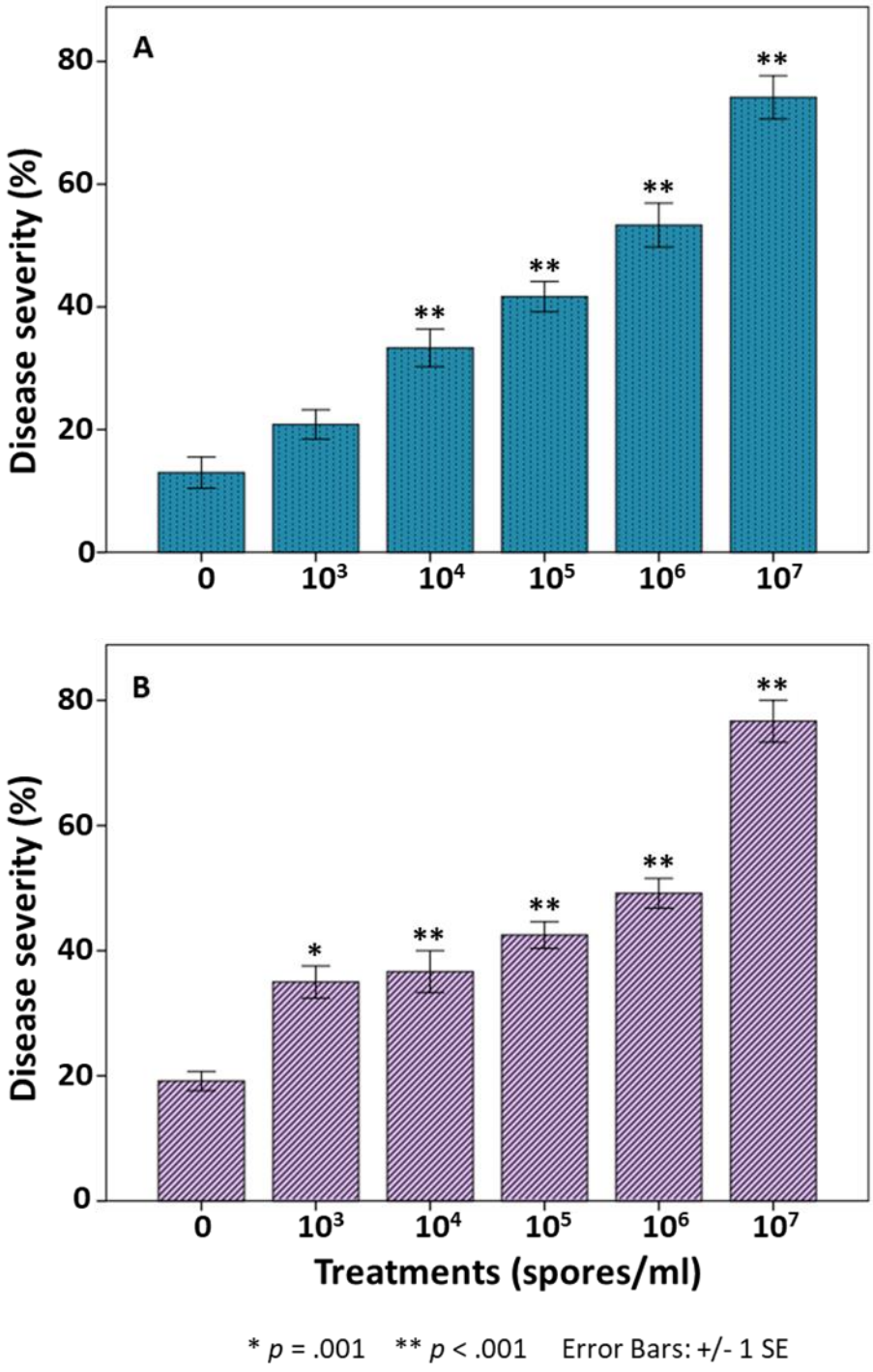

Figure 2.10 – Field experiment 2017: stripe rust disease severity rating (14 dai) under field conditions; trials one (A) and two (B).

trials (one in 2016 and two in 2017) that higher concentrations of spore cause higher disease severity under favorable conditions. However, it is also clear that the environmental conditions exert great influence on the disease severity when we look at the results of trials one and two of 2016 experiment.

2.5 Discussion and conclusions

The present experiments were conducted to test the hypothesis that there is a minimum threshold concentration of spores required for causing an infestation of stripe rust and powdery mildew in susceptible wheat under controlled environmental conditions and under field conditions in Southern Alberta for rust. This is an important question for which there was no answer in the literature up-to-now. To test this hypothesis susceptible wheat varieties were inoculated with five different concentrations (10^3, 10^4, 10^5, 10^6 and 10^7 spores/ml, and negative controls) of fungal pathogen spores; subsequently, the disease infection was rated according to the standard protocols. The first sign of stripe rust sporulation appeared 14 days after inoculation (Chen 2005) and 9 days after inoculation for powdery mildew (Orton & Brown 2016). No results were found in the literature to compare with our results as usually an excess of pathogen spores is used in artificial inoculation studies (Su et al. 2003; Chen et al. 2010; Orton & Brown 2016).

Under growth chamber conditions, *Pst* and *Bgt* disease rating results of both trials showed that the disease severity caused by both pathogens increased over time for treatments 10^5 to 10^7 spores/ml for *Pst*, and for all treatments of *Bgt*. The results also showed that the concentration of 10^5 spores/ml is the possible threshold concentration of spores for stripe rust disease infection. However, the most representative disease development time is approximately at 14 dai because after the first cycle of sporulation starts, under favorable conditions, each uredium produces thousands of spores every day (Roelfs et al. 1992; Chen 2005). Signs of *Bgt* infection were observed in all treatments a few days after rating one in both trials. However, before the cross-contamination or reinfection by a new cycle of spores started, it was possible to identify in rating one (9 dai) a threshold concentration of spores for disease infection at 10^6 spores/ml. The life

cycle for *Bgt* is shorter than that for *Pst*, taking only 5 to 10 days from infection to the start of sporulation (Orton & Brown 2016), meaning a more rapid buildup of the pathogen. Thus, this phenomenon could explain why cross-contamination and possible re-infection occurred so soon during the *Bgt* experiment. At the last rating day for *Pst* under controlled conditions (28 dai), more than 45% of the inoculated leaves of the treatment 10^5 were infected, while for treatments 10^6 and 10^7 spores/ml more than 90% of the inoculated leaves were infected. After 21 days, the percentage of *Bgt* infected plants varied for all the different treatments, directly increasing with the increase of inoculum concentration. The infection incidence and disease severity results for *Pst* and *Bgt* illustrate that the higher concentration of inoculum causes a higher incidence and disease severity, suggesting that these two factors are related to inoculum concentration when under controlled conditions. Based on the results the most representative time for *Bgt* rating was 9 days after inoculation, which is around the time when the first sporulation cycle starts.

Field experiment results from the 2016 growing season showed that the only significantly different treatments were 10^6 and 10^7 spores/ml of trial three when compared with negative controls. This could be explained by the prevailing weather conditions on the day of inoculation which were calm winds and high humidity, which were favorable for infection. For the other two trials, environmental conditions were worse as a storm with strong winds occurred about two hours directly following inoculation likely introducing natural inoculum into the study and/or shifting inoculated spores between the different treatments. Despite efforts to reduce cross-contamination by organizing the field plots with triticale barriers and orienting plots to reduce between-plot spread of pathogen spores, it was not possible to avoid cross-contamination. Even though the other two trials

were not significantly different when compared with the controls, the disease severity was moderate to high, resulting in significant visual damage to the plant leaves. Controlling cross-contamination between treatments caused by the inoculated spores or by natural inoculum are additional challenges in field experiments.

For the 2017 field experiments, results were similar between both trial plots, with treatments 10^4 to 10^7 spores/ml for trial one and 10^3 to 10^7 spores/ml for trial two presenting significantly higher disease severities when compared to controls. Although the temperature was higher and there was less precipitation in 2017, extensive disease levels resulting from inoculation with rust were observed. Disease severity was influenced by a dose-response relationship even with some level of cross-contamination and/or natural inoculum occurring. Disease development could be explained by irrigation at the day of inoculation and dew formation during the night, which increased the humidity in the field, making the conditions more favorable for spore germination. Elevated levels of humidity in the field for more than 3 hours promotes spore germination and infection (Rapilly 1979; Chen 2005). In 2017, from June 1st to July 31st, the maximum temperatures were higher and average humidity was lower than in 2016, which may have influenced sporulation amount. Additionally, in 2017, inoculated wheat plants in the field exhibited mostly yellow stripes and some chlorosis, but only traces of sporulation on wheat leaves whereas in 2016, there were yellow stripes with traces to intermediate sporulation on wheat leaves. This illustrates the fact that disease assessment under field conditions is challenging and that variations between different year trials are expected. Also, these results showed the importance of controls to be able to detect possible cross-contamination or natural inoculation. An optimum time for stripe rust rating in the field is when the first symptoms of sporulation starts, which usually happens

at 14 dai. However, under natural favorable conditions both host and pathogen tends to develop faster than under controlled conditions. This happens because growth chamber light has a limiting luminescence, while natural sun light is much brighter. Based on these facts, a good approach would be to check the plants for signs of infection between 10 to 14 dai.

Variances in temperature, humidity, and wind speed exerted different influences on disease development, resulting in differences between stripe rust ratings in the field and growth chamber. This illustrates the influence of the environmental factor of the Disease Triangle Concept in the present study, whereby the presence of a virulent pathogen and a susceptible host is not always synonymous of high levels of disease. It was visually possible to conclude that the best rating times for *Pst* and *Bgt* under controlled growth chamber conditions were 14 dai and 9 dai, respectively; while for stripe rust under field conditions was 14 dai, but possibly being 10 to 14 dai under favorable conditions for the pathogen development. Based on the most representative time for disease development, the threshold concentration of spores needed for *Pst* and *Bgt* to establish the disease was 10^6 spores/ml under controlled conditions; whereas, for *Pst* under field conditions was 10^6 spores/ml in 2016 (trial three); while in 2017, were 10^3 to 10^4 spores/ml depending on the different environmental conditions during and after the inoculation day.

Economic threshold has been used as a method of decision for fungicide application based on the crop value and fungicide costs (McGrath 2004). Fungicide applications can increase yield when applied properly. However, they are costly and can be harmful for the environment. Thus, they should not be applied in the absence of disease threat. Establishing the critical number of airborne spores required to cause

damaging levels of disease in the field is one of the best approaches to ensure that disease threat exists. (Hollomon 2002; McGrath 2004; Wightwick et al. 2012; David et al. 2016). This is an efficient threshold concept, which can also assist in development of disease monitoring systems. This study demonstrated that field studies to investigate inoculum threshold levels are difficult because it is impossible to exclude natural inoculum from experiential plots. However, in three of the five trials during two years of the study, a dose-response relationship was demonstrated between stripe rust and a susceptible wheat variety, where *Pst* inoculum threshold approached 10^6 spores/ml under controlled conditions, and 10^6 spores/ml in 2016 and 10^3 to 10^4 in 2017 under field conditions in Southern Alberta. These results will be important in future disease forecasting models for stripe rust because they demonstrate that hundreds or perhaps thousands of spores/ml in inoculation studies are required to produce damaging levels of disease. Alongside the inoculum concentration threshold information, frequent detection and quantification of pathogen inoculum in air currents are important tools for the development of a reliable disease forecast. DNA-based detection methods can be sensitive, detecting pathogen spores in spore trapping systems for diseases such as stripe rust and powdery mildew in low ranges of spores per week. Future disease forecast models will need to consider the high sensitivity of DNA-based technologies to ensure that expensive fungicides are not applied to control diseases in which inoculum thresholds have not been reached in the field.

CHAPTER THREE: DETECTION AND QUANTIFICATION OF WHEAT FUNGAL PATHOGEN SPORES

3.1 Introduction

3.1.1 Important fungal diseases of wheat in Western Canada

A variety of pathogens infect wheat crops worldwide, causing a wide range of symptoms and disease severities in the host. Successful interactions occur when pathogens are able to establish a parasitic relationship with the host. In Western Canada, some of the most important fungal diseases of wheat are stripe rust (*Puccinia striiformis f. sp. tritici* Westend. (*Pst*)), leaf rust (*Puccinia triticina f. sp. tritici* Erikss. (*Pt*)), stem rust (*Puccinia graminis f. sp. tritici* Pers. (*Pgt*)), powdery mildew (*Blumeria graminis* (DC.) Speer *f. sp. tritici* Em. Marchal (*Bgt*)), tan spot (*Pyrenophora tritici-repentis* (Died.) Drechs. (*Ptr*)), and Fusarium head blight (FHB) caused predominantly by *Fusarium graminearum* (Schwein) Petch. (*Fg*) (Regional Plant Disease Diagnostic Labs 2010; Fernandez et al. 2010, 2016; Marone et al. 2013; Tittlemier et al. 2013). Yield losses caused by these wheat pathogens can vary from mild to severe depending on pathogen virulence and aggressiveness, host susceptibility and prevailing environmental conditions. Under optimum conditions, the majority of these pathogens are capable of causing severe losses up to 50-100% (Waalwijk et al. 2004; Chen 2005; FAO 2010; Huerta-Espino et al. 2011; Abdullah et al. 2017; University of Saskatchewan 2018).

3.1.1.1 The rusts

The three rusts of wheat, *Pst*, *Pgt*, and *Pt*, can occur across Canada. In the main wheat production area in Western Canada, the impact of stripe rust is greatest in Western Prairies where cooler dryer environmental conditions prevail whereas for leaf and stem rust, their impact is greatest in Eastern Prairies where warmer and more humid conditions prevail during the growing season (Eversmeyer & Kramer 2000; Xi et al 2015; Aboukhaddour 2017). Rusts are obligate biotrophic basidiomycete fungi that are dispersed primarily by asexual urediniospores. Several cycles of urediniospores can be produced during a single growing season on susceptible wheat varieties leading to vast quantities of inoculum being produced. Urediniospores are wind dispersed and capable of moving long distances within and even between continents (Wegulo & Byamukama 2012; Chen et al. 2014).

The urediniospores morphologies between the three rusts are very similar; all are characterized by the presence of germ pores (3 to 13 on the surface), echnulation (spines - surface ornamentation), outside hyaline walls with thickness varying from 0.8 to 1.8 µm, with shapes varying from round to obovoid, and sizes varying from 26-30 µm x 18-32 µm (Hiratsuka & Sato, 1982; Savile 1984; Liu & Hambleton 2010; Baka & Rabei 2013). Spore colour varies among the rust fungi, from yellow to orange for stripe rust (infect leaves), reddish to brown for leaf rust (infect leaves), and brown to black for stem rust (infect stem and leaves) (Agrios 2005; Baka & Rabei 2013). Traditionally, stem and leaf rust have been more important pathogens but through extensive programs for breeding resistant varieties, these two rusts do not currently cause significant losses to wheat in Western Canada (Brar et al. 2017). Stripe rust is currently the most prevalent rust

affecting wheat production in Western Canadian Prairies (Fetch et al. 2011; Kumar et al. 2013; Brar et al. 2017).

3.1.1.2 Powdery mildew

Powdery mildew is an obligate biotrophic ascomycete fungus that can cause extensive losses in wheat crops worldwide. It is a host-specific pathogen that produces asexual conidiospores (or conidia) throughout the growing season. While conidia are the primary dispersal stage of the fungus (Agrios 2005; Wicker et al. 2013), the sexual ascospores, produced close to the end of the season in structures called cleistothecia, serve as overwintering structures (Huang & Röder 2004; Parks et al. 2011; Wicker et al. 2013). Conidia are hyaline to white in color, oblong shaped, and vary from 25-40 µm x 8-10 µm in size (Bayer 2018). They are formed in chains that stick up in the air, ready to be detached and infect new host tissues (Esmail & Draz 2017). Conidia and ascospores are dispersed by air currents (Parks et al. 2011). The predominant signs and symptoms are a fluffy white to brownish mass formed on leaves, stem, and heads of wheat plants early in the growing season followed by chlorosis and necrosis, and eventual senescence of infected tissues later in the growing season (Agrios 2005).

3.1.1.3 Tan spot

Leaf spotting pathogens of wheat are necrotrophic foliar fungi that infect wheat and other grasses (Strelkov & Lamari 2003). They are stubble-borne, where they overwinter; they produce lesions on wheat leaves that decrease photosynthetic capacity and can lead to yield and quality losses (Faris et al. 2013). Among the leaf spotting

complex pathogens (*P. tritici-repentis, Phaeosphaeria nodorum*, and *Mycosphaerella graminicola*), *Ptr* is the predominant species in Western Canada (Fernandez et al. 2010, 2016). The predominant tan spot symptoms on leaves are necrotic or chlorotic lesions, or a combination of necrotic lesion with a chlorotic halo (Faris et al. 2013; Moffat et al. 2014). Later in the season, the fungus produces pseudothecia (overwintering structures) appearing as black dots within the lesion (McMullen & Adhikari 2009). *Ptr* produces host-selective toxins (HSTs) that can be identified by the lesion phenotype produced. Ptr ToxA, Ptr ToxB, and Ptr ToxC are the three HSTs known to be caused by different *Ptr* races (Martinez et al. 2001). Eight races of *Ptr* have been identified and characterized by their virulence factors so far (Strelkov & Lamari 2003). *Pyrenophora tritici-repentis* and *Parastagonospora nodorum* (previously named *Stagnospora nodorum*, anamorph of *P. nodorum*) shared the same ToxA gene and both produces the active toxin Ptr ToxA (Friesen et al. 2006). Ptr ToxA is the predominant HST and it was found in 98% of the tested isolates in Alberta; it is produced by the races 1 and 2 (Aboukhaddour et al. 2013). Under favorable weather conditions of prolonged wet periods *Ptr* can cause yield and quality losses of wheat (McMullen & Adhikari 2009). Yield losses ranging from 3 to 50% have been reported in USA and Canada (Hosford et al. 1987; Sykes & Bernier 1991; Ciuffetti & Tuori 1999). The tan spot pathogen produces sexual spores (ascospores) within pseudothecia during the end of winter, spring and beginning of summer, and asexual spores (conidia) on conidiophores, during the summer growing season (Ciuffetti & Tuori 1999; McMullen & Adhikari 2009). Conidia are multinucleate and cylindrical in shape with four to seven septa, and vary in size from 117-217 µm x 15-18 µm. Ascospores are also multinucleate with three septa, oval to globose shape, brown in color, and size varies from 48-58 µm x 18-24 µm (Ciuffetti & Tuori 1999; Benslimane 2014;

Benslimane et al. 2017). Both spore types are considered to be the primary inoculum of new infections (Ciuffetti & Tuori 1999).

3.1.1.4 Fusarium head blight

Fusarium head blight is one of the most important fungal diseases that can affect both yield and quality of wheat crops. FHB can be caused by many different facultative saprophytic species, but in Western Canada it is predominantly caused by *Fusarium graminearum* (Gräfenhan et al. 2013). *Fusarium* diseases can cause yield losses of 30 to 70% and further quality losses due to contamination of grains with toxins (Waalwijk et al. 2004; Harris et al. 2015). FHB produces a range of mycotoxins on wheat grains which make them unsuitable for consumption because these mycotoxins can be harmful to both humans and animals (Gautam & Dill-Macky 2012). Very low levels ($\leq$ 2 ppm) of the principal mycotoxin, deoxynivalenol (DON), are tolerated in grains to be sold (Fernando et al. 2000; van Egmond et al. 2007; Gautam & Dill-Macky 2012). Higher FHB severity and DON accumulation is correlated with high temperatures and humidity (rainfall, relatively air humidity, or long periods of moisture exposure) during or just after anthesis growth stage (Fernando et al. 2000; Kikot et al. 2011; Gautam & Dill-Macky 2012). *F. graminearum* overwinters on infected plant debris and generates ascospores (sexual stage) and conidia (asexual stage) during the warm and humid weather of spring. Both types of spores may serve as the primary inoculum, and are spread by rain, insects, and wind (Goswami & Kistler 2004). *F. graminearum* produces macroconidia which are translucent canoe or banana-shaped with five or more septa and a distinctly foot-shaped basal cell, and vary in size from 25-50 µm x 3-4 µm (Schmale & Bergstrom 2003; Leslie

& Summerell 2006; Keller et al. 2014). It is very challenging to distinguish the *Fusarium* macroconidia at species level because of their morphological similarities (Leslie & Summerell 2006). *F. graminearum* is considered homothallic, producing both the male and female reproductive structures on the same thallus (Schmale & Bergstrom 2003). Ascospores range from translucent to light brown in colour, and slightly curved with rounded ends, and vary in size from 19-24 µm x 3-4 µm (Schmale & Bergstrom 2003; Keller et al. 2014).

3.1.2 Crop disease monitoring

It would be important to employ disease forecasting systems, if available, to predict potential wheat diseases for helping producers to make better informed decisions to control diseases using fungicides or other control measures. The Disease Triangle Concept states that a susceptible host, virulent pathogen and appropriate environmental conditions are required for disease development (Scholthof 2007). Sufficient quantities of pathogen propagules are essential for establishing if damaging levels of disease will develop in fields. Disease forecasting systems increasingly rely on establishing the local levels of pathogen propagules, such as spores, in crop areas (Cao et al. 2016). Spore trapping methods are frequently used for monitoring and quantifying air-borne inocula of fungal plant pathogens (Cao et al. 2016). There are many different types of spore trapping methods, including air-sampling instruments, wax-coated film, and double-sided adhesive tape. These methods are essential tools for spore monitoring, understanding disease development, and forecasting crop disease development (Alcázar et al. 2003; Cao et al. 2016).

Studies to compare the adhesive efficiency of different types of tapes have concluded that there are small differences between the different tape types (Comtois & Mandrioli 1997; Alcázar & Comtois 1999; Alcázar et al. 2003). According to Alcázar & Comtois (1999), the acrylic double-sided adhesive tape 3M Scotch Brand (#9425) had slightly higher capturing efficiency than glycerine/gelatine coating.

Of the several commercial spore trapping instruments available, the Burkard 7-days sampler has been shown to be a reliable instrument for sampling airborne spores for DNA-based analyses (Cao et al. 2016; Núñez et al. 2017).

3.1.3 Molecular biology detection of fungal spores

Rapid and reliable methods for identification and quantification of airborne fungal pathogens make disease monitoring and management practical because they permit achievement of real-time detection for plant diseases. This aspect is critical if treatments such as fungicides are to be effective in mitigating the harmful impact of plant diseases. Molecular techniques have been shown to be rapid, sensitive, highly accurate, and cost effective and are the current focus of strategies to forecast diseases and protect crops (Khan et al. 2005; Friesen et al. 2006; Tsui et al. 2011; Randhawa et al. 2013; Cao et al. 2016). These techniques frequently employ methods such as real-time PCR (qPCR) assay, DNA sequencing, and multiplex PCR assay. There is a great variety of methods for extraction of nucleic acid, which have different applications depending on the type of experiment. Testing different methods, sometimes even adapting them for specific sample types, is important for adequate cell disruption and efficient DNA extraction (Tsui et al.

2011). In addition to representative DNA samples, the design of highly pathogen-specific primers and/or probes, and the optimization of methods and materials, are essential for the use of these molecular methods (Reischer et al. 2004; Nicolaisen et al. 2009; Cao et al. 2016). Pathogen-specific primers for PCR-based assays are often developed to target pathogen DNA regions such as ITS region, who's variability is limited and often not specific enough to identify all species. Therefore, the design of more specific assays targeting unique genes, such as toxins, has been recommended (Nicolaisen et al. 2009).

3.2 Objectives and hypothesis

3.2.1 Objectives

The overall aim of this project is to develop a methodology for efficient detection and quantification of airborne wheat fungal spores (*Pst*, *Pt*, *Pgt*, *Bgt*, *Ptr*, and *Fg*) in Western Canada. This project represents the initial step toward the development of a forecasting network which will provide the necessary information to producers about potential disease epidemics. The overall aim was addressed by completing the following objectives:

A) To design/adapt highly pathogen-specific PCR primers within a qPCR assay and assess their efficiency for detection and quantification of *Pst*, *Pt*, *Pgt*, *Bgt*, *Ptr*, and *Fg*.

B) To test double-sided adhesive tape on a microscope slide as a spore trapping system and to assess its efficiency by identifying and quantifying asexual spores of *Pst*, *Pt*, *Pgt*, *Bgt*, *Ptr*, and *Fg*.

C) To determine the incidence of airborne *Pst*, *Pt*, *Pgt*, *Bgt*, *Ptr*, and *Fg* fungal spores in air samples from wheat fields in Southern Alberta by using qPCR and microscopy analyses.

3.2.2 Hypothesis

It is possible to efficiently identify and determine the incidence of airborne spores of important wheat pathogens sampled at specific locations of Southern Alberta, during the growing season.

3.3 Materials and methods

3.3.1 Spore trapping

3.3.1.1 Burkard Cyclone instrument

The spores were collected with Burkard Automatic Cyclone Air Sampler (Burkard Manufacturing Co. Ltd., Rickmansworth, Hertfordshire, UK), which actively sample particles in air at a rate of 16.5 litres/min. The upper part (or cap) of the instrument supports a wind-vane, which orients the vertical orifice (9 x 3 mm) of the instrument to constantly face the prevailing wind. The instrument collects all particles present in air. Two models, the Burkard Cyclone One-vial and Burkard Cyclone Multi-vials were used. The one-vial model samples constantly into just one tube until the tube is manually changed, whereas the multi-vials model is integrated with timer and movement controls of the carousel that switches the sampling tubes every day (capacity for 8 tubes). This model automatically turns off after all tubes have been used (7 to 8 days depending on the sampling timer set up), so the tubes need to be changed and the instrument restarted. The sampled particulates were collected in an specific 1.5 ml microfuge tube (Burkard Manufacturing Co. Ltd., Rickmansworth, Hertfordshire, UK). The instruments were placed in or near wheat fields at a number of locations in Southern Alberta (Table 3.1). Instruments were set up on top of a pallet platform, and connected to a battery and solar panel (Appendix 5). During the 2015, 2016, and 2017 growing seasons, samples were mostly collected weekly. Collaborators were responsible for changing the tubes once a week and mailing the tube(s) to us. However, in some occasions, some collaborators were not able to do weekly tube changes, so a few samples were collected for more than seven days in the same tube. The air samples were stored in a -80°C freezer until DNA

Table 3.1 – Sampling sites in Southern Alberta where the Burkard Cyclone instruments were installed during the wheat growing seasons 2015, 2016, and 2017.

Growing season	Location	Coordinates
2015 **2016** **2017**	Weather Station - Lethbridge Research and Development Centre (LeRDC), Lethbridge, AB	N 49° 41.685' W 112° 46.080'
2015	Field Pathology Building - LeRDC, Lethbridge, AB	N 49° 42.067' W 112° 44.449'
2016	Crop Diversification Centre South, Brooks, AB	N 50° 32.612' W 111° 50.609'
2016	Penniket Acreage, Granum, AB	N 49° 52.490' W 113° 22.219'
2016 **2017**	Stanford Farm, Magrath, AB	N 49° 23.556' W 112° 56.510'
2016 **2017**	Stamp Seeds Farm, Enchant, AB	N 50° 10.047' W 112° 26.030'
2017	Welsh Farm, Milk River, AB	N 49° 6.423' W 111° 55.137'
2017	Fairfield – LeRDC, Lethbridge, AB	N 49° 42.493' W 112° 41.738'

extraction was conducted. Samples were dried using a Savant SpeedVac® SC110 Concentrator before being stored at -80°C.

3.3.1.2 Adhesive tape

A second method, referred to as the passive method of spore trapping, was employed around the Lethbridge Research and Development Centre field areas. Double-sided adhesive tape (3M Scotch® Removable Poster Tape, 3/4" (19 mm) wide, clear) was applied to an area of 19 mm X 50 mm of a microscope slide (25 mm X 75 mm) (Appendix 6 A). Slides were attached on the cap of the Burkard Cyclone instrument, just below the collection orifice. Thus, the slide was always facing the prevailing wind. The slides were stored in a microscope slide box at room temperature for few days until analysed using a light microscope.

3.3.2 Microscopic analyses

The slides with the adhesive tape were observed, directly without any staining, using brightfield microscopy (Leica Microsystems DM6000 B) and pictures were taken with the attached camera (Leica Microsystems DFC310 FX). Six different fungal spores were identified based on their morphology (shape, size, and color) (Appendix 7) and quantified using a grid slide underneath (with a defined area of 40 quadrants of 5 mm x 5 mm in size, covering a total area of 20 mm x 50 mm) to facilitate the orientation on the slide while counting the spores (Appendix 6 B).

Identification of fungal spores by morphology requires knowledge of taxonomy and training because there are many similar features between spores of different fungi species. For approximately two months prior to the study, I was self-trained to identify

the asexual spores stage of all six fungi by analysing known fungi spores in isolation or mixed with other fungi spores and soil. Occasionally, I consulted experts about certain pathogens identification. Only the asexual spores stage was employed in the training because they are the repeating spore stage during growth season; in many cases, they can travel long distances by wind, and thus are the most important in the epidemiology of the individual plant diseases. In most cases, the asexual spores are considered as the primary inoculum. The morphologies of rust uredineospores are very similar; practically, it was not possible to distinguish them. For this reason, rust spores were grouped as "rust spores" and not identified to species level. Also, *Fg* macroconidia are very similar to other *Fusarium* species, so they were identified as "*Fusarium spp. (F.spp)*".

3.3.3 DNA extraction

The DNA extraction protocol was optimized by performing several trials using pure spore preparations from the six pathogens studied and four different protocols; Alkaline polyethylene glycol (PEG)-based (Chomczynski & Rymaszewski 2006), OmniPrep kit (Biosciences), NaOH solution (Werner et al. 2002, modifications made), and PowerSoil kit (QIAGEN). The six different fungal spores used for the extraction protocol optimization were: i) collected from wheat plants at the greenhouse (*Pst* and *Bgt*), ii) cultivated in agar media in the lab (*Ptr*), or iii) provided by other labs (*Pt*, *Pgt*, and *Fg*). *Ptr* initial cultures were provided by Dr. Reem Aboukhaddour from Dr. Stephen Strelkov's lab at University of Alberta, *Pt* and *Pgt* spores were provided by Dr. Harpinder Randhawa's lab at Lethbridge Research and Development Centre (LeRDC), and *Fg* spores were provided by Dr. Nora Foroud's lab at LeRDC. Following DNA extraction, samples were kept in a -20°C freezer until analysed.

3.3.4 Optimization of pathogen-specific primers

Several sets of pathogen-specific primers were selected from the literature and were tested using standard PCR with the QIAGEN HotStar Taq Master Mix kit and protocol (2.5 µl DNA template added). Cycle conditions were: 1 cycle at 94 °C for 15 min, 35 cycles at 94°C for 1 min, 55° to 65°C for 1 min and 72°C for 1 min; followed by a final extension period at 72°C for 10 min after the last cycle. After six pairs of PCR primer pairs were selected (Table 3.2), one pair for each pathogen; they were adapted and/or optimized. They were further evaluated using different qPCR assay approaches for quantitative determination of the pathogens (*Pst*, *Pt*, *Pgt*, *Bgt*, *Ptr*, and *Fg*).

3.3.5 Molecular analyses methods

Different qPCR approaches (singleplex, duplex, and multiplex) and digital droplet PCR (ddPCR) method were tested to detect and quantify the six important wheat pathogens. The materials used for these tests were PerfeCTa® SYBR® Green SuperMix Low Rox (QantaBio) for singleplex and duplex qPCR; and Prime Time® Gene Expression Master Mix - probe-based (IDT) (TaqMan) for multiplex qPCR. QX200™ ddPCR™ EvaGreen Supermix was used for ddPCR. All methods were tested with clean DNA samples from the six pathogens. One probe was designed for each primer set.
Samples collected by the Burkard Cyclone instruments were analysed by qPCR assay using the PerfeCTa® SYBR® Green kit and protocol (2.5 µl DNA template added) for identification and quantification of the pathogens in the air samples. The qPCR instrument used to analyse the samples was an Applied Biosystems™ QuantStudio™ 6

Table 3.2 – Primer sets selected for standard PCR and qPCR assays to identify the six wheat pathogens.

Primer pairs	Targets	Sequences (5'-3')	Size (bp)	Tm (°C)	GeneBank	References
PSBTQ	*Pst*	**F:** CAATCACCGTCC CAGAGTTGACATC **R:** ACGGACAGCAT GTTCTCTTCGACT Beta tubulin gene	151	74	HM067995	Liu et al. 2015
Pg2BTQ	*Pgt*	**F:** AAGAGAACATG CTGTCCGTT **R:** TTTGGAACTACA AGGGTATCAAG Beta tubulin; mRNA	146	61	HQ317591	Liu et al. 2015
EF1-Pt2-032 **EF1-Pt1-113** **EF1-Pt1-113***	*Pt*	**F:** TCGTCATTGGAC ACGTCGATTCGT **R:** ATCCTCACAGCG GTAAATCCACCA **R:** TGGTGGATTTAC CGCAGTGAGGAT Elongation factor 1-alfa	504 104	72 72	JX533507.1 JX533507.1	Liu et al. 2013 This thesis
Bgt-6	*Bgt*	**F:** CGAGGGTTGGA ACTGGATAA **R:** TTCTCTGTTTGA CGCTCTCG Bgt-6 microsatellite sequence	157	60	HQ631368	Parks et al. 2011
Tox A1 **Tox A2**	*Ptr*	**F:** GTCATGCGTTCT ATCCTC **R:** CCTATAGCACCA GGTCGTCC ToxA-like gene	294	59	HM234155.1	GeneBank
Fgram379 **Fgram411** **Fgram411***	*Fg*	**F:** CCATTCCCTGG GCGCT **R:** CCTATTGACAGG TGGTTAGTGACTGG **R:** CAGGTGGTTAG TGACTGG Elongation factor 1-alfa	95 90	55 56	KX702800.1 KX702800.1	Nicolaisen et al. 2009 This thesis

*****: Modifications made on the original sequence.

Flex Real-Time PCR System. Cycle conditions were: 1 cycle at 95 °C for 3 min, 40 cycles at 94°C for 15 s, 55°C for 30 s, and 72°C for 30 s, with melting curve formation at the end of run. Preliminary analyses of the results (standard curve, Ct values, melt curve, and other parameters) were conducted using the software QuantStudio™ Software V1.3.

Standard curves to determine the quantity of DNA amplified, using qPCR, were done by using known spore numbers for each different fungal pathogen. These results were used to evaluate the method consistency, and also, to calculate how many spores are needed to amount 1 ng of DNA for each different pathogen. The qPCR results of the air samples (in ng of DNA) were then translated into spore numbers.

3.3.6 Statistical analyses

All statistical analyses were performed using SPSS Statistics (IBM Analytics, release 23.0.0.0). Descriptive statistics analyses were conducted on the data. Simple Linear Regression (SLR) was used to analyse the results of air samples. Pearson correlation test was used to evaluate the relationship between spores counted under the microscope and spores' quantity detected by qPCR assays. A data clean-up removing zeros (no spores detected) and logarithm base 10 transformations (log10) of spore numbers were used to correct for skewed data (McDonald 2014).

3.4 Results

3.4.1 Adhesive tape trap

The number of spores collected during a 1-week interval at the Weather Station location were counted during the 2015, 2016, and 2017 growing seasons (Figure 3.1), whereas for Field Pathology Building and Fairfield locations, number of spores were evaluated only in 2015 and 2017 growing seasons, respectively (Figures 3.2 A and B). During 2015, the peaks of spore numbers were observed at both Weather Station and Field Pathology Building locations later in July (Figures 3.1 and 3.2 A), whereas, during 2016, highest spore numbers were observed during early August for Weather Station location. During the dry summer of 2017, peaks of spore numbers were observed in late June for Weather Station and early August for Fairfield location. During the 3-year monitoring study at the Lethbridge locations, the highest spore numbers counted for each species were 429 for rust and 106 for *Bgt* at the Fairfield site in 2017, 9 for *Ptr* at the Weather Station location in 2016, and 2 for *F.spp* at the Weather Station and Field Pathology Building sites in 2015. It is important to highlight that every year Fairfield wheat fields are artificially inoculated with *Pst* for research experiment purposes, so this can explain the differences in spore numbers encountered between Weather Station and Fairfield in 2017. The results show that great variation in spore numbers occurs during and between the growing seasons, and among the different locations. The variations occurred, possibly, due to weather conditions, new inocula carried on prevailing winds, and/or physical differences in each location (e.g.; if it is an open area or surrounded by wheat crops). Also, results showed that among the pathogens examined, rusts had the highest incidence of asexual spores.

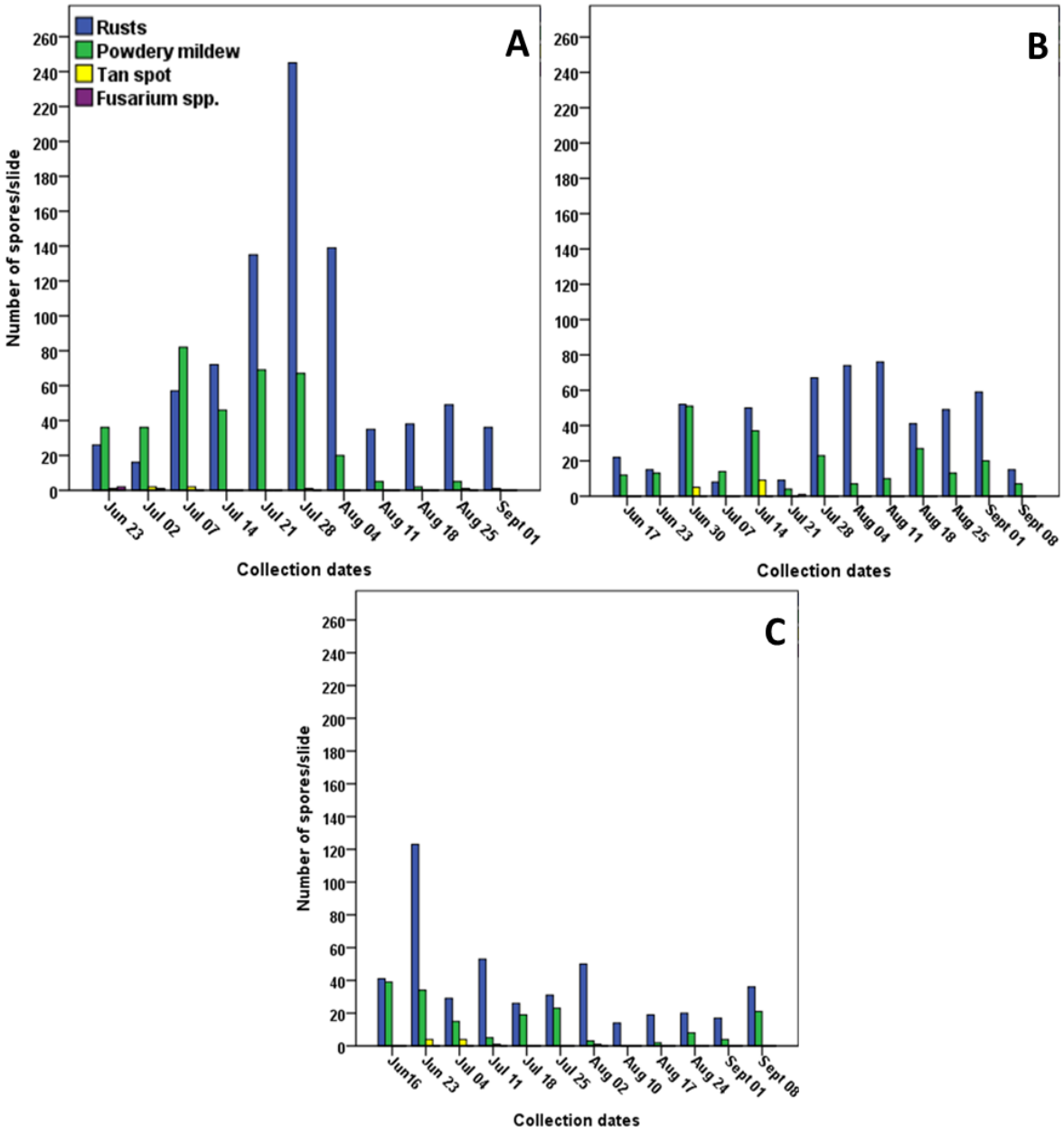

Figure 3.1 – Weekly number of fungal spores collected with adhesive tape traps and counted using brightfield microscopy. Samples were collected at the Weather Station – Lethbridge, during the wheat growing seasons 2015 (A), 2016 (B), and 2017 (C). The collection dates mark the beginning of the sampling week.

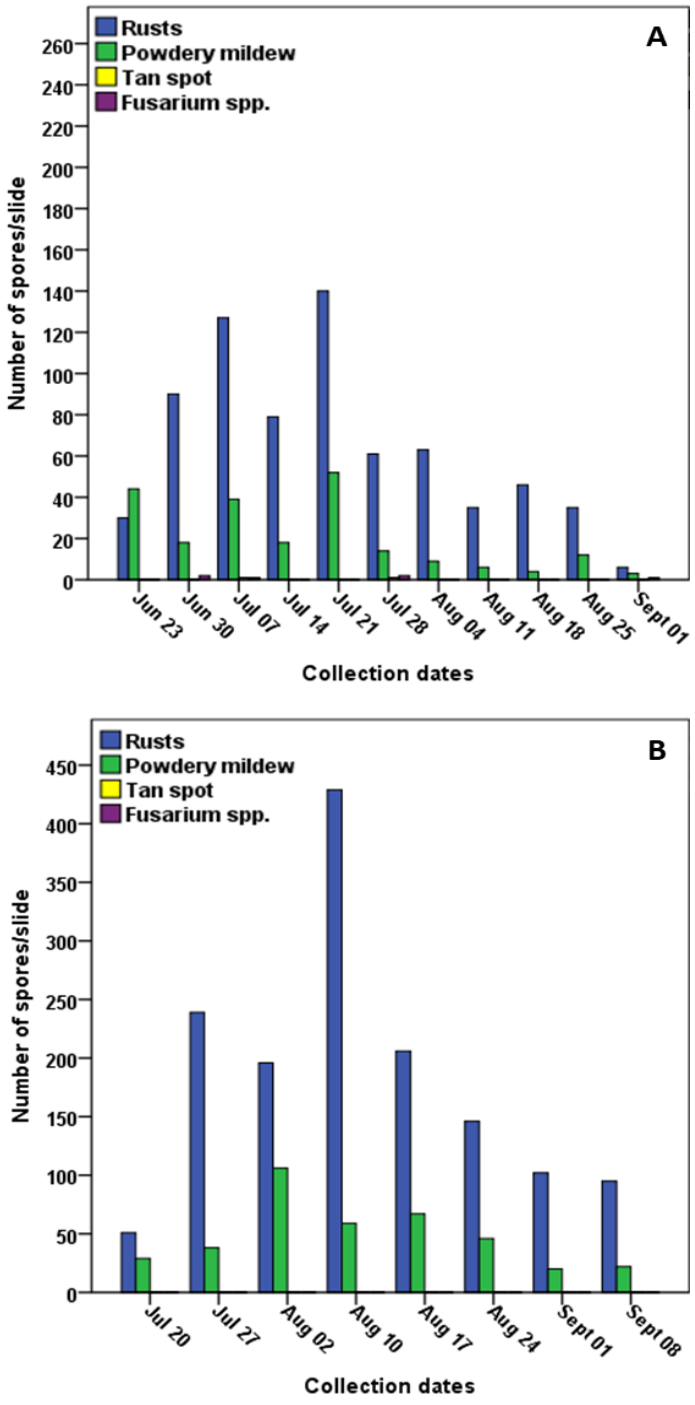

Figure 3.2 – Weekly number of fungal spores collected with adhesive tape trap and counted using a brightfield microscopy. Samples were collected at the Field Pathology Building site in Lethbridge, during the 2015 growing season (A) and at the Fairfield site in Lethbridge, during the 2017 growing season (B). The collection dates mark the beginning of the sampling week.

3.4.2 DNA extraction methods

NaOH solution and Alkaline PEG protocols used only alkaline chemical reactions to break cells and isolate DNA, while OmniPrep and PowerSoil protocols included chemical and mechanical reactions. Based on PCR results, the most effective DNA extraction protocols tested was the DNeasy PowerSoil kit (QIAGEN) because it yielded better DNA quality and consistent technical replicates results. Minor adaptations made to the QIAGEN original protocol consisted of the following: air sample tubes were washed (4x) with the beads buffer and C1 solution, and spores were ground at room temperature using a PRECELLYS® 24 (Bertin Instruments) (program 5000 - 2 x 30 s grinding with a 10 s pause between the two periods); following the extraction process, DNA was eluted in 60 µl of C6 solution to increase DNA concentrations.

3.4.3 Optimization of primers and PCR methods

The most consistent six primers out of thirty-two pairs tested (Appendix 8), one pair for each pathogen target, were optimized. All primers were first tested on a temperature gradient (55 to 65°C) on a standard PCR test to identify the temperature range of detection. The optimum annealing temperatures represented by the brightest bands were 55 to 60°C, 53 to 55°C, 53 to 59°C, 55 to 57°C, 53 to 57°C, and 53 to 57°C for for *Pst*, *Pgt*, *Pt*, *Bgt*, *Ptr*, and *Fg* primer pairs, respectively. A minimum of two replicates for each primer set including three technical reps for each sample was conducted. Several tests were conducted using standard PCR before advancing to qPCR tests (data not shown). In order to test these primer pairs on a multiplex qPCR assay, an annealing temperature common to all six primer pairs was selected on the combined results of the standard PCR tests. The chosen temperature was 55°C. Before starting

multiplex qPCR tests, each primer pair was singly tested by qPCR assays using 10-fold serial dilutions of a known amount of DNA. Results showed that the limit of detection for primer pairs ranged from 0.0001 to 0.001 ng of DNA for *Pst*, *Pgt*, *Pt*, *Bgt*, and *Fg*, and 0.001 ng for *Ptr* (Table 3.3). Following a minimum of five independent multiplex qPCR tests conducted using TaqMan and SYBR Green, it was clear that there were interactions between primer sets because different problems occurred (e.g.: amplification failure for pure DNA samples; amplification of additional products resulting in more melting curves than expected; or bright primer dimerization). Duplex qPCR was tested with all possible combinations of these primers sets; even then, some of the problems cited above persisted. Designing new primer sets and probes to keep up with multiplex qPCR tests was not an option because it is costly and time consuming to design and test all possible sets. Using ddPCR as an alternative procedure, showed no significant improvements over qPCR. Based on overall testing, qPCR (singleplex) was the chosen method to analyse the air samples and employed the 55°C annealing temperature for all six primer sets because strong and consistent amplifications were obtained. Additionally, all six primer sets could be used on the same qPCR plate/run.

3.4.4 Air sample analyses

Preliminary qPCR results showed great differences in spore numbers among the eight different locations and three growing seasons (Figures 3.3 to 3.8). Differences were mainly observed for the locations that were sampled during consecutive years. These differences in spore numbers might be related to weather conditions (rainfall and temperature) and/or inoculum abundance. Total rainfall and average of maximum temperature from June to August for Weather Station location were 60 mm and 27°C in

Table 3.3 – Limit of DNA detection of PCR primers on qPCR assay.

Primer set (F/R)	Target	Detection level (ng)	Detection level (No. of spores)
PSBTQ	*Pst*	0.0002	1
Pg2BTQ	*Pgt*	0.0001	1
EF1-Pt2-032 **EF1-Pt1-113 (al.)**	*Pt*	0.0002	1
Bgt6	*Bgt*	0.0002	1
ToxA1 **ToxA2**	*Ptr*	0.001	3
Fgram379 **Fgram411 (al.)**	*Fg*	0.0002	35

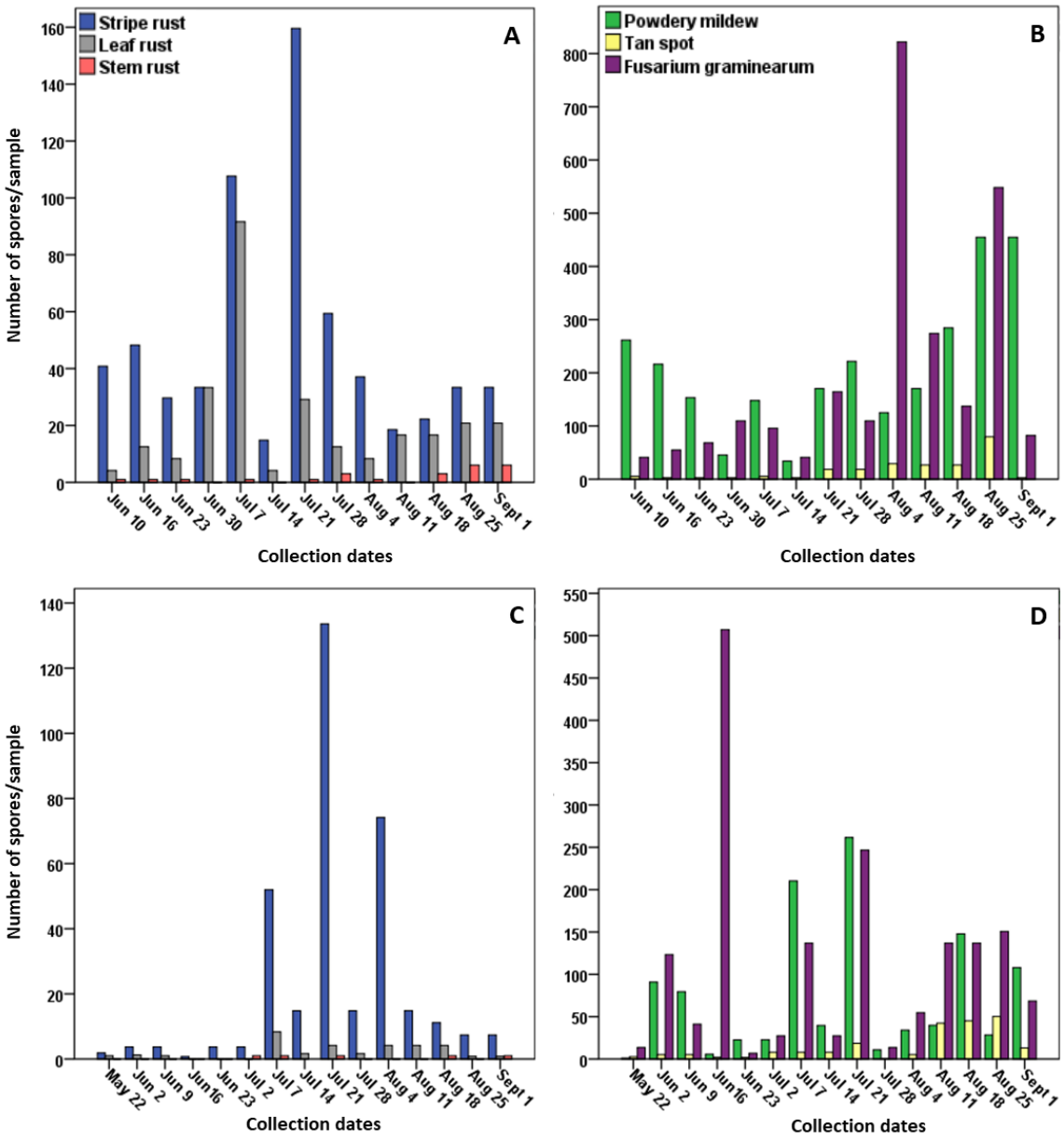

Figure 3.3 – Number of spores detected in air samples collected in 2015 at LeRDC Field Pathology Building (A-B) and Weather Station sites (C-D).

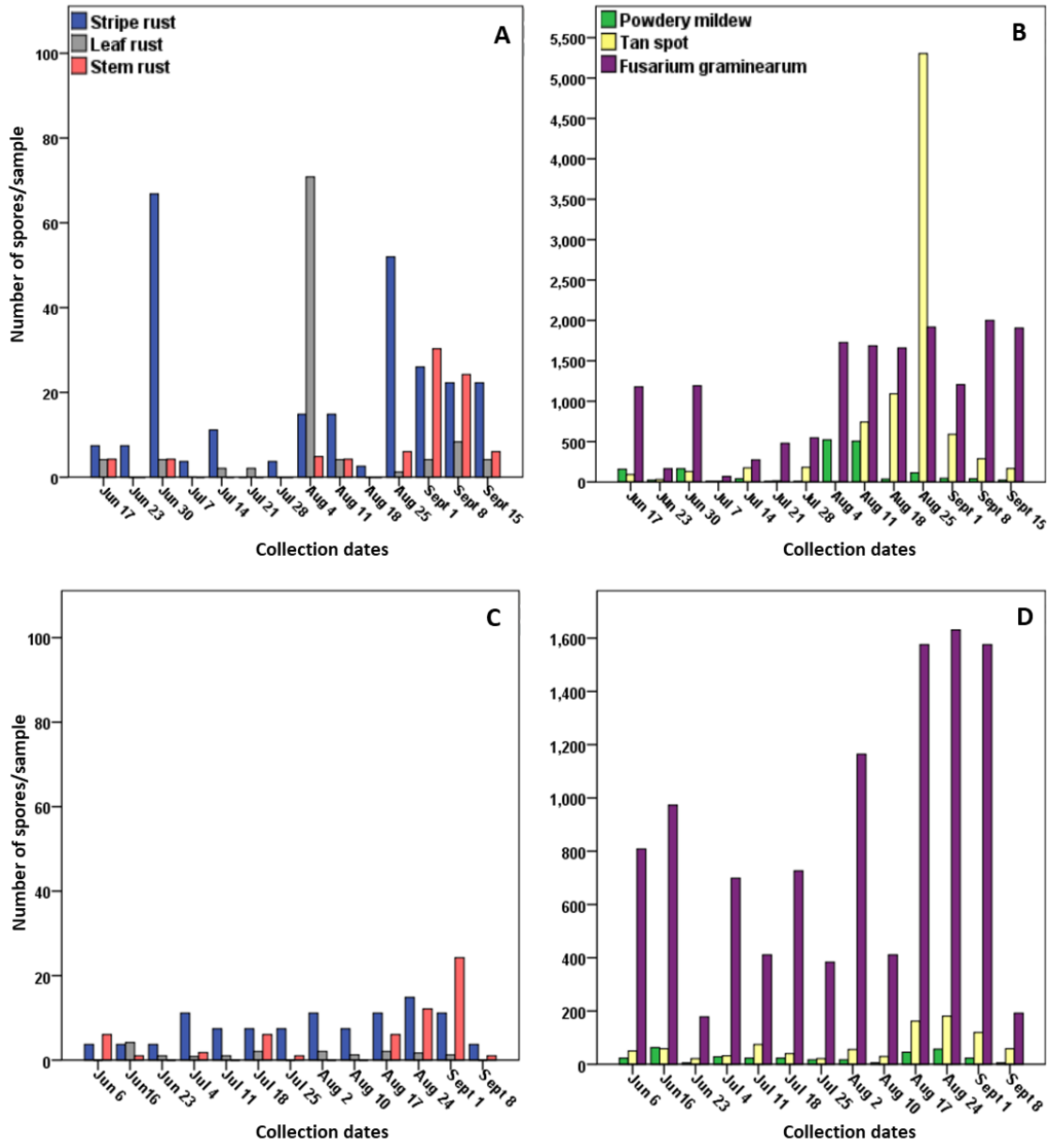

Figure 3.4 – Number of spores detected in air samples collected in 2016 (A-B) and 2017 (C-D) at LeRDC Weather Station site.

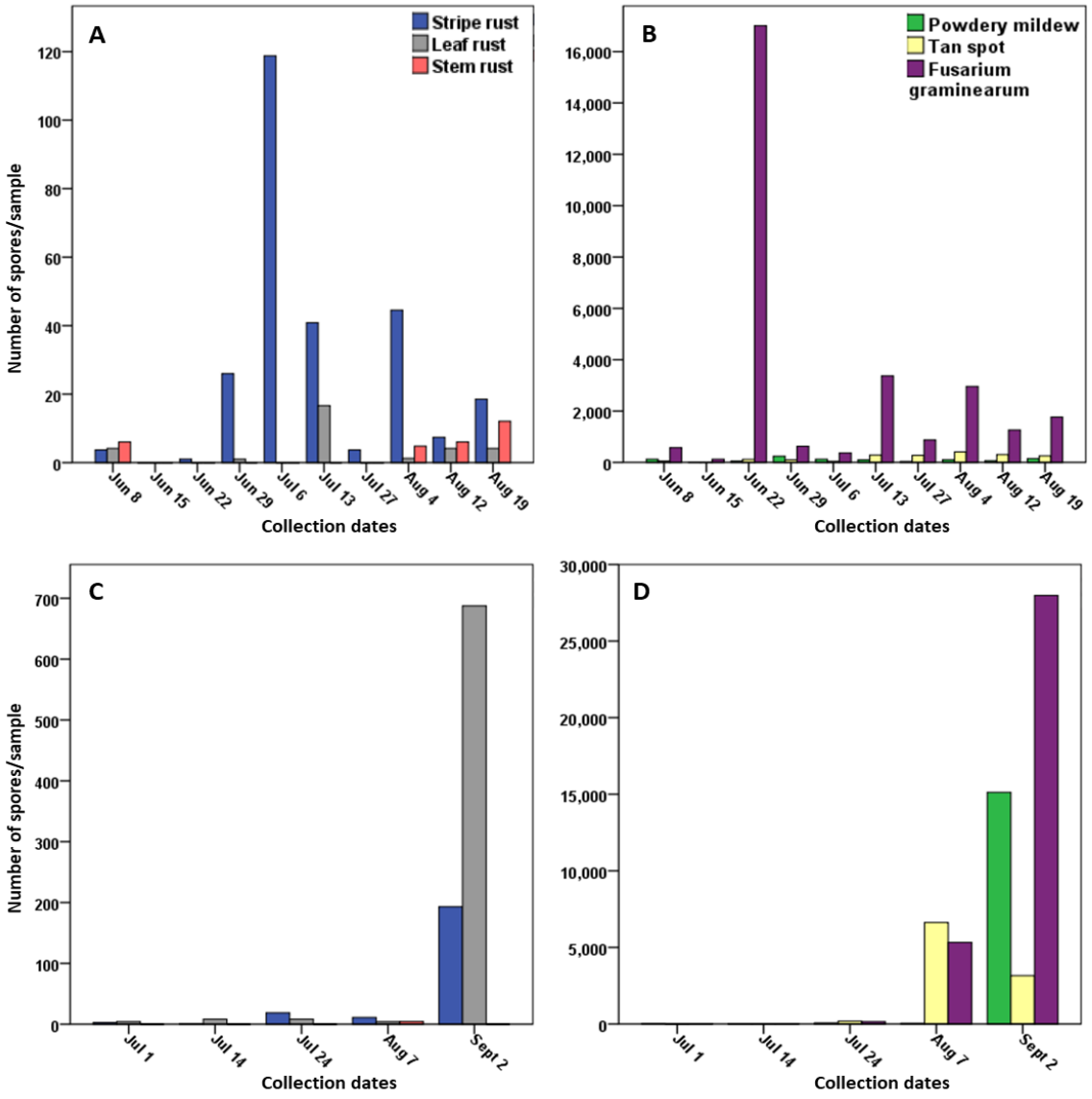

Figure 3.5 – Number of spores detected in air samples collected in 2016 at Brooks (A-B) and Granum sites (C-D). Samples collected at Granum were collected for more than a week, resulting in higher number of spores in each sample and fewer individual samples.

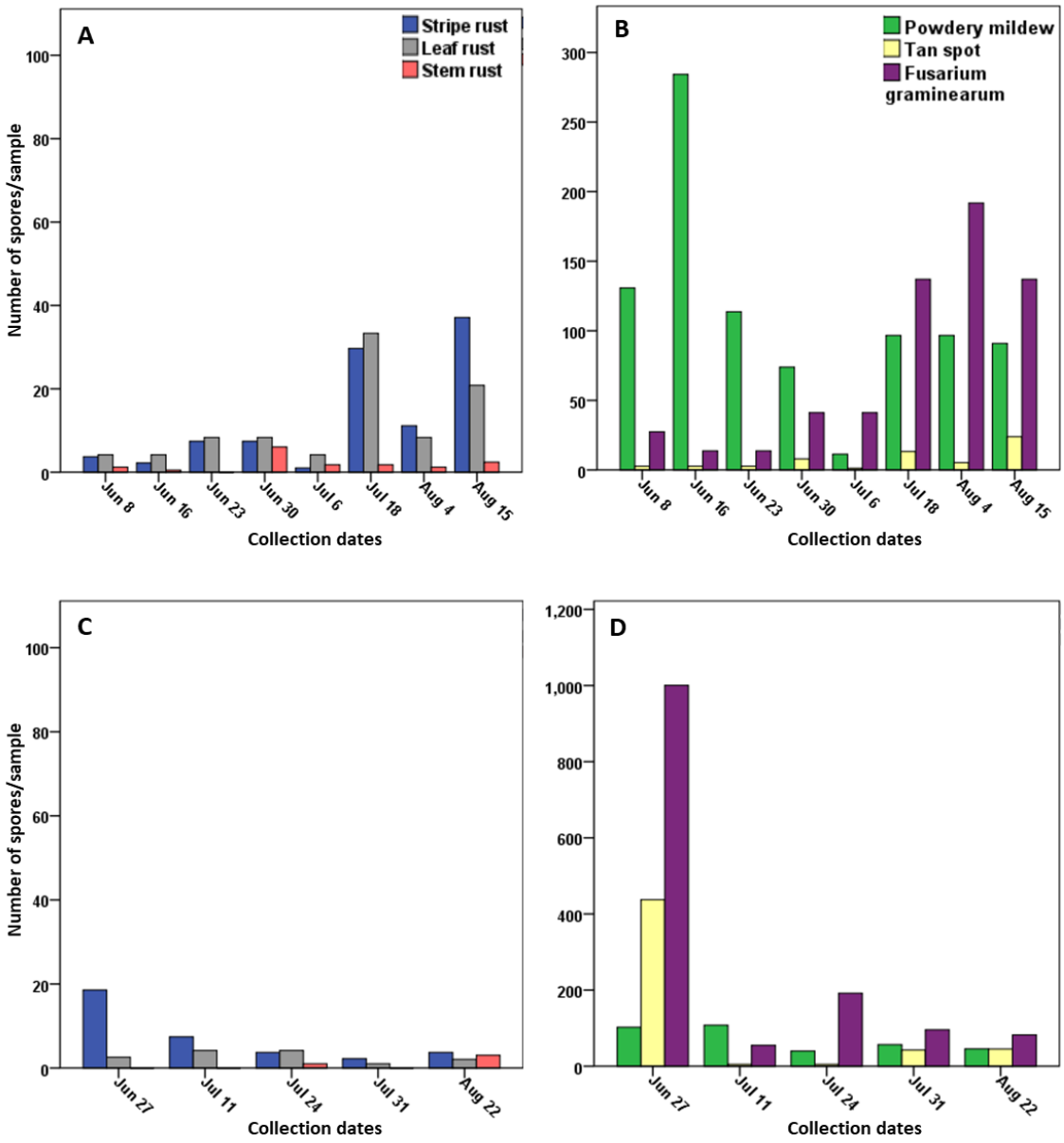

Figure 3.6 – Number of spores detected in air samples collected in 2016 (A-B) and 2017 (C-D) at Magrath site. Samples collected in 2017 were collected for more than a week, resulting in higher number of spores in each sample and fewer individual samples.

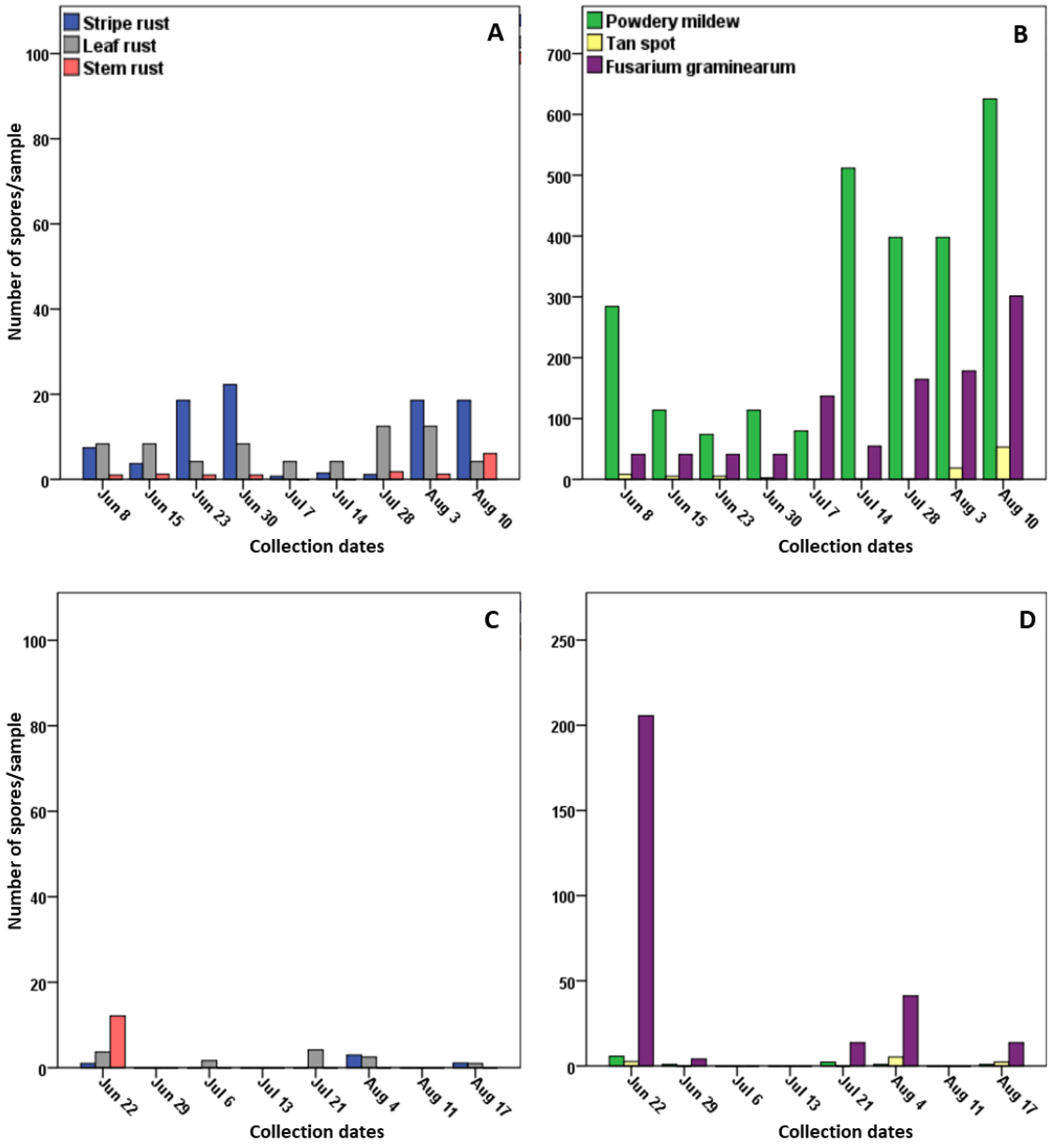

Figure 3.7 – Number of spores detected in air samples collected in 2016 (A-B) and 2017 (C-D) at Enchant site.

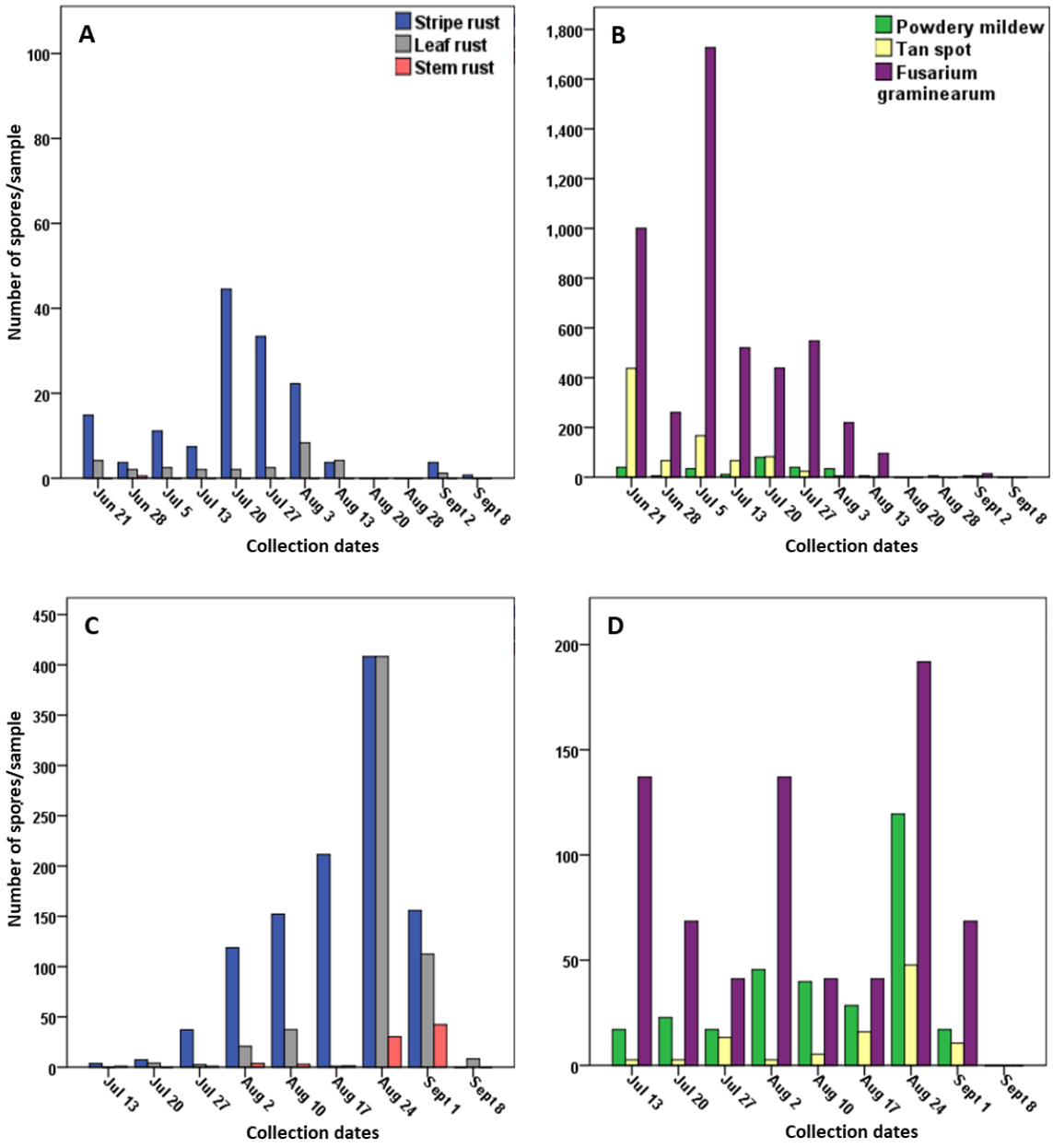

Figure 3.8 – Number of spores detected in air samples collected in 2017 at Milk River (A-B) and LeRDC Fairfield sites (C-D).

2015;142 mm and 25°C in 2016; 79 mm and 28°C in 2017 (AAF 2015, 2016 B & 2017 B). For Magrath, total of rainfall and average temperature were 178 mm and 25°C in 2016 and 84 mm and 27°C in 2017 (AAF 2016 C and 2017 C) and for Enchant 161 mm and 25°C in 2016 and 88 mm and 27°C in 2017 (AAF 2016 D and 2017 D).

A simple linear regression statistical test was used to analyse the qPCR results. qPCR standard curves generated for each pathogen (eight standard curves for each target, total of 30 to 37 samples) showed significant relationships (Figures 3.9 to 3.11). Standard curves were generated to test the efficiency of the qPCR assays as they were conducted with known DNA samples of spores from each pathogen and amplified using pathogen-specific primers.

Air sample analyses showed that all six pathogens were present at all of the eight collected sites in Southern Alberta. *F. graminearum* spores were the most predominant species among all the other pathogens detected at all eight collected sites and in most samples. On the other hand, stem rust spores were the least predominant with spores in at least one sample per collected site. The majority of the air sample results presented significant linear relationship between log10 of spore numbers and Ct value, except for 11 out of 72 analyses (Table 3.4). One of these exceptions was a *Pt* analyses from Fairfield site ($p < .052$). Even though it was not statistically significant, it is possibly biologically significant because it is extremely close to the *p*-value threshold ($p < .05$). Most of the other exceptions were *Pgt* analyses from various locations because of the small number of samples or of spore samples with the same Ct value, resulting in not enough different data points to generate the F-value or *p*-value. This issue could be possibly solved with higher sample size, which is also an alternative for the non-significant results.

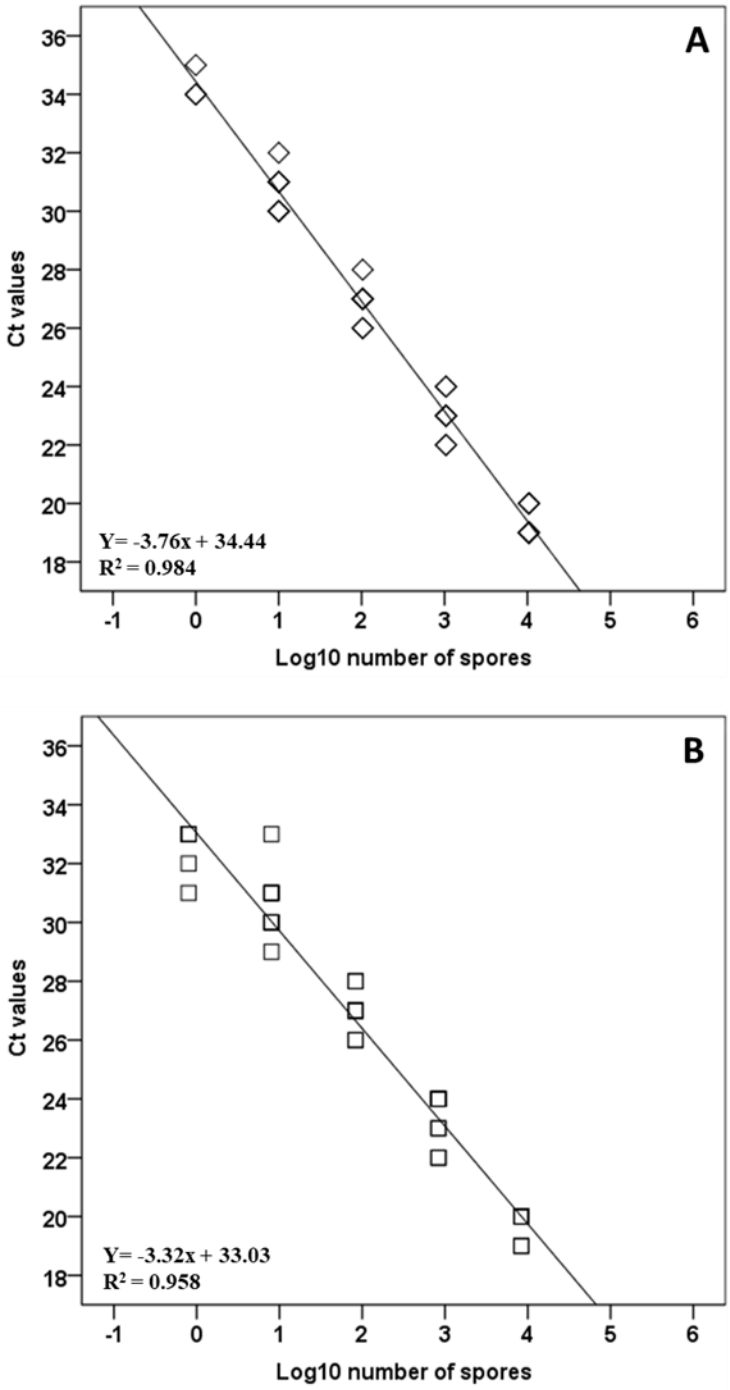

Figure 3.9 – Relationship between log number of spores used to generate standard curves and Ct values in qPCR assays. A) *Pst* and B) *Pt*. Overlapping data points are represented with symbols with a darker outline (in some cases, more than two data points were overlapping).

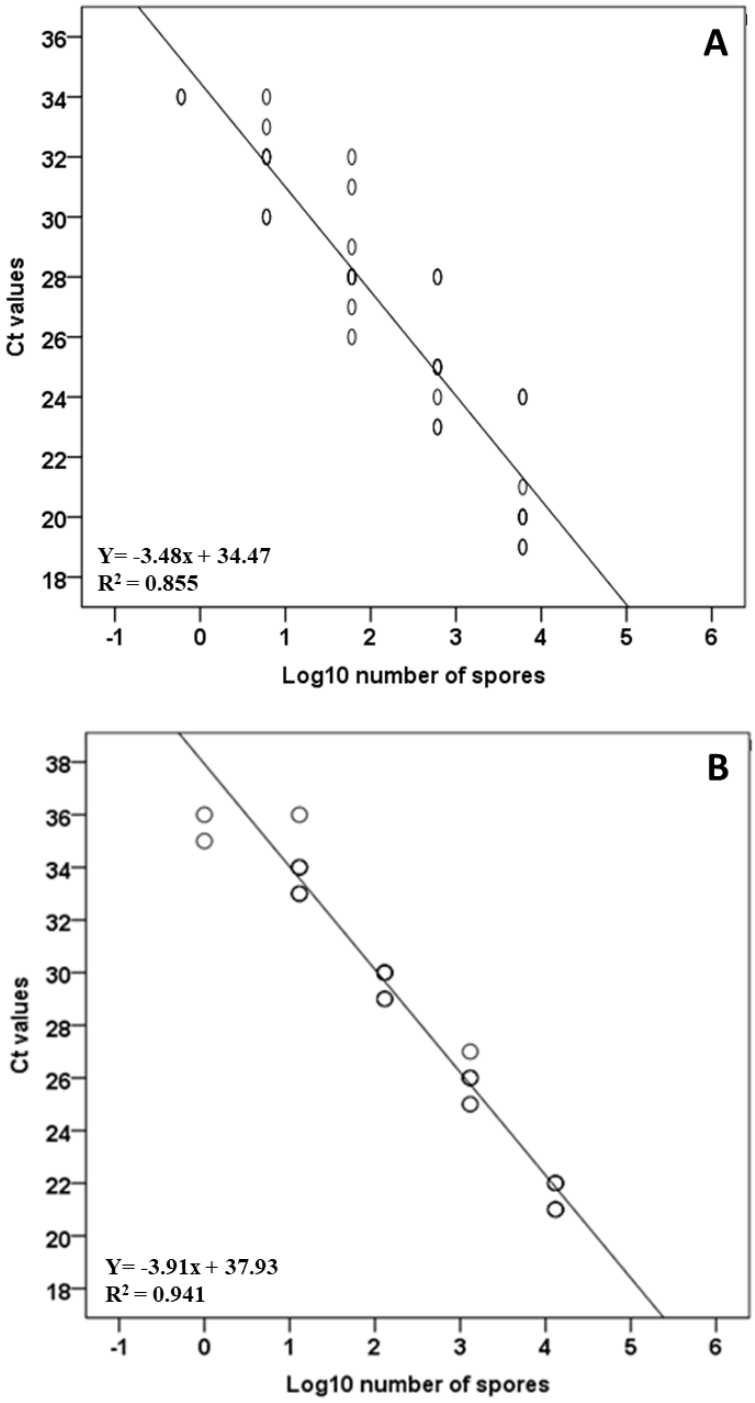

Figure 3.10 – Relationship between log number of spores used to generate standard curves and Ct values in qPCR assays. A) *Pgt* and B) *Bgt*. Overlapping data points are represented with symbols with a darker outline (in some cases, more than two data points were overlapping).

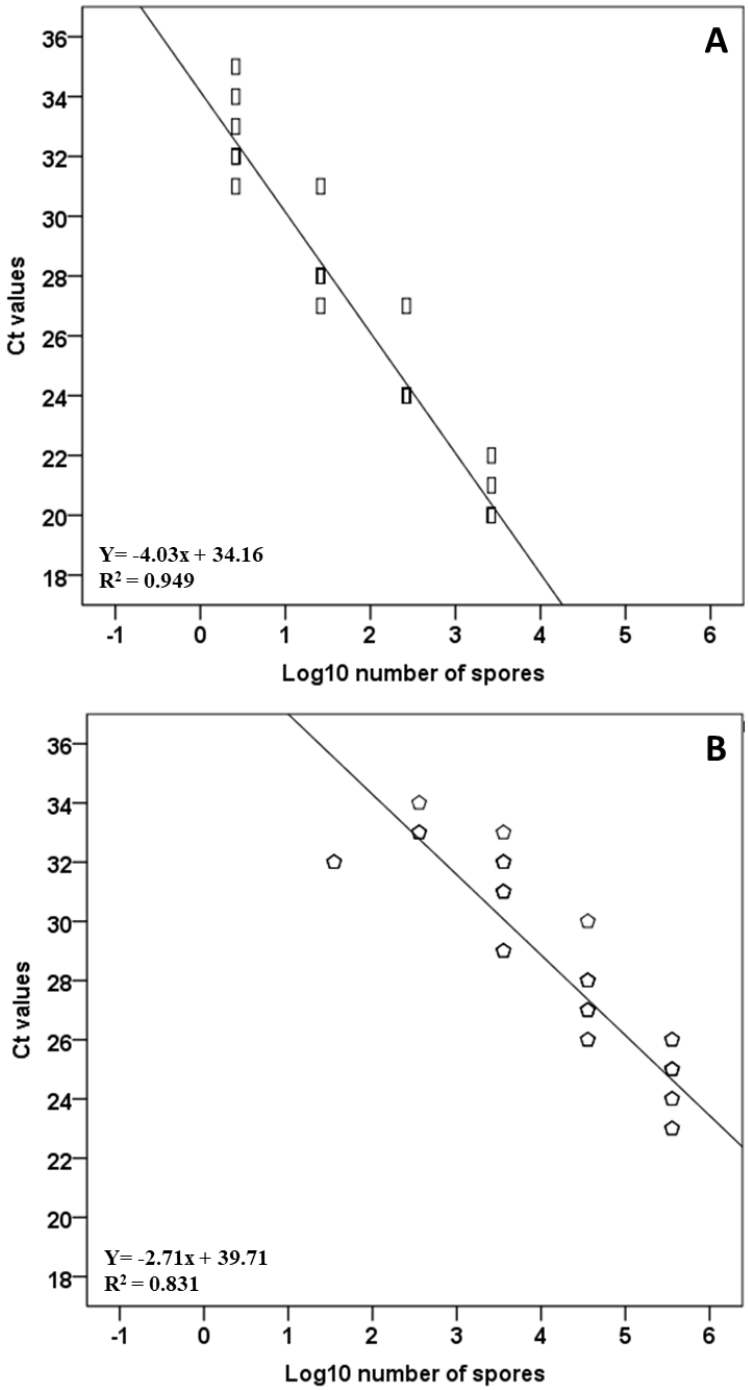

Figure 3.11 – Relationship between log number of spores used to generate standard curves and Ct values in qPCR assays. A) *Ptr* and B) *Fg*. Overlapping data points are represented with symbols with a darker outline (in some cases, more than two data points were overlapping).

Table 3.4: Simple linear regression results of standard curve samples and air samples collected in Southern Alberta.

Samples ID	Pathogen	F-value	*p*-value	Graphic
Standard curve	*Pst*	$F_{(1, 35)} = 747.38$	$p < .001$*	Figure 3.9 A
	Pt	$F_{(1, 35)} = 794.07$	$p < .001$*	Figure 3.9 B
	Pgt	$F_{(1, 31)} = 182.35$	$p < .001$*	Figure 3.10 A
	Bgt	$F_{(1, 32)} = 506.48$	$p < .001$*	Figure 3.10 B
	Ptr	$F_{(1, 28)} = 513.16$	$p < .001$*	Figure 3.11 A
	Fg	$F_{(1, 32)} = 157.50$	$p < .001$*	Figure 3.11 B
Field Pathology Building 2015	*Pst*	$F_{(1, 11)} = 40.05$	$p < .001$*	
	Pt	$F_{(1, 11)} = 3.42$	$p = .091$	
	Pgt	$F_{(1, 8)} = 1.48$	$p = .258$	Appendix 9
	Bgt	$F_{(1, 11)} = 67.18$	$p < .001$*	
	Ptr	$F_{(1, 11)} = 224.28$	$p < .001$*	
	Fg	$F_{(1, 11)} = 109.23$	$p < .001$*	
Weather Station 2015	*Pst*	$F_{(1, 13)} = 217.96$	$p < .001$*	
	Pt	$F_{(1, 10)} = 19.60$	$p = .001$*	
	Pgt	N/A	N/A	Appendix 10
	Bgt	$F_{(1, 13)} = 62.35$	$p < .001$*	
	Ptr	$F_{(1, 13)} = 64.38$	$p < .001$*	
	Fg	$F_{(1, 13)} = 101.37$	$p < .001$*	
Weather Station 2016	*Pst*	$F_{(1, 11)} = 95.45$	$p < .001$*	
	Pt	$F_{(1, 8)} = 17.26$	$p = .003$*	
	Pgt	$F_{(1, 6)} = 9.28$	$p = .023$*	Figure 3.12
	Bgt	$F_{(1, 12)} = 140.48$	$p < .001$*	
	Ptr	$F_{(1, 11)} = 2145.25$	$p < .001$*	
	Fg	$F_{(1, 12)} = 455.45$	$p < .001$*	

N/A: Not applicable because it was not possible to generate a F-value or *p*-value because of the number of samples or repetitive number of spores available.
*Significant linear relationships

Table 3.4 (continued)

Samples ID	Pathogen	F-value	*p*-value	Graphic
Weather Station 2017	*Pst*	$F_{(1,11)} = 14.01$	$p = .003$*	
	Pt	$F_{(1,8)} = 63.06$	$p < .001$*	
	Pgt	$F_{(1,7)} = 77.43$	$p < .001$*	Appendix 11
	Bgt	$F_{(1,11)} = 105.62$	$p < .001$*	
	Ptr	$F_{(1,11)} = 361.70$	$p < .001$*	
	Fg	$F_{(1,11)} = 341.10$	$p < .001$*	
Brooks 2016	*Pst*	$F_{(1,7)} = 137.56$	$p < .001$*	
	Pt	$F_{(1,4)} = 108.20$	$p < .001$*	
	Pgt	$F_{(1,2)} = 0.82$	$p = .460$	Appendix 12
	Bgt	$F_{(1,8)} = 219.61$	$p < .001$*	
	Ptr	$F_{(1,8)} = 333.32$	$p < .001$*	
	Fg	$F_{(1,8)} = 379.01$	$p < .001$*	
Granum 2016	*Pst*	$F_{(1,3)} = 15.15$	$p = .030$*	
	Pt	$F_{(1,3)} = 23.52$	$p = .017$*	
	Pgt	N/A	N/A	Appendix 13
	Bgt	$F_{(1,3)} = 51.97$	$p = .006$*	
	Ptr	$F_{(1,3)} = 16.48$	$p = .027$*	
	Fg	$F_{(1,3)} = 50.63$	$p = .006$*	
Magrath 2016	*Pst*	$F_{(1,6)} = 155.62$	$p < .001$*	
	Pt	$F_{(1,6)} = 45.61$	$p = .001$*	
	Pgt	$F_{(1,5)} = 0.55$	$p = .490$	Appendix 14
	Bgt	$F_{(1,6)} = 57.74$	$p < .001$*	
	Ptr	$F_{(1,6)} = 13.37$	$p = .011$*	
	Fg	$F_{(1,6)} = 19.86$	$p = .004$*	
Magrath 2017	*Pst*	$F_{(1,3)} = 12.10$	$p = .040$*	
	Pt	$F_{(1,3)} = 91.76$	$p = .002$*	
	Pgt	N/A	N/A	Appendix 15
	Bgt	$F_{(1,3)} = 35.40$	$p = .009$*	
	Ptr	$F_{(1,3)} = 27.67$	$p = .013$*	
	Fg	$F_{(1,3)} = 217.91$	$p = .001$*	
Enchant 2016	*Pst*	$F_{(1,7)} = 24.74$	$p = .002$*	
	Pt	$F_{(1,7)} = 13.71$	$p = .008$*	
	Pgt	$F_{(1,5)} = 24.59$	$p = .004$*	Appendix 16
	Bgt	$F_{(1,7)} = 782.70$	$p < .001$*	
	Ptr	$F_{(1,7)} = 8.36$	$p = .023$*	
	Fg	$F_{(1,7)} = 1.04$	$p = .342$	

N/A: Not applicable because it was not possible to generate a F-value or *p*-value because of the number of samples or repetitive number of spores available.
*Significant linear relationships

Table 3.4 (continued)

Samples ID	Pathogen	F-value	*p*-value	Graphic
Enchant 2017	*Pst*	$F_{(1,1)} = 170.78$	$p = .049$*	
	Pt	$F_{(1,3)} = 32.51$	$p = .011$*	
	Pgt	N/A	N/A	Appendix 17
	Bgt	$F_{(1,3)} = 47.15$	$p = .006$*	
	Ptr	$F_{(1,1)} = 5.62$	$p = .254$	
	Fg	$F_{(1,3)} = 84.82$	$p = .003$*	
Milk River 2017	*Pst*	$F_{(1,8)} = 118.50$	$p < .001$*	
	Pt	$F_{(1,7)} = 10.14$	$p = .015$*	
	Pgt	N/A	N/A	Appendix 18
	Bgt	$F_{(1,9)} = 44.62$	$p < .001$*	
	Ptr	$F_{(1,9)} = 24.72$	$p = .001$*	
	Fg	$F_{(1,8)} = 238.97$	$p < .001$*	
Fairfield 2017	*Pst*	$F_{(1,6)} = 499.39$	$p < .001$*	
	Pt	$F_{(1,6)} = 5.82$	$p = .052$	
	Pgt	$F_{(1,5)} = 111.73$	$p < .001$*	Appendix 19
	Bgt	$F_{(1,6)} = 35.15$	$p = .001$*	
	Ptr	$F_{(1,6)} = 374.68$	$p < .001$*	
	Fg	$F_{(1,6)} = 30.04$	$p = .002$*	

N/A: Not applicable because it was not possible to generate a F-value or *p*-value because of the number of samples or repetitive number of spores available.
*Significant linear relationships

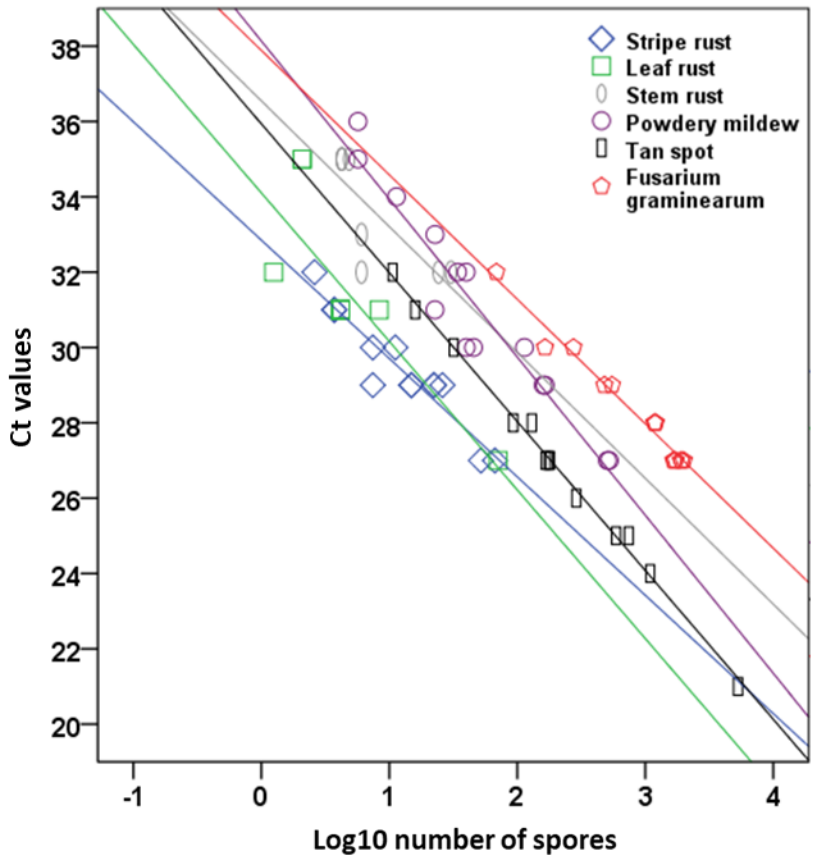

Target	Linear regression equations
Pst	$Y = -3.14x + 32.85$, $R^2 = 0.90$
Pt	$Y = -3.94x + 34.10$, $R^2 = 0.68$
Pgt	$Y = -3.34x + 36.55$, $R^2 = 0.61$
Bgt	$Y = -4.20x + 38.14$, $R^2 = 0.92$
Ptr	$Y = -3.95x + 35.94$, $R^2 = 0.99$
Fg	$Y = -3.30x + 37.89$, $R^2 = 0.97$

Figure 3.12 – Linear relationship between log number of spores collected at the LeRDC Weather Station in 2016 and Ct values in qPCR assays. Overlapping data points are represented with symbols with a darker outline (in some cases, more than two data points were overlapping).

3.4.5 Spores counted vs. spores detected

The spore counts determined by microscopy were compared with spores detected by qPCR assays (Figures 3.13 to 3.17). These results showed that in most occasions, for rusts, these two methods of analyses (microscopy and qPCR) revealed similar results. However, for *Bgt* the differences in spore numbers were moderate; whereas for the other two pathogens (*Ptr*, and *F.spp*) results were very different between the two methods. This could have occurred due to the microscopy analyses of only asexual spores, while qPCR analyses based on DNA content would detect both sexual and asexual spores.

Pearson correlation statistical analyses were done to evaluate the relationship between results found by both methods of spore analyses. Results of samples collected at the LeRDC Weather Station location in 2015 and 2017, showed a significant relationship between rusts spores detected by both methods, but no significant relationships were found for rusts at this location in 2016 (Table 3.5). No significant relationships were found for the other pathogen spores in all the three sampling years.

Samples collected at the LeRDC Field Pathology Building location in 2015, showed a significant linear relationship between rusts spores detected by both methods, but no significant relationship were found for the other pathogen spores, whereas at the LeRDC Fairfield site in 2017, no significant relationship were found for any of the pathogens spores (Table 3.6).

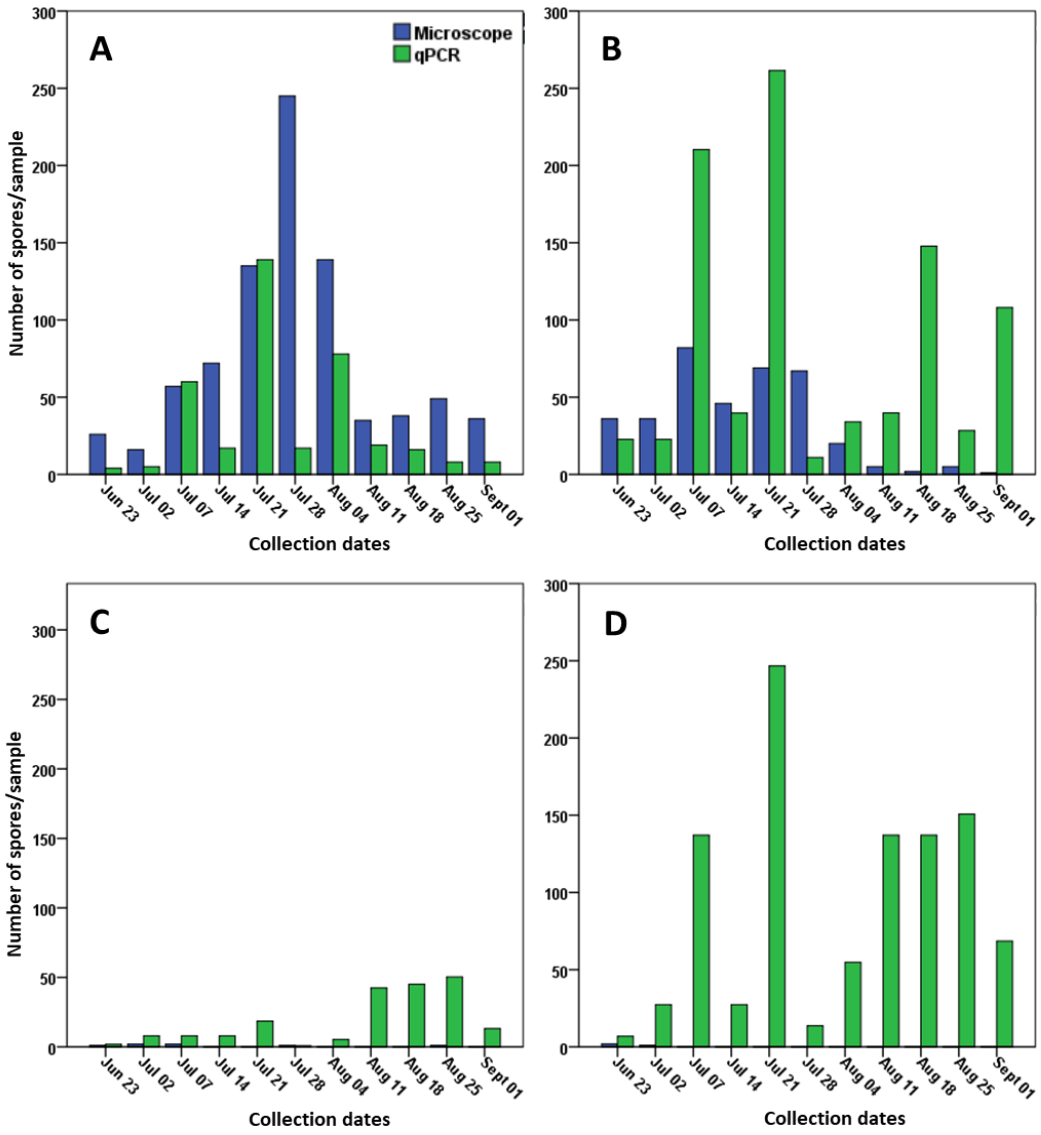

Figure 3.13 – Comparison between spore numbers counted using microscopy and spores detected by qPCR assay during the 2015 growing season at the LeRDC Weather Station site, A) rusts, B) powdery mildew, C) tan spot, and D) *F.spp* vs. *F. graminearum*.

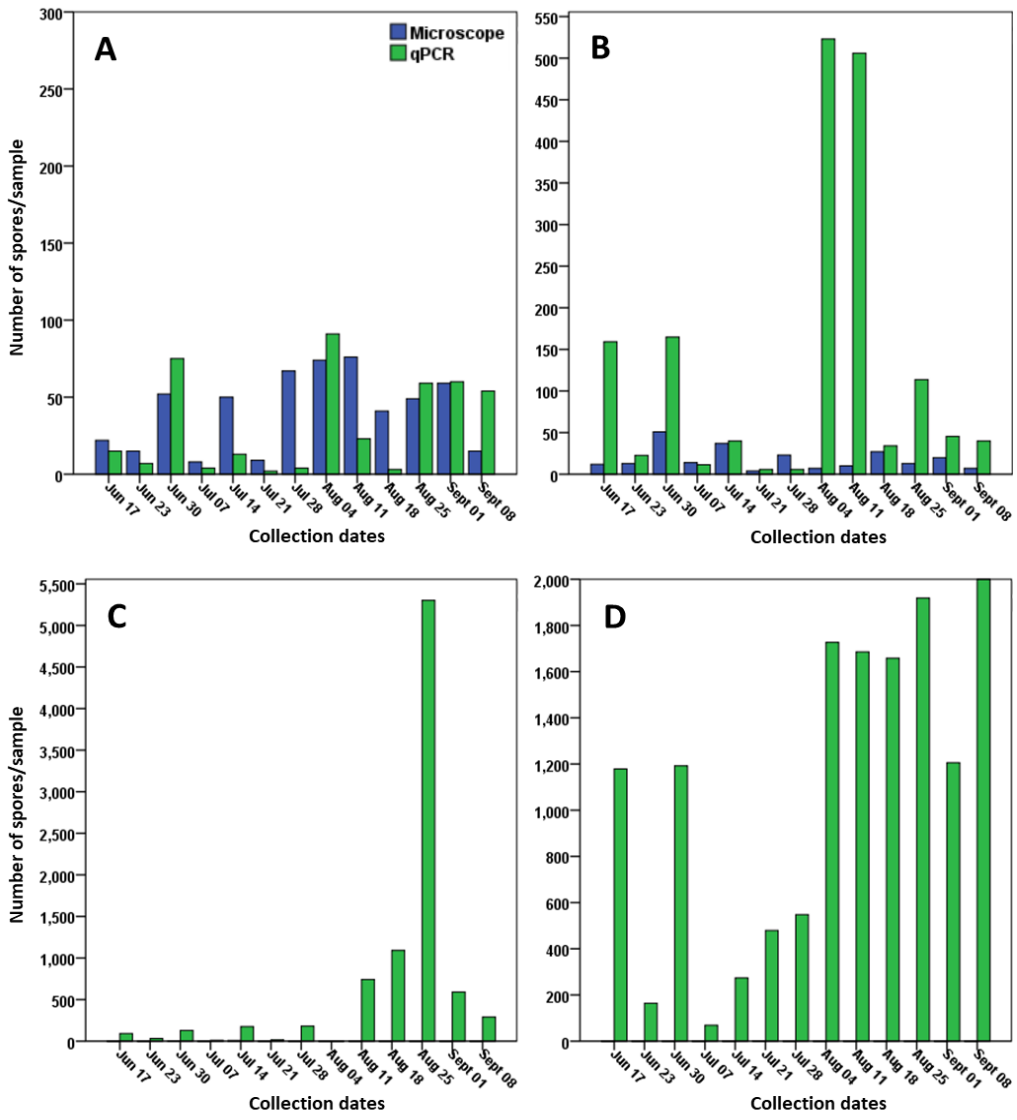

Figure 3.14 – Comparison between spore numbers counted using microscopy and spores detected by qPCR assay during the 2016 growing season at the LeRDC Weather Station site, A) rusts, B) powdery mildew, C) tan spot, and D) *F.spp* vs. *F. graminearum*.

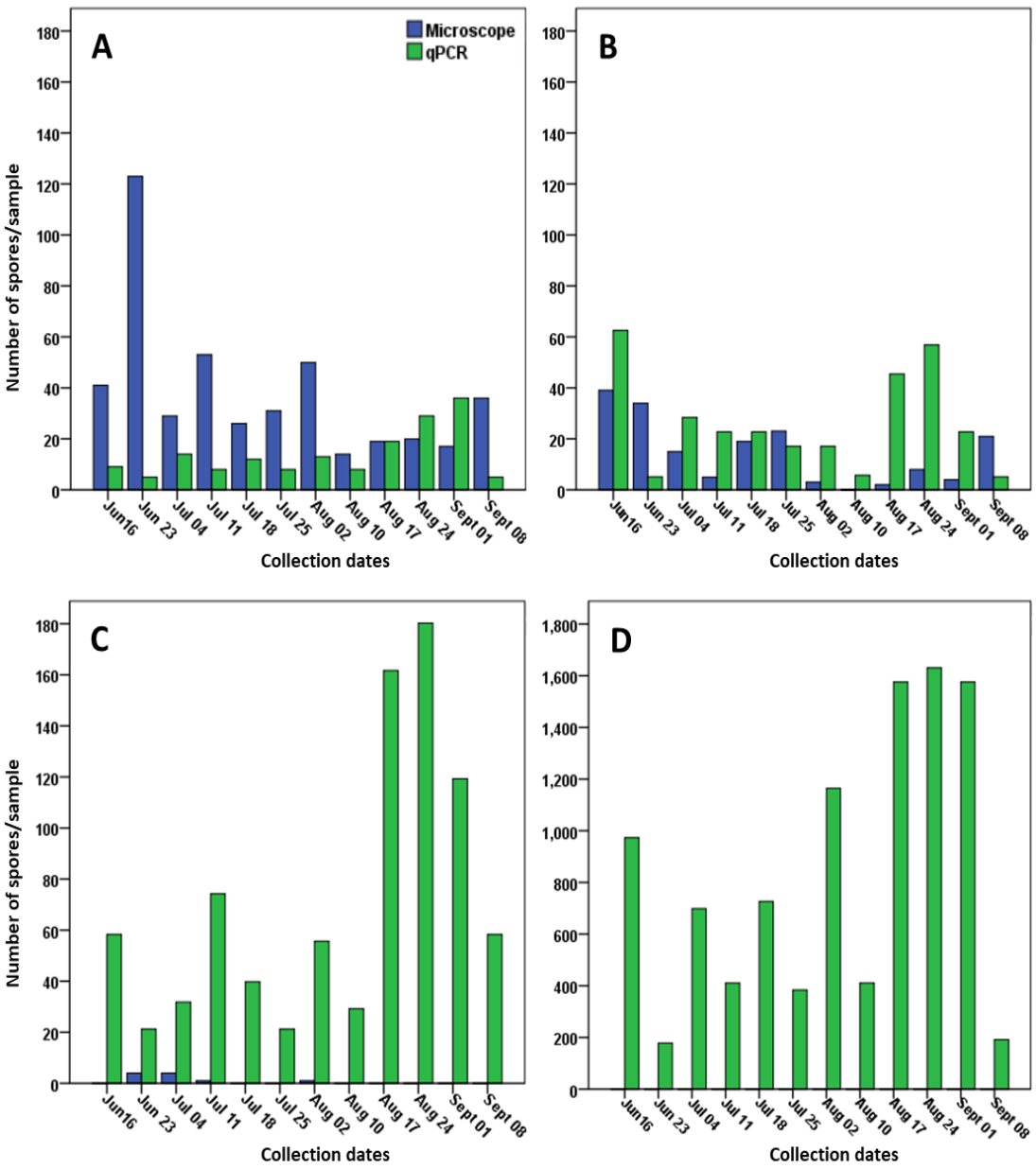

Figure 3.15 – Comparison between spore numbers counted using microscopy and spores detected by qPCR assay during the 2017 growing season at the LeRDC Weather Station site, A) rusts, B) powdery mildew, C) tan spot, and D) *F.spp* vs. *F. graminearum*.

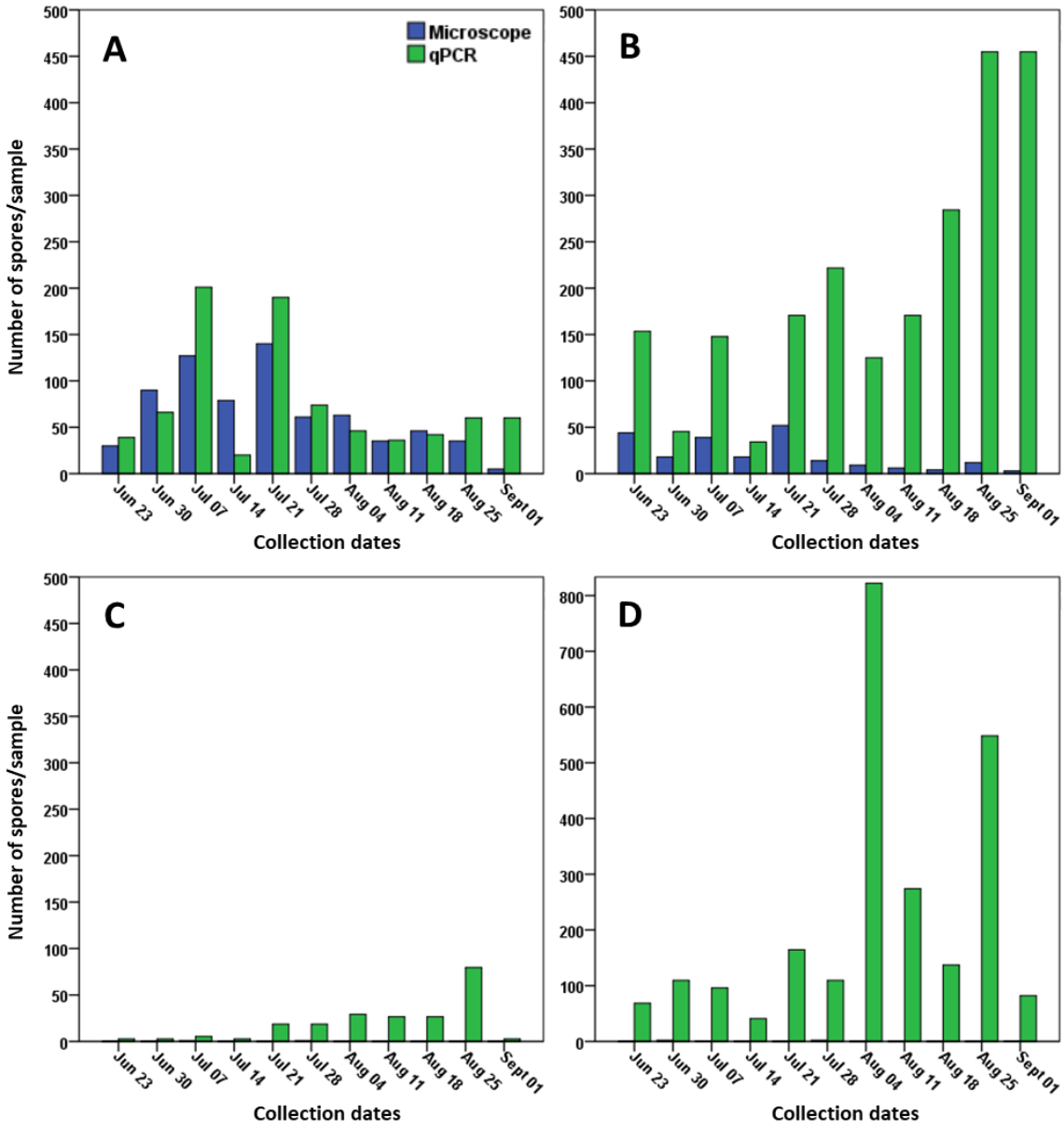

Figure 3.16 – Comparison between spore numbers counted using microscopy and spores detected by qPCR assay during the 2015 growing season at the LeRDC Field Pathology Building site, A) rusts, B) powdery mildew, C) tan spot, and D) *F.spp* vs. *F. graminearum*.

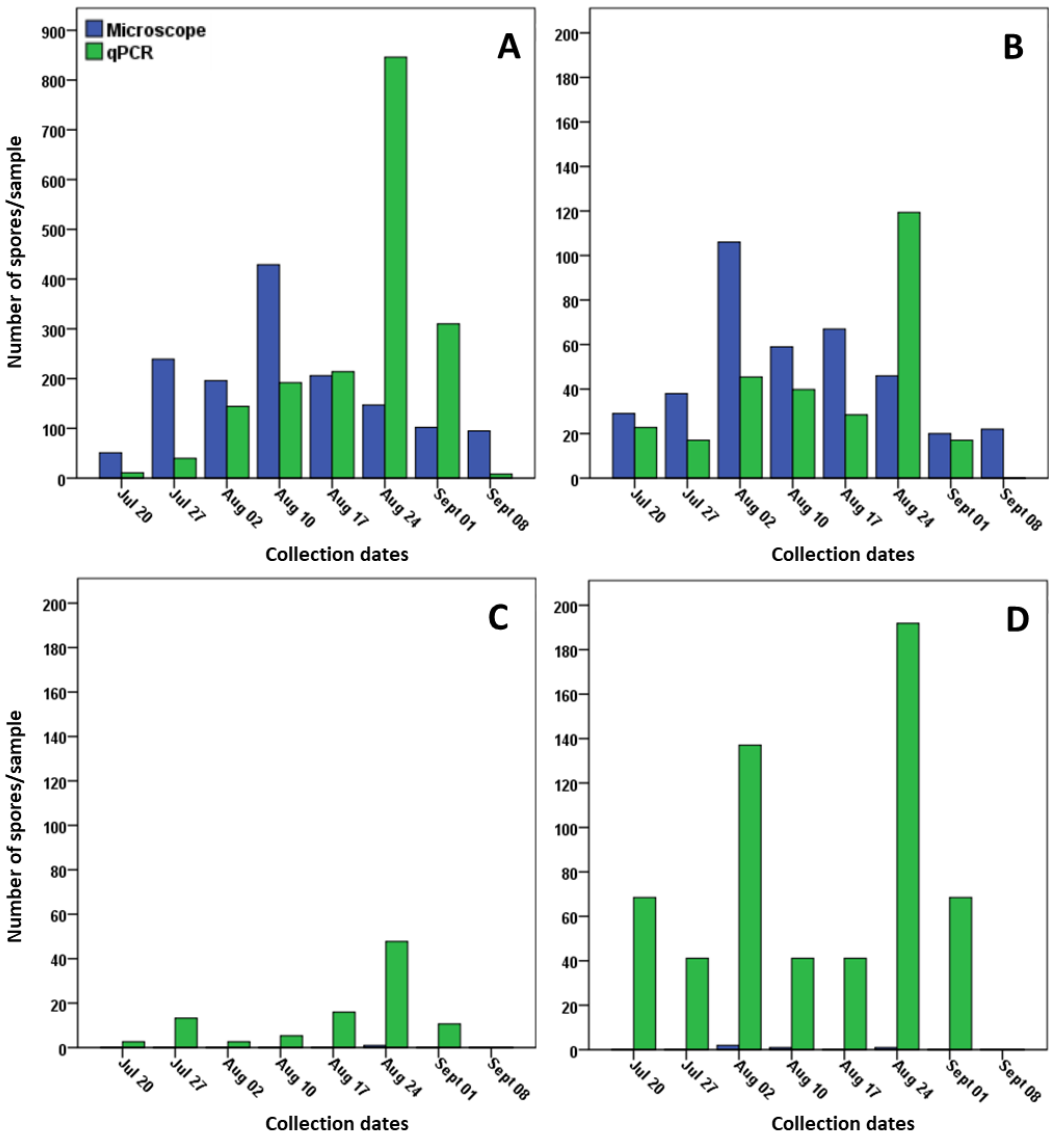

Figure 3.17 – Comparison between spore numbers counted using microscopy and spores detected by qPCR assay during the 2017 growing season at the LeRDC Fairfield site, A) rusts, B) powdery mildew, C) tan spot, and D) *F.spp* vs. *F. graminearum*.

Table 3.5 – Correlation results of the relationship between spore numbers counted using microscopy and spores detected by qPCR assay. Samples collected in Lethbridge, Weather Station site.

Year of collection	Target	R-value	*p*-value
2015	Rusts	R = 0.680	*p* = .021*
	Bgt	R = 0.386	*p* = .241
	Ptr	R = -0.424	*p* = .194
	F.spp/Fg	R = -0.478	*p* = .137
2016	Rusts	R = 0.503	*p* = .080
	Bgt	R = -0.204	*p* = .505
	Ptr	R = -0.50	*p* = .878
	F.spp/Fg	R = -0.127	*p* = .680
2017	Rusts	R = -0.615	*p* = .033*
	Bgt	R = -0.308	*p* = .356
	Ptr	R = -0.360	*p* = .251
	F.spp/Fg	N/A	N/A

*Significant relationship results.

Table 3.6 – Correlation results of the relationship between spore numbers counted using microscopy and spores detected by qPCR assay. Samples collected at the LeRDC Field Pathology Building and Fairfield sites.

Location and year of collection	Target	R-value	*p*-value
Field Pathology Building 2015	Rusts	R = 0.783	*p* = .004*
	Bgt	R = -0.409	*p* = .211
	Ptr	R = -0.017	*p* = .960
	F.spp/Fg	R = -0.351	*p* = .290
Fairfield 2017	Rusts	R = 0.484	*p* = .224
	Bgt	R = 0.537	*p* = .170
	Ptr	R = 0.397	*p* = .329
	F.spp/Fg	R = 0.388	*p* = .342

*Significant relationship results.

3.5 Discussion and conclusions

Several studies on identification and quantification of airborne plant pathogens have been reported worldwide (Fernando et al. 2000; West et al. 2008; Isard et al. 2011; Guarín et al. 2015; Cao et al. 2016) but only a few related to wheat pathogens could be identified (Fernando et al. 2000; Cao et al. 2016). In this present study, two methods for air sampling were used, the passive method using adhesive tape trap and the active method Burkard cyclone instrument (Alcázar & Comtois 1999; Alcázar et al. 2003; West & Kimber 2015; Cao et al. 2016).

The present study focused on the detection and quantification of six important fungal airborne wheat pathogens (*Pst*, *Pt*, *Pgt*, *Bgt*, *Fg*, and *Ptr*) using both molecular and microscopic approaches. Results demonstrated that it was possible to optimize a quantitative PCR assay using highly sensitive and specific primers to identify and determine, in real-time, the incidence of airborne spores of wheat pathogens sampled at specific locations in Southern Alberta. These results were confirmed, in part, using microscopic analyses as a complementary technique for identification and quantification of airborne fungal spores. The results of this study will be used in the development of a forecasting network to predict, on the basis of inoculum prevalence, infections of important wheat pathogens before the first signs of the disease are evident.

For the qPCR-based analyses, the best six out of the 29 pathogen-specific PCR primer pairs were chosen for their ability to reliably amplify target sequences from wheat pathogen genomes during the optimization period. Results showed that the limit of detection of the six primers pairs varied from 0.0001 to 0.001 ng of DNA which corresponds to 1 to 35 spores. These results demonstrate the high sensitivity of the PCR primers. Challenges were encountered in the adaptation or redesign of primer sequences,

annealing temperature tests, different qPCR kits tests, and different qPCR-based methods tests (single and multiplex). Even though all six primer pairs are highly pathogen-specific, *Pst* and *Ptr* PCR primers could potentially detect one more pathogen beside stripe rust and tan spot of wheat. *Pst* PCR primers (PSBTQ) amplified an uncharacterized sample of stripe rust collected from foxtail barley (*Hordeum jubatum*) in Southern Alberta (data not shown). In a survey carried out in Central and Southern Alberta, Holtz et al. (2013) reported that frequency of stripe rust infection was much higher in wheat than in barley as of the nine rust isolates collected on foxtail barley, seven isolates were infecting wheat (*Pst*) and two barley (*Psh*). It is not clear at this point if the rust collected represents *Pst* or *Psh* (*Puccinia striiformis* f. sp. *hordei* - stripe rust of barley) as both rusts can be detected on this host in Alberta (Holtz et al. 2013) and sequences for the amplified locus are identical between *Pst* and *Psh* (Xia et al 2018). A biological assay infecting both susceptible wheat and barley will be needed to resolve this question. *Ptr* PCR primers (Tox A1/2) have the potential to amplify sequences for leaf blotch of wheat (*P. nodorum (Pn)*), also a producer of the Ptr ToxA protein (Phan et al. 2016). For ToxA PCR primers, this finding may be less important because *Ptr* is the predominant leaf spot pathogen in Alberta (Aboukhaddour et al. 2013). This fact should be considered in other Canadian regions where *Pn* is abundant.

For the microscopy analyses, morphological identification and quantification of asexual spores were possible; however, the three rusts were not distinguishable because of morphological similarities among spores. In Southern Alberta, this may be less important depending on the year because leaf and stem rust usually infect later in the growing season and do not cause infection and yield losses whereas stripe rust will overwinter or arrive early in the spring (Brar et al. 2017). Incidence of asexual spores of

Ptr and *F.spp* in the adhesive tape trap were extremely low compared with the other four pathogens. This observation could be explained by the fact that *Fg* macroconidia are harder to find at the height of wheat heads (Fernando et al. 2000); microscope slides were set at 90 to 100 cm height above the ground on the upper lid of the Burkard Cyclone. For *Ptr*, conidial dispersal might be similar to that of tan spot of barley (*Pyrenophora teres*), which has limited horizontal and vertical spreading thus leaving most of the conidia present below 100 cm height above ground level (Martin et al. 1984). A few slides seemed to have been washed by rainfall and/or irrigation, which might illustrate a disadvantage of this trapping method. Alcázar et al. (2003) suggested that rain could be a factor to be considered when using the adhesive tape method.

Identification and quantification of all six pathogens spores among air samples were possible using qPCR analyses. Significant linear correlations between log10 number of spores and Ct values were detected for most of the air samples collected by the cyclone instruments. This demonstrated the consistency and efficiency of analyses method. qPCR results showed the presence of all six fungal pathogens at all eight locations at some point during the sampling periods. The highest spores incidence found among all six pathogens was for *Fg* with spore numbers varying from 0 to 2,000 spores, including samples with greater than 10,000 spores. These results are similar to those reported by Fernando et al. (2000) in Eastern Canada. According to the qPCR analyses, spore numbers averaged over the eight locations showed that the most abundant pathogen spores were *Fg* with an average of 866 spores/sample. The second most abundant pathogen spores were *Bgt or Ptr* depending on the location; averages of 224 spores/sample and 201 spores/sample, respectively. These pathogens overwinter in the stubble and are always present in Western Canada (Aboukhaddour et al. 2013; Gräfenhan et al. 2013; Abdullah et al. 2017;

University of Saskatchewan 2018). Spore numbers found for powdery mildew and tan spot varied mainly between 0 to 1,000 spores. The numbers of *Bgt* spores detected in the present study were lower than the amount described by Cao et al. (2016) in Hebei Province, China (ranged from 50 to 500,000 spores/sample). No related studies were found to compare with the rusts and tan spot spores detected. For stripe and leaf rust, spore numbers varied mainly from 0 to 200 and for stem rust, from 0 to 30 spores. Among the three rusts, *Pst* was the predominant species in all eight locations of Southern Alberta whereas the least abundant pathogen was *Pgt* at 3 spores/sample. *Pst* is endemic to Western Prairies and occurs in most years (Brar et al. 2017). The lower incidence of both *Pgt* and *Pt* is likely due to their regular occurrence along *Puccinia* pathway in the Central Prairies of North America, resulting in late entry of these two species in Southern Alberta in most years (Wegulo & Byamukama 2012).

Variances in spore numbers for the different pathogens in air samples were observed among the different locations that had samples collected in two or three consecutive years. In general, there was an increase in spore numbers from 2015 to 2016 at LeRDC Weather Station location while a decrease was observed from 2016 to 2017. These changes closely followed average rainfall/moisture and temperature in these years. At the Magrath location, increases in *Fg*, *Ptr*, and *Bgt* spores were observed, while a small decrease occurred for rusts. The decrease in rusts spore numbers were likely due to the higher temperature in 2017, which is not favorable for rusts spore germination. At the Enchant location, from 2016 to 2017, a decrease in spore numbers was noticed for all six pathogens, which might be related to the decrease of spores in the Lethbridge location and the higher temperature in 2017 for the rusts. The prevailing wind directions in Southern Alberta are from West and Southwest to East and Northeast (Vickers et al.

2001; AAF 2017 E) which would likely influence the secondary spread of rust spores from Magrath to Lethbridge, to Enchant, and to Brooks. During the season 2016, it was interesting to note that the maximum peak for stripe rust only in Brooks was one week later than that for the Weather Station in Lethbridge. A similar trend was not observed in 2017 for stripe rust or the other pathogens. Results suggest that among the three locations Lethbridge, Enchant and Brooks; Lethbridge might be a representative area for stripe rust spore collection in Southern Alberta since the prevailing winds in this region tend to pass through Lethbridge first.

Advantages and disadvantages were apparent between the two spore trapping methods. A Burkard Cyclone instrument is expensive, requiring an external power source and there is a risk of instrument failure due to low battery or mechanical issues. Additionally, the field set up can be a bit more laborious. However, this instrument was generally a more effective and representative trapping method compared to the adhesive tape method. The Burkard Cyclone instrument was set up around 90 to 100 cm from the ground surface to the collector orifice which was appropriate for the rusts because this height is close to that for the upper leaves and wheat heads. However, this sampling height was less effective for *Fg* and *Ptr* spores in both methods (Martin et al. 1984; Fernando et al. 2000). However, the primary interest of this study was related to wheat rusts and powdery mildew. The adhesive tape and microscope slides were much less expensive, easy to carry and place in the field, and easily distributed in different study areas. Additionally, the convenient size and weight of the microscope slides made it possible to set them up in the moving cap of the Burkard cyclone, which allowed the slide to always face the prevailing wind; therefore, increasing efficiency of the adhesive tape trap method. However, this method is subject to environmental influences, for example

higher temperatures can make the tape stickier (Alcázar et al. 2003). Also, rainfall and irrigation might influence sampling by washing the tape or making it less sticky, which was occasionally observed during this study and was suggested to be a possible issue by Alcázar et al. (2003). Additionally, this method required an extensive training to reliably count and identify the asexual spores for the six pathogens. Microscopic analyses are often limited to identification at the genus level rather than species level as for rust and Fusarium. *Ptr* and *F.spp* spore counts varied greatly between the two analyses methods, with average counts being much higher in the qPCR-based detection method. For *Bgt* and rusts, the variations between the analyses were moderate to small. These differences illustrate the importance of looking for asexual and sexual spores in air samples, which was done using qPCR because the pathogen-specific primers targeted both types of spores by opposition of microscopy analyses. Other explanations for the differences found by both methods are possible losses of spores during DNA extraction, influence of rain/irrigation on adhesive tape stickiness, and losses of tape adhesiveness due to saturation by other particulates (dust, debris, and crop residue) and insects.

Significant linear correlations between both methods of analyses (qPCR and microscopy) were found for rusts spores at Weather station (2015 and 2017) and Plant Pathology building (2015) locations. These correlations are likely due to the fact that asexual spores are the primary inoculum, which arrives in spore showers from Pacific Northwest in USA (Brar & Kutcher 2016; Aboukhadour 2017). This is not the case for the other three fungi which mostly originate from infested crop residue within the field or from nearby fields (Fernando et al. 2000; Heffer et al. 2006; Abdullah et al. 2017; Wicker et al. 2013). No significant correlations were detected for rusts at Weather Station (2016)

and Fairfield locations (2017), and for the other pathogen spores at any location, possibly because of some of the reasons described above. Differences in rust spore numbers for both methods between Fairfield and the other two locations in Lethbridge are possibly because wheat fields at Fairfield are artificially inoculated with *Pst*. These results demonstrate divergence in spore quantification by these methods as comparative techniques, but they can be used as complementary techniques especially if total spore numbers need to be quantified and if the ratio of asexual to sexual spore types need to be determined. However, both methods need to be improved to reliably collect both asexual and sexual spores by setting up the traps at a favorable height for both types of spores for all six pathogens.

This study demonstrated that it was possible to reliably identify and quantify six fungal wheat pathogens in air samples from Southern Alberta areas by selecting pathogen-specific primers and qPCR protocol. qPCR-based technique coupled with Burkard Cyclone instruments for air sampling provided a means of generating efficient pathogen identification and monitoring in real-time. The study results also illustrated the importance of understanding how individual pathogens move via air currents above and within the crop canopy. By establishing the presence and quantity of airborne spores of specific wheat pathogens that could potentially cause infections and integrate this information with prevailing weather conditions and long term environmental data, it should be possible to estimate the risk to wheat plants throughout the growing season and decide what, if any, fungicide controls to apply. Additionally, these methods may be adapted to new introduced pathogens and races such as *Pgt* Ug99 (TTKSK) that started

evolving in Uganda and has spread throughout many regions in Africa and Asia (FAO 2010).

In summary, an efficient method of air sampling was coupled with a qPCR-based method for identification and quantification of airborne wheat pathogens. These methods will be important in developing reliable forecasting models based on pathogen presence, for estimating risk for crop loss. The forecasting will also assist in reducing fungicide use, maintaining fungicide efficacy through the reduction of fungicide over applications, reducing production costs, and protecting the environment from harmful fungicide chemicals. A complementary study of this thesis, establishing the threshold levels of stripe rust and powdery mildew inoculum to cause disease is also key in developing reliable crop forecasting models.

CHAPTER FOUR: SUMMARY OF CONCLUSIONS

4.1 Conclusions

Any sustainable approach to fungal disease control in a susceptible crop species requires that fungicides only be applied when there is a direct threat from plant pathogens. Consequently, establishing the direct threat of air-borne pathogen, i.e. the aerobiological surveillance of crop pathogens in real-time, remains the goal of sustainable approaches to pathogen control in agriculture. This approach requires accurate biological and meteorological information. On the biological side, methods for establishing the abundance and prevalence of individual plant pathogens within defined geographic areas are needed. Information about minimum threshold number of spores of a given fungal pathogen necessary to cause significant disease must also be determined. The goals of this project were to determine the minimum threshold concentration of stripe rust and powdery mildew spores required to damage wheat plants, and to develop microscopy and qPCR methods to identify and quantify six wheat fungal pathogen spores in air samples collected in Southern Alberta.

The minimum threshold number of *Pst* and *Bgt* spores required to cause significant disease under controlled growth chamber conditions was 10^6 spores/ml for both pathogens. However, for *Pst* under field conditions the results varied from 10^6 spores/ml in 2016 and 10^3 to 10^4 spores/ml in 2017. These results reflect the influence exerted by the natural weather conditions on the disease pressure. This demonstrated that year-to-year variations in disease severity are expected in wheat plants given the same concentration of inoculum. In a more practical way, this information could be integrated with environmental disease risk models in a Wheat Disease Forecasting System.

Identification and quantification of airborne wheat pathogens were possible using the microscopy analyses. However, difficulties were encountered using this method because of similarities between the three rust asexual spores and the trap height set up for *Ptr* and *Fg*. The highest asexual spore numbers counted using this method were 429 spores in one sample for *Pst*, and the lowest was for *Ptr* and *F.spp* with absence of asexual spores in many samples. Microscopy results showed that *Ptr* and *F.spp* asexual spores were rarely present at 1 m above ground. This result suggests that the asexual spore of *Fg* might be the source of initial infection in some cases, but it is not the primary inoculum of wheat heads, as confirmed by Fernando et al. (2000).

Both identification and quantification of the six airborne wheat pathogens were possible using qPCR. After optimization of the qPCR methodology, the analyses were consistent and reliable because of the highly pathogen-specific PCR primers used. These PCR primers were able to detect as few as 1 spore for the three rusts and *Bgt*, 3 spores for *Ptr*, and 35 spores for *Fg*. qPCR results for all eight locations sampled in Southern Alberta showed that *Fg* was the most predominant inoculum with an average of 866 spores/sample. The lowest level of inoculum was for *Pgt* with an average of 3 spores/sample. Among the three rusts *Pst* was the most predominant. Results varied according to year and location but spore numbers for all six pathogens were higher in 2016 and lower in 2017 because of the warmer and drier weather. The identification of pathogen spores in air currents is important for the recognition of the local pathogens and for application of an adequate disease control method for each specific pathogen.

Prevailing winds in Alberta are likely influencing the trajectories of rust spores and illustrate the importance of employing multiple sampling points and consecutive sampling years for a more accurate understanding disease development in Southern

Alberta. Pathogen spore concentrations must be kept below the minimum threshold in order to prevent disease epidemics in susceptible wheat cultivars. These results provide information, in conjunction with available weather data, for the development of a Wheat Disease Forecasting System to predict possible disease development before the first signs of the disease appear on the wheat plants.

References

AAF (Alberta Agriculture and Forestry) 2015. Current and historical Alberta weather station data viewer. https://agriculture.alberta.ca/acis/weather-data-viewer/graph.jsp?stations=2154&elements=PRCIP,ATX&startdate=20150601&enddate=20150830&interval=DAILY&precipunit=mm (last access: Jun16, 2018).

AAF (Alberta Agriculture and Forestry) 2016 A. Current and historical Alberta weather station data viewer. http://www.agric.gov.ab.ca/acis/weather-data-viewer/graph.jsp?Stations =2154&elements=PRCIP,ATN,DEW&startdate=20160624&enddate=20160713& interval= DAILY&precipunit=mm (last access: Jan 26, 2018).

AAF (Alberta Agriculture and Forestry) 2016 B. Current and historical Alberta weather station data viewer. https://agriculture.alberta.ca/acis/weather-data-viewer/graph.jsp?stations=2154&elements=PRCIP,ATX&startdate=20160601&enddate=20160830&interval=DAILY&precipunit=mm (last access: Jun 16, 2018).

AAF (Alberta Agriculture and Forestry) 2016 C. Current and historical Alberta weather station data viewer. https://agriculture.alberta.ca/acis/weather-data-viewer/graph.jsp?stations=9815&elements=ATX,PRCIP,HX&startdate=20160601&enddate=20160831&interval=DAILY&precipunit=mm (last access: Jun 16, 2018).

AAF (Alberta Agriculture and Forestry) 2016 D. Current and historical Alberta weather station data viewer. https://agriculture.alberta.ca/acis/weather-data-viewer/graph.jsp?stations=9942&elements=ATX,PRCIP,HX&startdate=20160601&enddate=20160831&interval=DAILY&precipunit=mm (last access: Jun 16, 2018).

AAF (Alberta Agriculture and Forestry) 2017 A. Current and historical Alberta weather station data viewer. http://www.agric.gov.ab.ca/acis/weather-data-viewer/graph.jsp?stations =21 54&elements=PRCIP,ATN,DEW&startdate=20170706&enddate=20170720& interval= DAILY&precipunit=mm (last access: Jan. 26, 2018).

AAF (Alberta Agriculture and Forestry) 2017 B. Current and historical Alberta weather station data viewer. https://agriculture.alberta.ca/acis/weather-data-viewer/graph.jsp?stations=2154&elements=PRCIP,ATX&startdate=20170601&enddate=20170830&interval=DAILY&precipunit=mm (last access: Jun 16, 2018).

AAF (Alberta Agriculture and Forestry) 2017 C. Current and historical Alberta weather station data viewer. https://agriculture.alberta.ca/acis/weather-data-viewer/graph.jsp?stations=9815&elements=ATX,PRCIP,HX&startdate=20170601&enddate=20170831&interval=DAILY&precipunit=mm (last access: Jun 16, 2018).

AAF (Alberta Agriculture and Forestry) 2017 D. Current and historical Alberta weather station data viewer. https://agriculture.alberta.ca/acis/weather-data-viewer/graph.jsp?stations=9942&elements=ATX,PRCIP,HX&startdate=20170601&enddate=20170831&interval=DAILY&precipunit=mm (Jun 16, 2018).

AAF (Alberta Agriculture and Forestry) 2017 E. Mean wind speed and prevailing direction (June, July and August): 1971 to 2000. https://www1.agric.gov.ab.ca/$department/dept docs.nsf/all/sag6452?opendocument (last access: June 18, 2018).

AAFC (Agriculture and Agri-Food Canada) 2015 A. New hope in fight to protect global wheat supply from Ug99 stem rust. http://www.agr.gc.ca/eng/news/scientific-achievements-in-agriculture/cereals-and-pulses/new-hope-in-the-fight-to-protect-global-wheat-supply-from-ug99-stem-rust/?id=1382645939207 (last access: Mar 4, 2018).

AAFC (Agriculture and Agri-Food Canada) 2015 B. From a single seed – tracing the Marquis wheat success story in Canada to its roots in Ukraine. http://www.agr.gc.ca/eng/news/ scientific-achievements-in-agriculture/from-a-single-seed-tracing-the-marquis-wheat-success-story-in-canada-to-its-roots-in-ukraine-4of11/?id=1181305178350 (last access: Feb 26, 2018).

AAFC (Agriculture and Agri-food Canada) 2016. Canada: outlook for principal field crops, February 16, 2016. http://www.agr.gc.ca/eng/industry-markets-and-trade/market-information-by-sector/crops/outlook-for-principal-field-crops-in-canada/canada-outlook-for-principal-field-crops-february-16-2016/?id=1455720699951 (last access: Jan 25, 2018).

Abdullah S, Sehgal SK, Jin Y, Turnipseed B, Ali S. 2017. Insights into tan spot and stem rust resistance and susceptibility by studying the pre-green revolution global collection of wheat. Plant Pathol J. 33:125-132.

Aboukhaddour R. 2017. Stripe rust in Canada. Alberta Wheat Commission. http://www.alberta wheat.com/media/blog-the-wheat-sheaf/stripe-rust-in-canada (last access: Nov 27, 2017).

Aboukhaddour R, Turkington TK, Strelkov SE. 2013. Race structure of *Pyrenophora tritici-repentis* (tan spot of wheat) in Alberta, Canada. Can J Plant Pathol. 35:256-268.

Agrios GN. 2005. Plant Pathology (5th edition). San Diego, CA: Elsevier-Academic Press.

Alcázar P, Comtois P. 1999. A new adhesive for airborne pollen sampling. Aerobiology. 15:105-108.

Alcázar P, Galán C, Carinanos P, Dominguez-Vilches. 2003. A new adhesive for airborne pollen sampling in Spain. Aerobiology. 19:57-61.

Andrie RM, Pandelova I, Ciuffetti LM. 2007. A combination of phenotypic and genotypic characterization strengthens *Pyrenophora tritici-repentis* race identification. Phytopathology. 97:694-701.

Bailey KL, Gossen BD, Gugel RK, Morrall RAA. 2009. Diseases of field crops in Canada (3rd edition, second printing). Saskatoon, SK: Houghton Boston. Published by The Canadian Phytopathological Society.

Baka ZAM, Rabei S. 2013. Morphology of uredinia and urediniospores of seven *Puccinia* species attacking Poaceae in Egypt. Egypt J Bot. 3:407-421.

Bayer. 2018. *Blumeria graminis f. sp. tritici*. https://www.cropscience.bayer.com/en /crop-compendium/pests-diseases-weeds/diseases/blumeria-graminis-f-sp-tritici (last access: Feb 22, 2018).

Beddow JM, Pardey PG, Chai Y, Hurley TM, Kriticos DJ, Braun HJ, Park RF, Cuddy WS, Yonow T. 2015. Research investment implications of shifts in global geography of wheat stripe rust. Nat Plants. 1:1-5.

Benslimane H. 2014. Simple method to produce *in vitro Pyrenophora tritici-repentis* teleomorph. Plant Pathol J. 30:437-439.

Benslimane H, Aouali S, Khalfi A, Ali S, Bouznad Z. 2017. *In vitro* morphological characteristics of *Pyrenophora tritici-repentis* isolates from several Algerian agro-ecological zones. Plant Pathol J. 33:109-117.

Beyer M, Roding S, Ludewig A, Verreet JA. 2004. Germination and survival of *Fusarium graminearum* macroconidia as affected by environmental factors. J Pythopathol. 152:92-97.

Bock CH, El Jarroudi M, Kouadio LA, Mackels C, Chiang KS, Delfosse P. 2015. Disease severity estimates-effects of rate accuracy and assessment methods for comparing treatments. Plant Dis. 99:1104-1112.

Boodly JW, Sheldrake RJr. 1972. Cornell peat-lite mixes for commercial plant growing. Plant Sciences: information bulletin. Cornell University, Ithaca, NY. 43:1-8.

Brar GS, Graf R, Knox R, Campbell H, Kutcher HR. 2017. Reaction of differential wheat and triticale genotypes to natural stripe rust [*Puccinia striiformis f. sp. tritici*] infection in Saskatchewan, Canada. Can J Plant Pathol. 39:138-148.

Brar GS, Kutcher HR. 2016. Race characterization of *Puccinia striiformis f. sp. tritici*, the cause of wheat stripe rust, in Saskatchewan and Southern Alberta, Canada and virulence comparison with races from United States. Plant Dis. 100:1744-1753.

CAFTA (Canadian Agri-Food Trade Alliance) 2018. Agri-food exports. http://cafta.org/agri-food-exports/ (last access: Jan 12, 2018).

Cao X, Yao D, Zhou Y, West JS, Xu X, Luo Y, Ding K, Fan J, Duan X. 2016. Detection and quantification of airborne inoculum of *Blumeria graminis* f. sp. *tritici* using quantitative PCR. Eur J Plant Pathol. 146:225-229.

Charmley LL, Trenholm HL. 2017. Fact sheet – Mycotoxins. http://www.inspection.gc.ca/ animals/feeds/regulatory-guidance/rg-8/eng/1347383943203/1347384015909?chap=1 (last access: Mar 2, 2018).

Chen W, Wellings C, Chen X, Kang Z, Liu T. 2014. Wheat stripe (yellow) rust caused by *Puccinia striiformis* f. sp. *tritici*. Mol Plant Pathol. 15:433-446.

Chen X. 2013. Review article: high-temperature adult-plant resistance, key for sustainable control of stripe rust. Am J Plant Sci. 4:608-627.

Chen X, Penman L, Wan A, Cheng P. 2010. Virulence races of *Puccinia striiformis* f. sp.*tritici* 2006 and 2007 and development of wheat stripe rust and distributions,

dynamics, and evolutionary relationships of races from 2000 to 2007 in the United States. Can J Plant Pathol. 32:315-333.

Chen XM. 2005. Epidemiology and control of stripe rust [*Puccinia striiformis* f. sp. *tritici*] on wheat. Can J Plant Pathol. 27:314-337.

Chen XM. 2007. Challenges and solutions for stripe rust control in the United States. Aust J Agric Res. 58:648-655.

Chisholm ST, Coaker G, Day B, Staskawicz BJ. 2006. Host-microbe interactions: Shaping the evolution of the plant immune response. Cell. 124:803-814.

Chomczynski P, Rymaszewski M. 2006. Alkaline polyethylene glycol-based method for direct PCR from bacteria, eukaryotic tissue samples, and whole blood. BioTechiniques. 40:454-458.

Ciuffetti LM, Tuori RP. 1999. Advances in the characterization of the *Pyrenophora tritici-repentis*-wheat interaction. Phytopathology. 89:444-449.

Comtois P, Mandrioli P. 1997. Pollen capture media: a comparative study. Aerobiology. 13:149-154.

Conner RL, Kuzyk AD, Su H. 2003. Impact of powdery mildew on the yield of soft white spring wheat cultivars. Can J Plant Sci. 83:725-728.

Conner RL, Thomas JB, Kuzyk AD. 1988. Overwintering of stripe rust in Southern Alberta. Can Plant Dis Surv. 68:153-155.

Costamilan LM. 2005. Variability of the wheat powdery mildew pathogen *Blumeria graminis* f. sp. *tritici* in the 2003 crop season. Fitopatol Bras. 30:420-422.

Cunnington J, Takamatsu S. 2003. Molecular identification of anamorphic powdery mildew (*Erysiphales*). Aust Plant Pathol. 32:421-428.

Cuomo CA, Bakkeren G, Khalil HB, Panwar V, Joly D, Linning R, Sakthikumar S, Song X, Adiconis X, Fan L, Goldberg JM, Levin JZ, Young S, Zeng Q, Anikster Y, Bruce M, Wang M, Yin C, McCallum B, Szabo LJ, Hulbert S, Chen X, Fellers JP. 2017.

Comparative analysis highlights variable genome content of wheat rusts and divergence of the mating loci. G3: Gen Genom Genet. 7:361-376.

David A, Botías C, Abdul-Sada A, Nicholls E, Rotheray EL, Hill EM, Goulson D. 2016. Widespread contamination of wildflower and bee-collected pollen with complex mixtures of neonicotinoids and fungicides commonly applied to crops. Environ Int. 88:169-178.

De Wolf E. 2008. Tan spot. https://www.plantpath.k-state.edu/extension/publications/tan-spot-ep134.pdf (last access: Jan 14, 2018).

Djian-Caporalino C, Palloix A, Fazari A, Marteu N, Barbary A, Abad P, Sage-Palloix AM, Mateille T, Risso S, Lanza R, Taussig C, Castagnone-Sereno P. 2014. Pyramiding, alternating or mixing: comparative performances of deployment strategies of nematode resistance genes to promote plant resistance efficiency and durability. BMC Plant Biol. 14:53.

DPIRD (Department of Primary Industries and Regional Development) 2016. Diagnosing leaf rust of wheat. https://www.agric.wa.gov.au/mycrop/diagnosing-leaf-rust-wheat (last access: Mar 4, 2018).

DPIRD (Department of Primary Industries and Regional Development) 2017. Managing powdery mildew in wheat. https://www.agric.wa.gov.au/spring/managing-powdery-mildew-wheat (last access: Mar 4, 2018).

Dubin HJ, Brennan JP. 2009. Combating stem rust and leaf rust of wheat: Historical perspective, impacts, and lessons learned. International Food Policy Research Institute. Discussion paper series 00910.

Duveiller E, Singh PK, Mezzalama M, Singh RP, Dababat A. 2012. Wheat diseases and pests: A guide for field identification (2nd edition). Mexico, DF: CIMMYT.

Esmail SM, Draz IS. 2017. Fungal morphogenesis tracking of *Blumeria graminis f. sp. tritici* on leaf freed of epicuticular wax using scanning electron microscopy. Intl J Microbiol Biothecnol. 2:181-188.

Eversmeyer MG, Kramer CL. 2000. Epidemiology of wheat leaf and stem rust in the Central Great Plains of the USA. Annu Rev Phytopathol. 38:491-513.

Ezzahiri B, Diouri S, Roelfs AP. 1992. The role of the alternate host, *Anchusa italica*, in the epidemiology of *Puccinia recondita f. sp. tritici* on durum wheats in Morocco. In: Zeller FJ, Fischbeck G, editors. Proceedings of the 8th European and Mediterranean Cereal Rusts and Mildews Conference. Weihenstephen, Germany: Vortrage fur Pflanzenzuchtung (Society of Plant Breeding), p. 69–70.

FAO (Food and Agriculture Organization of the United Nations) 2010. Wheat stem rust – Ug99 (race TTSKS). http://www.fao.org/agriculture/crops/rust/stem/rust-report/stem-ug99racettksk/en/ (last access: Mar 4, 2018).

Faris JD, Liu Z, Xu SS. 2013. Genetics of tan spot resistance in wheat. Theor Appl Genet. 126:2197-2217.

Fernandez MR, Clarke FR, Knox RE, Clarke JM, Singh AK. 2010. Quantification of effects of leaf spotting diseases on grain yield and market quality of durum wheat using near-isogenic lines TCJP. Can J Plant Pathol. 32:177-187.

Fernandez MR, Stevenson CF, Hodge K, Dokken-Bouchard, Pearse PG, Waelchli F, Brown A, Peluola C. 2016. Assessing effects of climatic change, region and agronomic practices on leaf spotting of bread and durum wheat in Western Canada Prairies, from 2001 to 2012. Agron J. 108:1180-1195.

Fernando WGD, Miller JD, Seaman WL, Seifert K, Paulitz TC. 2000. Daily and seasonal dynamics of airborne spores of *Fusarium graminearum* and other *Fusarium* species sampled over wheat plots. Can J Bot. 78:497-505.

Fetch T, McCallum B, Menzies J, Rashid K, Tenuta A. 2011. Rust diseases in Canada. Prairie Soils Crops J. 4:86-96.

Fowler K. 2014. Yellow (leaf) spot. http://www.croppro.com.au/crop_disease_manual /ch02s10.php (last access: Mar 3, 2018).

Francl LJ. 2001. The Disease Triangle: A plant pathological paradigm revisited. The Plant Health Instructor. https://www.apsnet.org/edcenter/instcomm /TeachingArticles/Pages/ DiseaseTriangle.aspx (last access: Jan 27, 2018).

Friesen TL, Stukenbrock EH, Liu Z, Meinhardt S, Ling H, Faris JD, Rasmussen JB, Solomon PS, McDonald BA, Oliver RP. 2006. Emergence of a new disease as a result of interspecific virulence gene transfer. Nat Genet. 38:953-956.

Galán C, Dominguez-Vilches E. 1997. The capture media in aerobiological sampling. Aerobiologia. 13:155-160.

Gaudet DA, Frick MJ, Kundrik K, Amundsen E. 2015. 2014 Stripe rust survey in Southern Alberta. Can Plant Dis Surv. 95:108-109.

Gautam P, Dill-Macky R. 2012. Impact of moisture, host genetics and *Fusarium graminearum* isolates on Fusarium head blight development and trichothecene accumulation in spring wheat. Mycot Res. 28:45-58.

Geo for CXC 2016. Wheat farming in Canada. http://www.geoforcxc.com/economic-activities/wheat-farming-in-canada/ (last access: Feb 26, 2018).

Ghemawat MS. 1979. Seedling resistance to wheat powdery mildew fungus, *Erysiphe graminis f. sp. tritici*. I. Resistance of first leaves. Mycopathologia. 68:131-137.

Glass GV, Peckham PD, Sanders JR. 1972. Consequences of failure to meet assumption underlying the fixed effects analyses of variance and covariances. Rev Educ Res. 43:237-288.

Goswami RS, Kistler HC. 2004. Heading for disaster: *Fusarium graminearum* on cereal crops. Mol Plant Pathol. 5:515-525.

Government of Saskatchewan. 2018. Fusarium Head Blight. https://www.saskatchewan.ca/business/agriculture-natural-resources-and-industry/agribusiness-farmers-and-ranchers/crops-and-irrigation/crop-protection/disease/fusarium-head-blight (last access: Jan 4, 2018).

Gräfenhan T, Patrick SK, Roscoe M, Trelka R, Gaba D, Chan JM, McKendry T, Clear RM, Tittlemier. 2013. Fusarium damage in cereal grains from Western Canada. 1. Phylogenetic analysis of moniliformin-producing *Fusarium* species and their natural occurrence in mycotoxin-contaminated wheat, oats, and rye. J Agric Food Chem. 61:5425-5437.

Green SB, Salkind NJ. 2017. Using SPSS for Windows and Macintosh: Analyzing and understanding data (8th edition). New York, US: Pearson Education Inc., p. 130-184

Guarín FA, Abril MAQ, Alvarez A, Fonnegra R. 2015. Atmospheric pollen and spore content in the urban area of the city of Medellin, Colombia. Hoehnea. 42:9-19.

Harris LJ, Balcerzak M, Johnston A, Scheiderman D, Ouellet T. 2015. Host-preferential *Fusarium graminearum* gene expression during infection of wheat, barley, and maize. Fungal Biol. 120:111-123.

Heffer V, Johnson KB, Powelson ML, Shishkoff N. 2006. Identification of powdery mildew fungi anno 2006. The Plant Health Instructor. DOI: 10.1094/PHI-I-2006-0706-01.

Hershman DE. 1985. Leaf rust of wheat. https://uknowledge.uky.edu/anrreports/41/?utm_source= knowledge.uky.edu%2Fanr_reports%2F41&utm_medium=PDF&utm_campaign=PDFCoverPages (last access: Feb 27, 2018).

Hiratsuka Y, Sato S. 1982. Morphology and taxonomy of rust fungi. In: Scott K, Chakravorty AK, editors. The Rust Fungi. New York (NY): Academic Press, p. 1-36.

Hollomon D. 2002. Fungicides. In: Waller JM, Lenné JM, Waller SJ, editors. Plant pathologist's pocketbook (3rd edition). New York, USA: CABI Publishing, p. 336-344.

Holtz MD, Kumar K, Xi K. 2013. Virulence phenotypes of *Puccinia striiformis* in Alberta from 2009-2011. Can J Plant Pathol. 35:241-250.

Hosford Jr RM, Larez CR, Hammond JJ. 1987. Interaction of wet period and temperature on *Pyrenophora tritici-repentis* infection and development in wheats of differing resistance. Phytopathology. 77:1021-1027.

Huang XQ, Röder MS. 2004. Molecular mapping of powdery mildew resistance genes in wheat: A review. Euphytica. 137:203–223.

Huerta-Espino J, Singh RP, German S, McCallum BD, Park RF, Chen WQ, Bhardwaj SC, Goyeau H. 2011. Global status of wheat leaf rust caused by *Puccinia triticina*. Euphytica. 179:143-160.

Hutcheon JA, Jordan VWL. 1992. Fungicide timing and performance for *Fusarium* control in wheat. In: British crop protection council, Farnham editor. Brighton, England. Brighton crop protection conference: Pests and diseases, 2:633-638.

Ireta MJ, Gilchrist SL. 1994. Fusarium head scab of wheat (*Fusarium graminearum* Schwabe). Wheat special report No. 21b. Mexico, D.F.: CIMMYT.

Isard SA, Barnes CW, Hambleton S, Ariatti A, Russo JM, Tenuta A, Gay DA, Szabo LJ. 2011. Predicting soybean rust incursions into the North American continental interior using crop monitoring, spore trapping, and aerobiological modeling. Plant Dis. 95:1346-1357.

Jankovics T, Komaromi J, Fabian A, Jager K, Vida G, Kiss L. 2015. New insights into the life cycle of the wheat powdery mildew: direct observation of ascosporic infection in *Blumeria graminis f. sp. tritici*. Phytopathology. 105:797-804.

Jin Y, Szabo LJ, Carson M. 2010. Century-old mystery of *Puccinia striiformis* life history solved with the identification of *Berberis* as an alternate host. Phytopathology. 100:432-435.

Keller MD, Bergstrom GC, Shields EJ. 2014. The aerobiology of *Fusarium graminearum*. Aerobiologia. 30:123-136.

Kelly HM. 2016. Rusts and other diseases to be on the lookout for in wheat. http://news.utcrops.com/2016/03/rusts-diseases-lookout-wheat/ (last access: Mar 4, 2018).

Khan RR, Bariana HS, Dholakia BB, Naik SV, Lagu MD, Rathjen AJ, Bhavani S, Gupta VS. 2005. Molecular mapping of stem and leaf rust resistance in wheat. Theor Appl Genet. 111:846-850.

Kikot GE, Moschini R, Consolo VF, Rojo R, Salerno G, Hours RA, Gasoni L, Arambarri AM, Alcanada TM. 2011. Occurrence of different species of fusarium from wheat in relation to disease levels predicted by a weather-based model in Argentina Pampas region. Mycopathology. 171:139-149.

Kumar K, Holtz MD, Xi K, Turkington TK. 2013. Overwintering potential of the stripe rust pathogen (*Puccinia striiformis*) in central Alberta. Can J Plant Pathol. 35:304-314.

Laerd Statistics. 2013. Sphericity. https://statistics.laerd.com/statistical-guides/sphericity-statistical-guide.php (last access: Apr 12, 2018).

Lagudah E, Pretorius Z. 2013. Australian wheat has a new defence to a rusty old problem. The Conversation. http://theconversation.com/australian-wheat-has-a-new-defence-to-a-rusty-old-problem-15960 (last access: Jul 12, 2018).

Leslie JF, Summerell BA. 2006. The *Fusarium* laboratory manual. Blackwell Publishing, p. 176.

Liu M, Hambleton S. 2010. Taxonomic study of stripe rust, *Puccinia striiformis sensu lato*, based on molecular and morphological evidence. Fungal Biol. 114:881-899.

Liu M, McCabe E, Chapados JT, Carey J, Wilson SK, Tropiano R, Redhead SA, Lévesque CA, Hambleton S. 2015. Detection and identification of selected cereal rust pathogens by TaqMan® real-time PCR. Can J Plant Pathol. 37:92-105.

Liu M, Szabo LJ, Hambleton S, Anikster Y, Kolmer JA. 2013. Molecular phylogenetic relationships of the brown leaf rust fungi on wheat, rye, and other grasses. Plant Dis. 97:1408-1417.

Lubeck M, Lubeck PS. 1996. PCR-based methods – A promising tool for detection and identification of fungi in soil. In: Jensen DF, Jansson HB, Tronsmo A, editors. Monitoring antagonistic fungi deliberately released into the environment. Kluwer Academic Publishers, p. 113-121.

Marone D, Russo MA, Laidò G, De Vita P, Papa R, Blanco A, Gadaleta A, Rudiales D, Mastrangelo AM. 2013. Genetic basis of qualitative and quantitative resistance to powdery mildew in wheat: from consensus regions to candidate genes. BMC Genom. 14:562.

Martens G, Lamari L, Grieger A, Gulden RH, McCallum B. 2014. Comparative yield, disease resistance and response to fungicide for forty-five historic Canadian wheat cultivars. Can J Plant Sci. 94:371-381.

Martin RA, Clough KS, Johnston HW. 1984. Vertical and horizontal distribution of conidia of *Pyrenophora teres* in barley fields. Can J Plant Pathol. 6:280-282.

Martinelli F, Scalenghe R, Davino S, Panno S, Scuderi G, Ruisi P, Villa P, Stroppiana D, Boschetti M, Goulart LR, Davis CE, Dandekar AM. 2015. Advanced methods of plant disease detection. A review. Agron Sustain Dev. 35:1-25.

Martinez JP, Ottum SA, Ali S, Francl LJ, Ciuffetti LM. 2001. Characterization of ToxB gene from *Pyrenophora tritici-repentis*. Mol Plant-Microbe Interac. 14:675-677.

McCallum B, Fetch TJr, Seto-Goh P, Xi K, Turkington TK. 2006. Stripe rust of wheat and barley in Manitoba, Saskatchewan and Alberta in 2005. Can Plant Dis Surv. 86:50.

McCallum BD, Hiebert CW, Cloutier S, Bakkeren G, Rosa SB, Humphreys DG, Marais GF, McCartney CA, Panwar V, Rampitsch C, Saville BJ, Wang X. 2016. A review of wheat leaf rust research and the development of resistant cultivars in Canada. Can J Plant Pathol. 38:1-18.

McDonald JH. 2014. Data transformations. In: Handbook of Biological Statistics (3rd edition). Baltimore, USA: Sparky House Publishing, p. 140-144.

McGrath MT. 2004. What are fungicides? The Plant Health Instructor. DOI: 10.1094/PHI-I-2004-0825-01.

McInnis M. 2015. Canadian economic development in the wheat boom era: a reassessment. http://qed.econ.queensu.ca/faculty/mcinnis/Cda development1.pdf (last access: Dec 10, 2017).

McIntosh RA, Wellings CR, Park RF. 1995. Wheat rusts: An atlas of resistance genes. Victoria, AU: CSIRO Publications, p. 8.

McKie R, Rice X. 2007. Millions face famine as crop disease rages. https://www.theguardian. com/science/2007/apr/22/food.foodanddrink (last access: Mar 4, 2018).

McMullen M, Adhikari T. 2009. Fungal leaf spot diseases of wheat: tan spot, *stagonospora nodorum* blotch and *septoria tritici* blotch. https://www.ag.ndsu.edu/publications/crops/funga l-leaf-spot-diseases-of-wheat-tan-spot-septoria-stagonospora-nodorum-blotch-and-septoria-tritici-blotch/pp1249.pdf (last access: Jan 4, 2018).

McNeal FH, Konzak CS, Smith EP, Tate WS, Russell TS. 1971. A uniform system for recording and processing cereal data. USDA, Washington: ARS Bulletin, 34:121-143.

Mills K, Salgado JD, Paul A. 2016. Fusarium head blight or head scab of wheat, barley and other small grain crops. https://ohioline.osu.edu/factsheet/plpath-cer-06 (last access: Mar 3, 2018).

Milus G, DeWolf E, Dill-Macky R, Steffeson B, Wegulo S, Bergstrom G, Sorrells M, McMullen M, Paul P, Hunger R, Mundt C, Isard S, Stein J, Murray T, Baker H, Bulluck R, Divan C, Engle J, Hebbar P, Bowden B, Carson M, Chen X, Jin Y, Marshall D, Smith K, Szabo L, Draper M. 2010. Recovery plan for stem rust of wheat. https://www.ars.usda.gov/ARSUserFiles/opmp/Wheat%20Stem%20Rust%20Ug99%20101016.pdf (last access: Feb 28, 2018).

Moffat CS, See PT, Oliver RP. 2014. Generation of ToxA knockout strain of the wheat tan spot pathogen *Pyrenophora tritici-repentis*. Mol Plant Pathol. 15:918-926.

Mongrain D, Couture L, Comeau A. 2000. Natural occurrence of *Fusarium graminearum* on adult wheat midge and transmission to wheat spikes. Cereal Res Commun. 28:173-180.

Nicolaisen M, Suproniene S, Nielsen LK, Lazzaro I, Spliid NH, Justesen AF. 2009. Real-time PCR for quantification of eleven individual *Fusarium* species in cereals. J Microbiol Meth. 76:234-240.

Núñez A, Amo de Paz G, Ferencova Z, Rastrojo A, Guantes R., García AM, Alcamí A, Gutiérrez-Bustillo M, Moreno DA. 2017. Validation of the Hirst-type spore trap for simultaneous monitoring of prokaryotic and eukaryotic biodiversities in urban air samples by next-generation sequencing. Appl Environ Microbiol. 83:1-14.

Oerke EC. 2006. Crop losses to pests. J Agric Sci. 144:31-43.

Orton ES, Brown JKM. 2016. Reduction of growth and reproduction of the biotrophic fungus *Blumeria graminis* in the presence of a necrotrophic pathogen. Front Plant Sci. 7:1-12.

Pandey P, Irulappan V, Bagavathiannan MV, Senthil-Kumar M. 2017. Impact of combined abiotic and biotic stresses on plant growth and avenues for crop improvement by exploiting physio-morphological traits. Front Plant Sci. 8:537.

Parks WR, Booth W, Cowger C. 2011. Characterization of polymorphic microsatellite loci of *Blumeria graminis f. sp. tritici*, the cause of powdery mildew of wheat. Mol Ecol Resour. 11:586-589.

Peterson DP. 2013. "The barberry of bread" – The public campaing to eradicate common barberry in the United States in the early 20th century. http://www.apsnet.org/publications /apsnetfeatures/Pages/Barberry.aspx (last access: Feb 28, 2018).

Phan HTT, Rybak K, Furuki E, Breen S, Solomon PS, Oliver RP, Tan KC. 2016. Differential effector gene expression underpins epistasis in plant fungal disease. Plant J. 87:343-354.

Pilet-Nayel ML, Moury B, Caffier V, Montarry J, Kerlan MC, Fournet S, Durel CE, Delourme R. 2017. Quantitative resistance to plant pathogens in pyramiding strategies for durable crop protection. Front Plant Sci. 8:1-9.

Rabbinge R, Jorritsma ITM, Schans J. 1985. Damage components of powdery mildew in winter wheat. Neth J P1ant Pathol. 91:235-247.

Randhawa HS, Asif M, Pozniak C, Clarke JM, Graf RJ, Fox SL, Humphreys DG, Knox RE, DePauw RM, Singh AK, Cuthbert RD, Hucl P, Spaner D. 2013. Application of molecular markers to wheat breeding in Canada. Plant Breed. 132:458-471.

Ransom JK, McMullen MV. 2007. Yield and disease control on hard winter wheat cultivars with foliar fungicides. Agr J. 100:1190-1137.

Rapilly F. 1979. Yellow rust epidemiology. Annu Rev Phytopathol. 17:59-73.

Regional Plant Disease Diagnostic Labs 2010. Identifying rust diseases of wheat and barley. http://www.ars.usda.gov/SP2UserFiles/ad_hoc/36400500Cerealrusts/ Rust_Diseases_National.pdf (accessed last: Mar 5, 2018).

Reischer GH, Lemmens M, Farnleitner A, Adler A, Mach RL. 2004. Quantification of *Fusarium graminearum* in infected wheat by species specific real-time PCR applying a TaqMan Probe. J Microbiol Meth. 59:141-146.

Riaz S, Tenscher AC, Ramming DW, Walker MA. 2011. Using a limited mapping strategy to identify QTLs for resistance to grapevine powdery mildew (*Erysiphe*

necator) and their use in marker-assisted breeding. Theor Appl Genet. 122:1059-1073.

Roelfs AP, Singh RP, Saari EE. 1992. Rust diseases of wheat: Concepts and methods of disease management. Mexico, DF: CIMMYT, p. 4-5.

Rong JK, Millet E, Manisterski J, Feldman M. 2000. A new powdery mildew resistance gene: Introgression from wild emmer into common wheat and RFLP-based mapping. Euphytica. 115:121-126.

Savile DBO. 1984. Taxonomy of cereal rust fungi. In: Bushnell WR, Roelfs AP (eds) The cereal rust: origins, specificity, structure, and physiology. United Kingdom, London: Academic Press Inc., p. 89-110.

Schmale III DG, Bergstrom GC. 2003. Fusarium head blight in wheat. http://www.apsnet.org/edcenter/intropp/lessons/fungi/ascomycetes/pages/fusarium.aspx (last access: Jan 15, 2018).

Scholthof KBG. 2007. The disease triangle: pathogens, the environment and society. Nat Rev Microbial. 5:152-156.

Simpfendorfer S. 2015. Think before you spray! https://grdc.com.au/news-and-media/news-and-media-releases/north/2015/07/think-before-you-spray (last access: Mar 4, 2018).

Singh RP, Hodson DP, Huerta-Espino J, Jin Y, Njau P, Wanyera R, Herrer-Foessel SA, Ward RW. 2008. Will stem rust destroy the world's wheat crop? Adv Agron. 98:271-309.

Statistics Canada 2016. Production of principal field crops, November 2016. http://www.statcan.gc.ca/daily-quotidien/161206/dq161206b-eng.pdf (last access: Jan 25, 2018).

Statistics Canada 2017 A. Farm cash receipts, January to September 2017. http://www.statcan. gc.ca/daily-quotidien/171124/dq171124c-eng.pdf (last access: Feb 26, 2018).

Statistics Canada 2017 B. Production of principal field crops, November 2017. http://www.statcan.gc.ca/daily-quotidien/171206/dq171206a-eng.htm (last access: Jan 25, 2018).

Strelkov SE, Lamari L. 2003. Host-parasite interactions in tan spot [*Pyrenophora tritici-repentis*] of wheat. Can J Plant Pathol. 25:339-349.

Su H, Conner RL, Graf RJ, Kuzyk AD. 2003. Virulence of *Puccinia striiformis* f.sp. *tritici*, cause of stripe rust on wheat, in Western Canada from 1984-2002. Can J Plant Pathol. 25:312-319.

Sykes EE, Bernier CC. 1991. Qualitative inheritance of tan spot resistance in hexaploid, tetraploid, and diploid wheat. Can J Plant Pathol. 13:38-44.

Takamatsu S, Kano Y. 2001. PCR primers useful for nucleotide sequencing of rDNA of the powdery mildew fungi. Mycoscience. 42:135-139.

Termorshuizen AJ. 2002. Cultural control. In: Waller JM, Lenné JM, Waller SJ, editors. Plant pathologist's pocketbook (3rd edition). New York, USA: CABI Publishing, p. 318-327.

Tittlemier SA, Roscoe M, Trelka R, Gaba D, Chan JM, Patrick SK, Sulyok M, Krska R, McKendry T, Gräfenhan T. 2013. Fusarium damage in small cereal grains from Western Canada. 2. Occurrence of *Fusarium* toxins and their source organisms in durum wheat harvested in 2010. J Agric Food Chem. 61:5438-5448.

Tsui CKM, Woodhall J, Chen W, Lévesque CA, Lau A, Schoen CD, Baschien C, Najafzadeh MJ, Sybren de Hoog G. 2011. Molecular techniques for pathogen identification and fungus detections in the environment. Ima Fungus. 2:177-189.

University of Saskatchewan 2018. Powdery mildew. https://www.usask.ca/agriculture/plantsci/ winter_cereals/winter-wheat-production-manual/chapter-22/powdery-mildew.php (last access: Mar 5, 2018).

USDA (United States Department of Agriculture). 2017. Wheat stem rust. https://www.ars.usda.gov/midwest-area/stpaul/cereal-disease-lab/docs/cereal-rusts/wheat-stem-rust/ (last access: Aug 14, 2018).

van Egmond HP, Schothorst RC, Jonker MA. 2007. Regulations relating to mycotoxins in food. Anal Bioanal Chem. 389:147-157.

Vickers G, Buzza S, Schmidt D, Mullock J. 2001. The weather of the Canadian Prairies: Graphic area forecast 32. NAV Canada, p.180-181.

Waalwijk C, van der Heide R, de Vries I, van der Lee T, Schoen C, Corainville GC, Hauser-Hahn I, Kastelein P, Kohl J, Lonnet P, Demarquet T, Kema GHJ. 2004. Quantitative detection of *Fusarium* species in wheat using TaqMan. Eur J Plant Pathol. 110:481-494.

Wan A, Zhao Z, Chen X, He Z, Jin S, Jia Q, Yao G, Yang J, Wang B, Li G, Bi Y, Yuan Z. 2004 Wheat stripe rust epidemic and and virulence of *Puccinia striiformis f. sp. tritici* in China in 2002. Plant Dis. 88:896-904.

Wegulo SN, Byamukama E. 2012. Rust diseases of wheat. http://extensionpublications.unl.edu/assets/pdf/g2180.pdf (last access: Feb 27, 2018).

Werner O, Ros RM, Guerra J. 2002. Direct amplification and NaOH extraction: two rapid and simple methods for preparing bryophyte DNA for polymerase chain reaction (PCR). J Bryol. 24:127-131.

West JS, Atkins SD, Emberlin J, Fitt BDL. 2008. PCR to predict risk of airborne disease. Trends Microbio. 16:380-387.

West JS, Kimber BRE. 2015. Innovations in air sampling to detect plant pathogens. Ann Appl Biol. 166:4-17.

Wharton P. 2011. Managing Fusarium head blight on wheat. http://msue.anr.msu.edu/news/managing_fusarium_head_blight_on_wheat (last access: Mar 5, 2018).

White TJ, Bruns T, Lee S, Taylor J. 1990. Amplification and direct sequencing of fungi ribosomal RNA genes for phylogenetics. In: Innis MA, Gelfand DH, Sninsky JJ, White TJ (eds) PCR protocols: A guide to methods and applications. New York: Academic Press, p. 315-322.

Wicker T, Oberhaensli S, Parlange F, Buchmann JP, Shatalina M, Roffler S, Ben-David R, Doleže J, Šimková H, Schulze-Lefert P, Spanu PD, Bruggmann R, Amselem J,

Quesneville H, Ver Loren van Themaat E, Paape T, Shimizu KK, Keller B. 2013. The wheat powdery mildew genome shows the unique evolution of an obligate biotroph. Nat Genet. 45:1092-1096.

Wightwick AM, Bui AD, Zhang P, Rose G, Allinson M, Myers JH, Reichman SM, Menzies NW, Pettigrove V, Allinson G. 2012. Environmental fate of fungicides in surface waters of a horticultural-production catchment in southeastern Australia. Arch Environ Contam Toxcol. 62:380-390.

WSU (Washington State University). 2015. Greenhouse protocols for handling and testing stripe rust. http://striperust.cw.wsu.edu/wp-content/uploads/sites/16/2015 /12/Greenhouse-Protocols- for-Testing-and-Handling-Stripe-Rust.pdf (last access: Nov 20, 2017).

WSU (Washington State University). 2018. Disease management: control. http://striperust.wsu.edu/disease-management/control/ (last access: Jan 27, 2018).

Xi K, Turkington TK, Salmon D, McCallum BD, Navabi A. 2015. Stripe Rust 101: What is it, why do we have it, what can be done about it. Government of Alberta, Agriculture and Rural Development. http://www1.agric.gov.ab.ca/$department/ deptdocs.nsf/all/prm11383 (last access: Mar 3, 2018).

Xia C, Wang M, Yin C, Cornejo OE, Hulbert SH, Chen X. 2018. Genome sequence resources for the wheat stripe rust pathogen (*Puccinia striiformis f. sp. tritici*) and the barley stripe rust pathogen (*Puccinia striiformis f. sp. hordei*). Mol Plant Microbe Interact. DOI: 10.1094/MPMI-04-18-0107-A.

Zadoks JC, Chang TT, Konzak CF. 1974. A decimal code for the growth stages of cereal. Weed Res. 14:415-421.

Appendix 1 –Stripe rust spores diluted with Soltrol® 170 Isoparaffin for inoculation of the different treatments.

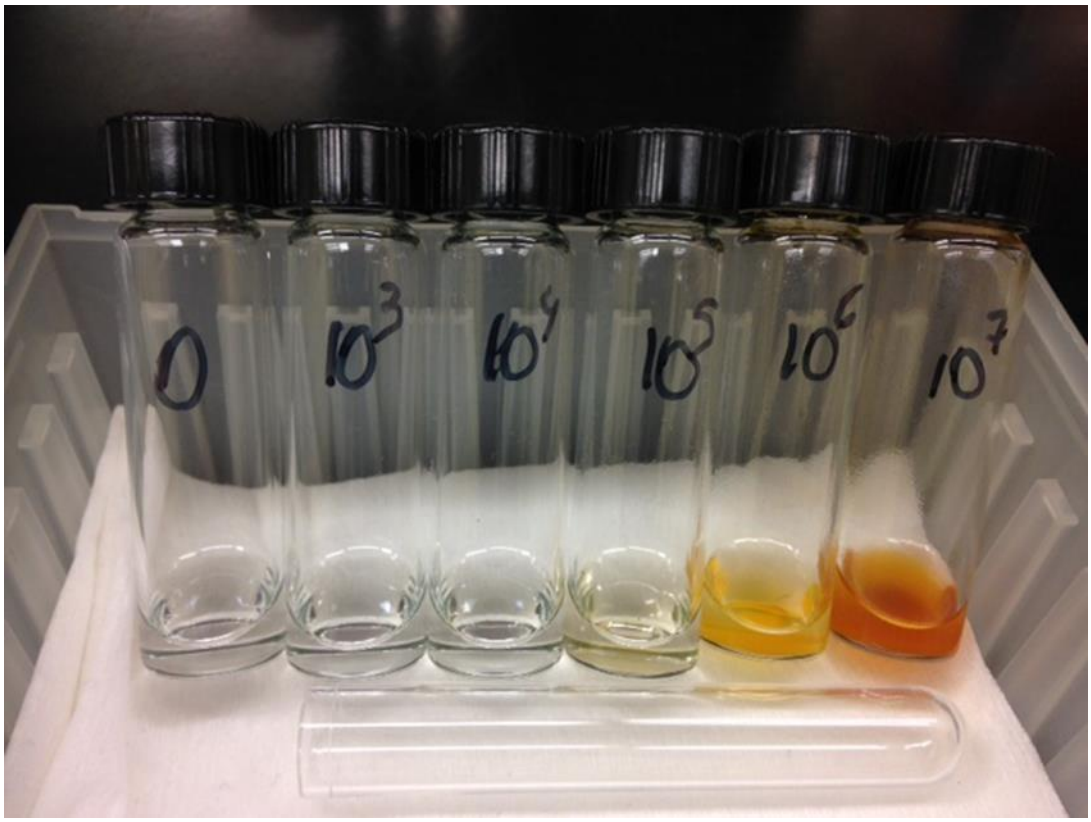

Appendix 2 – Sprayer used for wheat pathogens inoculation. A) Front view of the sprayer atomizer with stripe rust spores diluted with Soltrol® 170 Isoparaffin. B) Inoculation of wheat seedling using the sprayer atomizer. C) Side view of the sprayer atomizer and the handle of the air compressor used for inoculation. Pictures taken by Eric Amundsen**.**

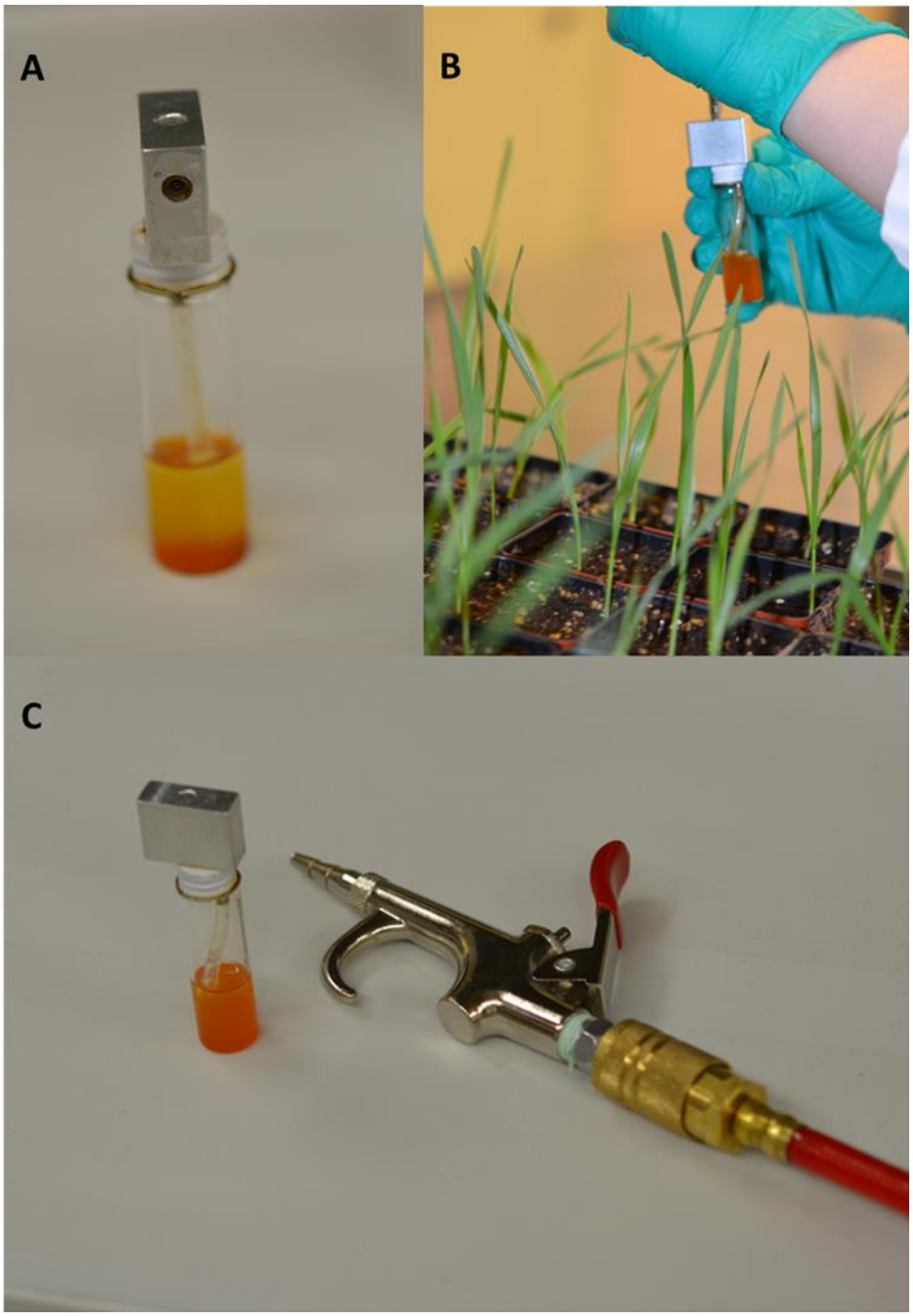

Appendix 3 – Descriptive statistics of the results from both trials of stripe rust disease severity (0-100% scale) under growth chamber conditions.

Trials	Ratings	Means	Standard deviation
One	**One**	**9.9**	**12.9**
	Two	**24.5**	**18**
	Three	**40.7**	**22.6**
Two	**One**	**8.1**	**11.9**
	Two	**17.2**	**19.1**
	Three	**35.9**	**27.5**

Appendix 4 – Descriptive statistics of the results of both trials of powdery mildew disease severity (0-100% scale) under growth chamber conditions.

Trials	Ratings	Means	Standard deviation
One	**One**	**5.5**	**12.6**
	Two	**21.3**	**26.7**
	Three	**26.8**	**29.7**
Two	**One**	**2.6**	**5.5**
	Two	**12.7**	**16.1**
	Three	**25.2**	**24.2**

Appendix 5 – View of Burkard Cyclone One-vial instrument set up in the field and connected to a battery (inside the plastic box) and solar panel.

Appendix 6 – Adhesive tape trap. A) Field slide covered with double-sided adhesive tape and B) Grid slide (with a defined area of 40 quadrants of 5 mm x 5 mm in size) used underneath the field slides to facilitate orientation on the slide while counting the spores.

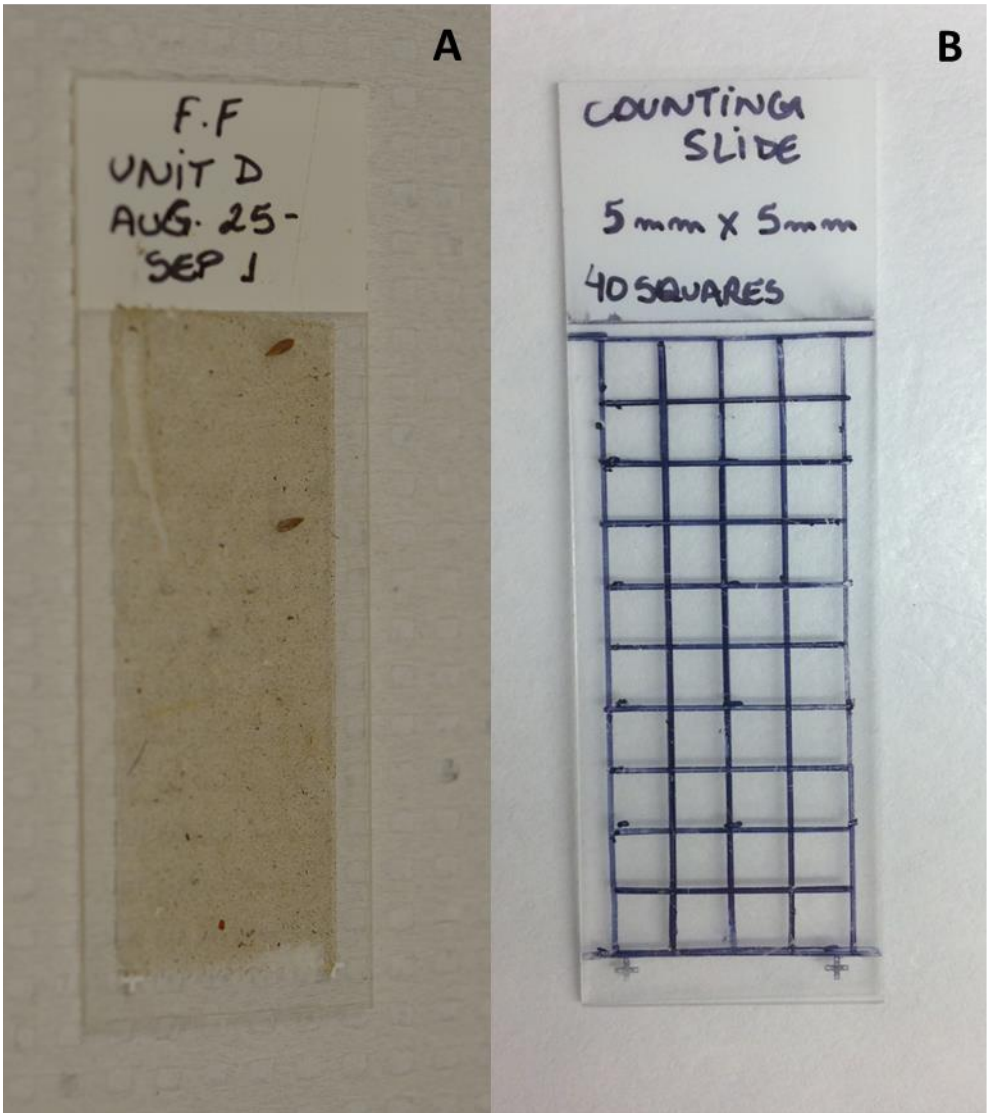

Appendix 7 – View of spore morphology under a light microscope (200 X). A) *Pst*, B) *Pt*, C) *Pg*, D) *Bgt*, E) *Ptr*, and F) *Fg*.

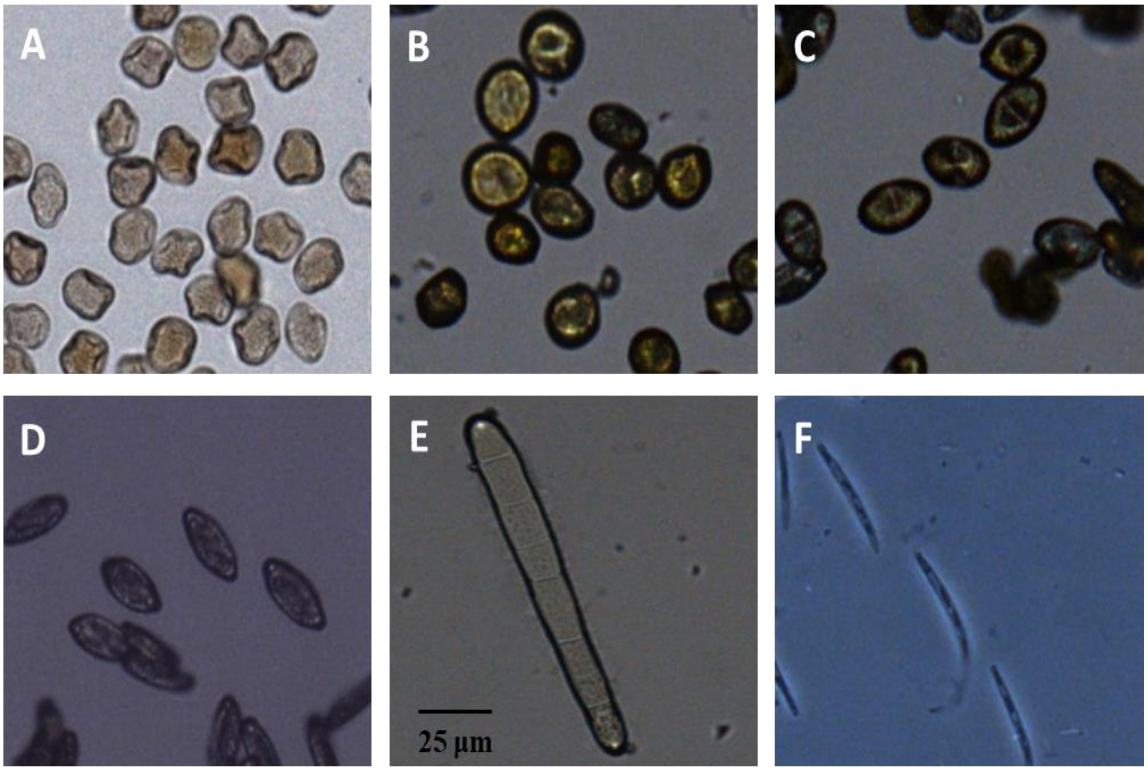

Appendix 8 – All PCR primers tested for the six pathogens.

Primer set	Target	Sequences (F/R) and annotation	Size (bp)	References
Pg2RPB2Q	*Pgt*	GMCCTGAAGTTTGTGAAGG/ ATGATGATATCTGGACACACGC Subunit RPB2 mRNA	158	Liu et al. 2015
Pg2BTQ	*Pgt*	AAGAGAACATGCTGTCCGTT/ TTTGGAACTACAAGGGTATCAAG Beta tubulin chain mRNA	146	Liu et al. 2015
PSBTQ	*Pst*	CAATCACCGTCCCAGAGTTGACATC/ ACGGACAGCATGTTCTCTTCGACT Beta tubulin gene	151	Liu et al. 2015
PSstrRPBQ	*Pst*	ACCTGAACCTGGAGATAAATTCGC/ CCTGTGATGGTGGACACTTTAC Ps28 RNA, second subunit gene	198	Liu et al. 2015
Pt1-113*/ Pt1-904	*Pt*	ATCCTCACAGCGGTAAATCCACCA/ ACACACCTCTTTGGTCCATCCCTT Elongation factor 1-alfa	792	Liu et al. 2013
Pt2-032/ Pt2-552*	*Pt*	TCGTCATTGGACACGTCGATTCGT/ AGTACCGGCAGCAATGATGAGGAT Elongation factor 1-alfa	521	Liu et al. 2013
Pt2-032/ Pt1-113*	*Pt*	TCGTCATTGGACACGTCGATTCGT/ TGGTGGATTTACCGCAGTGAGGAT Elongation factor 1-alfa	104	Liu et al. 2013
Pt2-552*/ Pt1-904	*Pt*	ATCCTCATCATTGCTGCCGGTACT/ ACACACCTCTTTGGTCCATCCCTT Elongation factor 1-alfa	353	Liu et al. 2013
PMITS1/PMITS2	*Bgt*	TCGGACTGGCCYGGGGAGA/ TCCGCTTCACTCGCCGTTAC 18S and 28S rRNA	455	Cunnington & Takamatsu 2003
ITS1/PM6	*Bgt*	TCCGTAGGTGAACCTGCGG/ GYCRCYCTGTCGCGAG 18S rRNA	427	Takamatsu & Kano 2001
ITS1/PM4	*Bgt*	TCCGTAGGTGAACCTGCGG/ CCGGCCCGCCAAAGCAAC 18S rRNA	118	Takamatsu & Kano 2001
Bgt -1	*Bgt*	TGGCTAATACTCACCAATCAGAA/ AGCAGAAGCCTTAGGACTTTAAT BgT-1 microsatellite sequence	241	Parks et al. 2011
Bgt -2	*Bgt*	GACCCAATGTGGAAAAGATAGC/ AGCAGAAGCCTCTTGTTTGT BgT-2 microsatellite sequence	151	Parks et al. 2011
Bgt -4	*Bgt*	TTCTGTAAACGCATTCTTGATA/ AAAAGAGGATAGGAGCACTGTA BgT-4 microsatellite sequence	166	Parks et al. 2011
Bgt -5	*Bgt*	GGAGAATGGAGGAACTTGTAT/ CCACAGAATGAGGAAAGATAAT BgT-5 microsatellite sequence	237	Parks et al. 2011

F/R: Forward/Reverse and *: Modifications made on the original sequence

Appendix 8 – Continued

Primer set	Target	Sequences (F/R) and annotation	Size (bp)	References
Bgt -6	*Bgt*	CGAGGGTTGGAACTGGATAA/ TTCTCTGTTTGACGCTCTCG BgT-6 microsatellite sequence	157	Parks et al. 2011
Bgt -7	*Bgt*	AGAAGGCTGGACAGATAGGT/ TTACCCTTCTCCTGATGTTGC BgT-7 microsatellite sequence	210	Parks et al. 2011
Bgt -8	*Bgt*	GGCATTCTGCTATATTCTATCCT A/ TGCTGCCAATGTCAAGATGT BgT-8 microsatellite sequence	366	Parks et al. 2011
Bgt -9	*Bgt*	AGCTCGCATAGGAGCTTTCA/ CTGACGTCGATGGTTCACTCA BgT-9 microsatellite sequence	260	Parks et al. 2011
Bgt -10	*Bgt*	CCAATCCTCAGGGTTCGGT/ TGGATGTCGCATGGTATCAGAGC BgT-10 microsatellite sequence	270	Parks et al. 2011
TA51/TA52	*Ptr*	GCGTTCTATCCTCGTACTTC/ GCATTCTCCAATTTTCACG Tox A-like gene	570	Andrie et al. 2007
Tox A1/ Tox A2	*Ptr*	GTCATGCGTTCTATCCTC/ CCTATAGCACCAGGTCGTCC Tox A-like gene	294	GeneBank HM234155.1
TB71/TB6	*Ptr*	GCTACTTGCTGTGGCTATC/ ACGTCCTCCACTTTGCACACTCT C Tox B-like gene	225	Andrie et al. 2007
TB71/TB60	*Ptr*	GCTACTTGCTGTGGCTAT C/ ACTAACAACGCTCTCCACTTTG Tox B-like gene	238	Andrie et al. 2007
TB71/TB58	*Ptr*	GCTACTTGCTGTGGCTATC/ TATGAATGATTGACTGGGGTTA Tox B-like gene	204	Andrie et al. 2007
Fgtub	*Fg*	GGTCTCGACAGCAATGGTGTT/ GCTTGTGTTTTTCGTGGCAGT Beta tubulin gene	120	Nicolaisen et al. 2009
Fgram379/Fgram411	*Fg*	CCATTCCCTGGGCGCT/ CCTATTGACAGGTGGTTAGTGAC TGG Elongation factor 1-alfa	100	Nicolaisen et al. 2009
Fgram379/Fgram411*	*Fg*	CCATTCCCTGGGCGCT/ CAGGTGGTTAGTGACTGG Elongation factor 1-alfa	90	Nicolaisen et al. 2009
ITS1/ITS4	Universal (Fungi)	TCCGTAGGTGAACCTGCGG/ TCCTCCGCTTATTGATATGC 18S rRNA	600	White et al. 1990

F/R: Forward/Reverse and *: Modifications made on the original sequence

Appendix 9 – Linear relationship between log number of spores collected at the LeRDC Field Pathology Building in 2015 and Ct values in qPCR assays. The darker points represent results that overlapped.

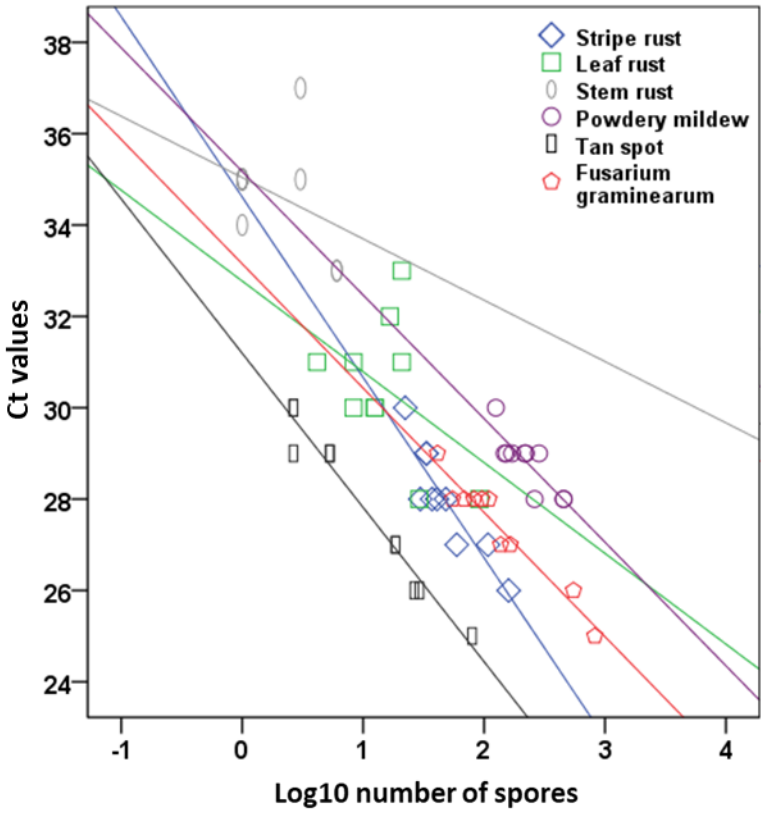

Target	Linear regression equations
Pst	$Y = -3.62x + 34.00$, $R^2 = 0.79$
Pt	$Y = -2.13x + 32.89$, $R^2 = 0.24$
Pgt	$Y = -1.34x + 35.04$, $R^2 = 0.16$
Bgt	$Y = -3.89x + 38.05$, $R^2 = 0.86$
Ptr	$Y = -3.35x + 31.10$, $R^2 = 0.95$
Fg	$Y = -2.68x + 33.10$, $R^2 = 0.91$

Appendix 10 - Linear relationship between log number of spores collected at the LeRDC Weather Station in 2015 and Ct values in qPCR assays. The darker points represent results that overlapped.

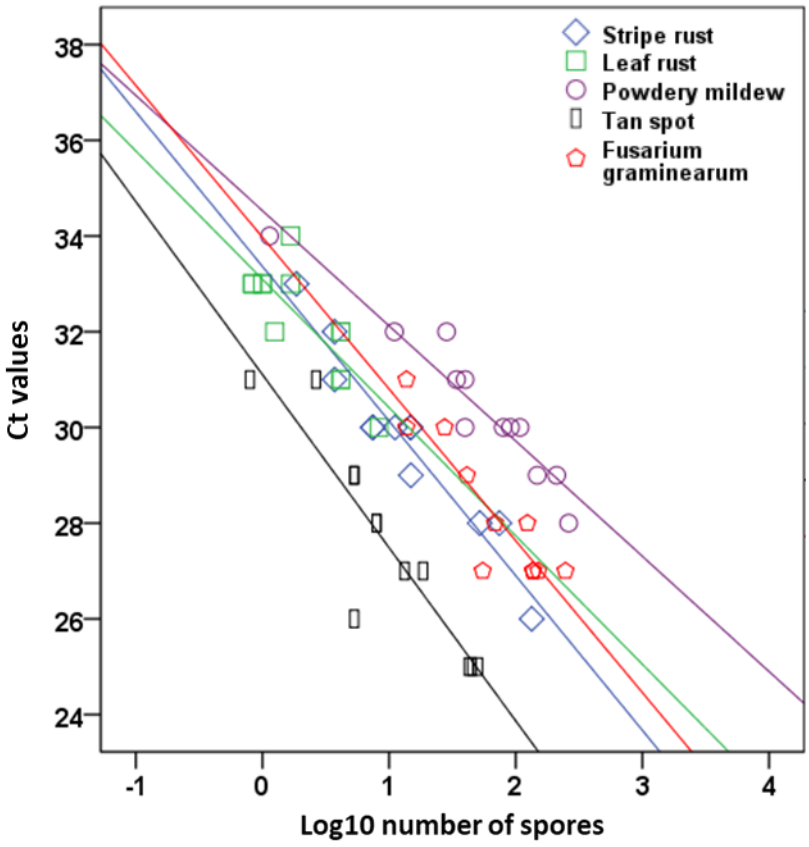

Target	Linear regression equations
Pst	Y = -3.27x + 33.42, R^2 = 0.94
Pt	Y = -2.68x + 33.10, R^2 = 0.66
Pgt	N/A
Bgt	Y = -2.81x + 35.41, R^2 = 0.83
Ptr	Y = -4.04x + 31.68, R^2 = 0.83
Fg	Y = -3.16x + 34.01, R^2 = 0.89

Appendix 11 - Linear relationship between log number of spores collected at the LeRDC Weather Station in 2017 and Ct values in qPCR assays. The darker points represent results that overlapped.

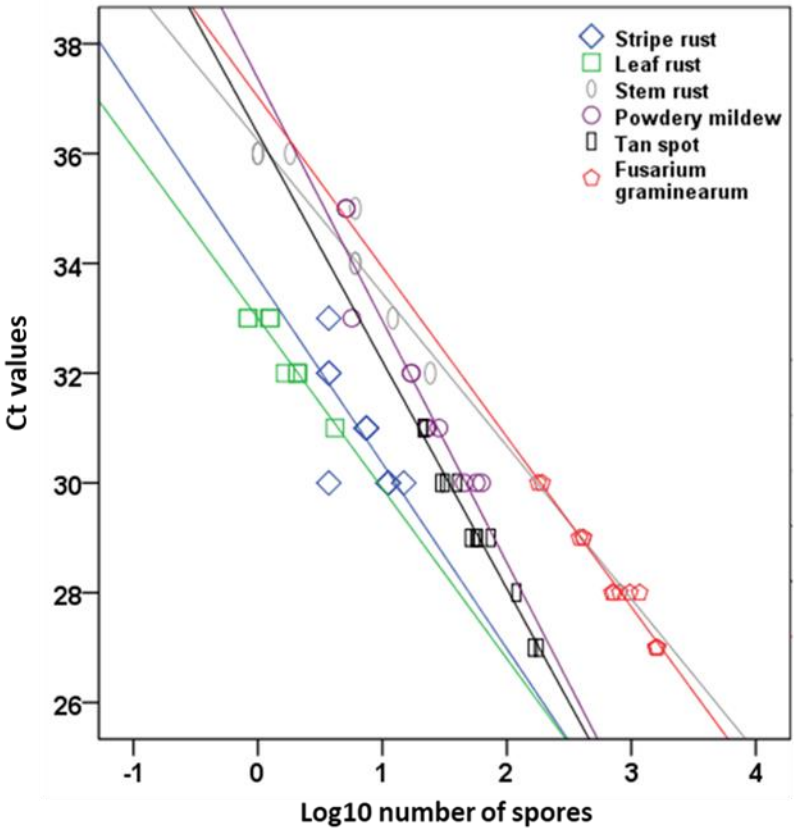

Target	Linear regression equations
Pst	$Y = -3.38x + 33.74$, $R^2 = 0.56$
Pt	$Y = -3.10x + 33.00$, $R^2 = 0.89$
Pgt	$Y = -2.78x + 36.24$, $R^2 = 0.91$
Bgt	$Y = -4.41x + 37.36$, $R^2 = 0.91$
Ptr	$Y = -4.14x + 36.36$, $R^2 = 0.97$
Fg	$Y = -3.10x + 37.03$, $R^2 = 0.97$

Appendix 12 - Linear relationship between log number of spores collected at the Brooks location in 2016 and Ct values in qPCR assays. The darker points represent results that overlapped.

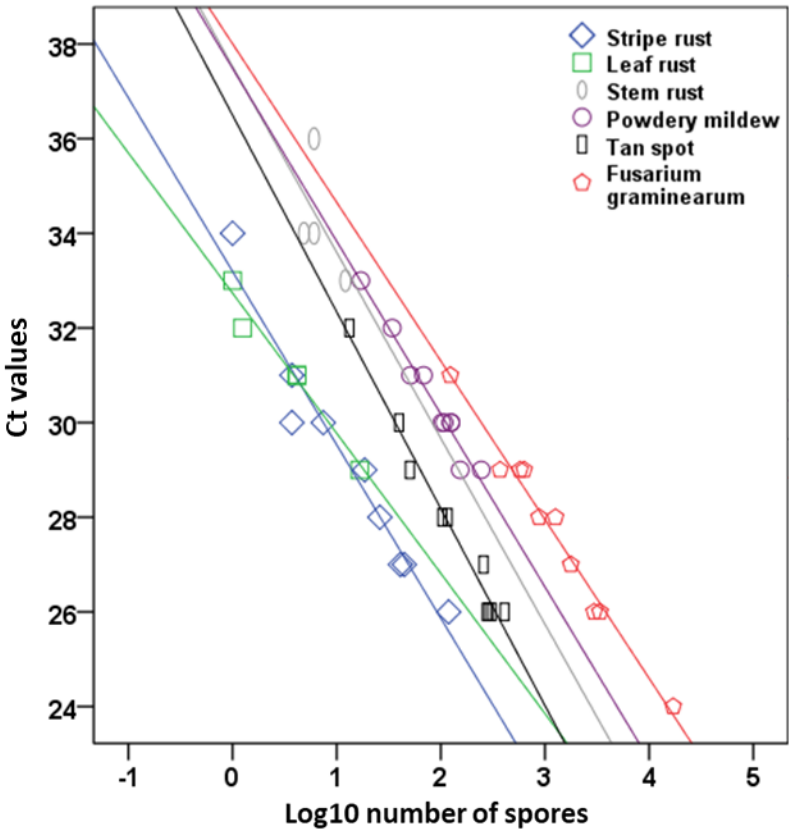

Target	Linear regression equations
Pst	Y = -3.67x + 33.20, R^2 = 0.95
Pt	Y = -2.96x + 32.74, R^2 = 0.96
Pgt	Y = -3.93x + 37.53, R^2 = 0.29
Bgt	Y = -3.65x + 37.50, R^2 = 0.97
Ptr	Y = -4.16x + 36.50, R^2 = 0.98
Fg	Y = -3.35x + 38.01, R^2 = 0.98

Appendix 13 - Linear relationship between log number of spores collected at the Granum location in 2016 and Ct values in qPCR assays. The darker points represent results that overlapped.

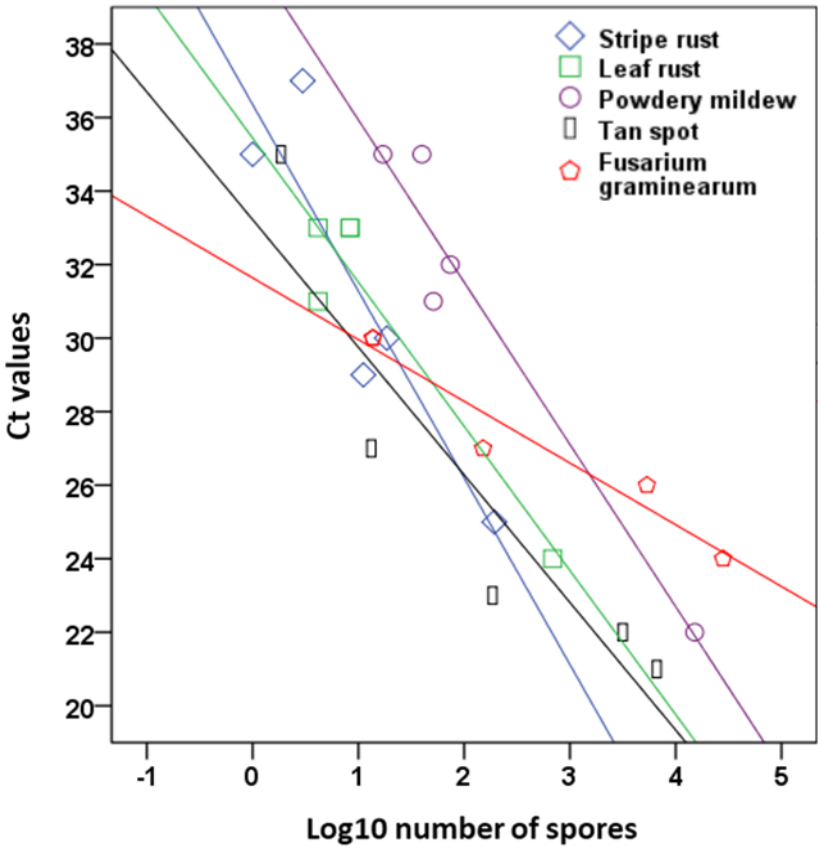

Target	Linear regression equations
Pst	Y = -5.10x + 36.35, R^2 = 0.84
Pt	Y = -3.92x + 35.44, R^2 = 0.89
Pgt	N/A
Bgt	Y = -4.41x + 40.35, R^2 = 0.95
Ptr	Y = -3.47x + 33.22, R^2 = 0.85
Fg	Y = -1.68x + 31.64, R^2 = 0.94

Appendix 14 - Linear relationship between log number of spores collected at the Magrath location in 2016 and Ct values in qPCR assays. The darker points represent results that overlapped.

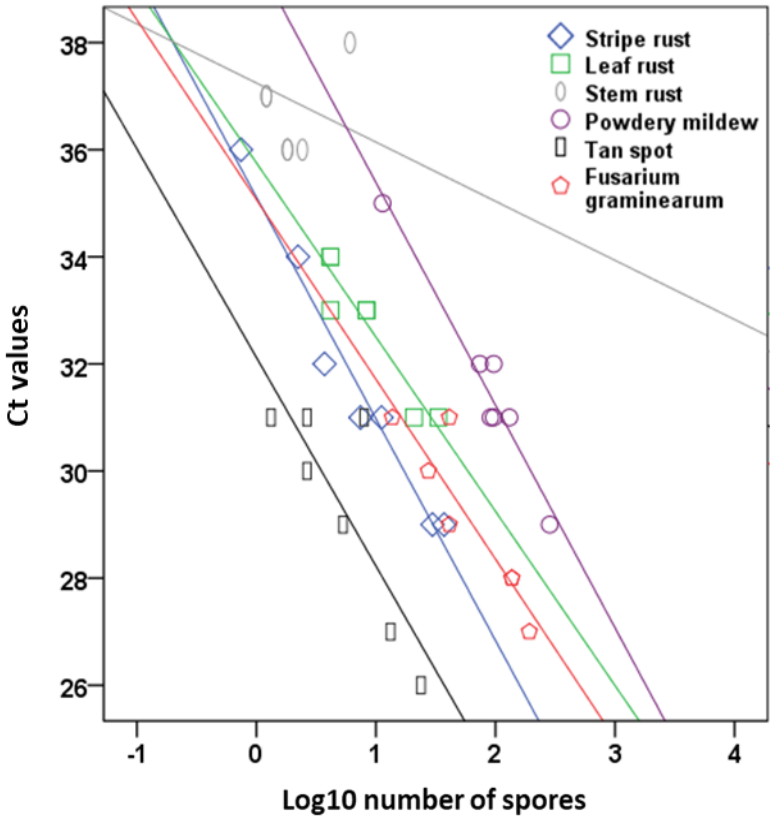

Target	Linear regression equations
Pst	$Y = -4.13x + 35.17$, $R^2 = 0.96$
Pt	$Y = -3.26x + 35.79$, $R^2 = 0.88$
Pgt	$Y = -1.10x + 37.25$, $R^2 = 0.10$
Bgt	$Y = -4.05x + 39.45$, $R^2 = 0.91$
Ptr	$Y = -3.80x + 32.00$, $R^2 = 0.69$
Fg	$Y = -288x + 34.10$, $R^2 = 0.77$

Appendix 15 - Linear relationship between log number of spores collected at the Magrath location in 2017 and Ct values in qPCR assays. The darker points represent results that overlapped.

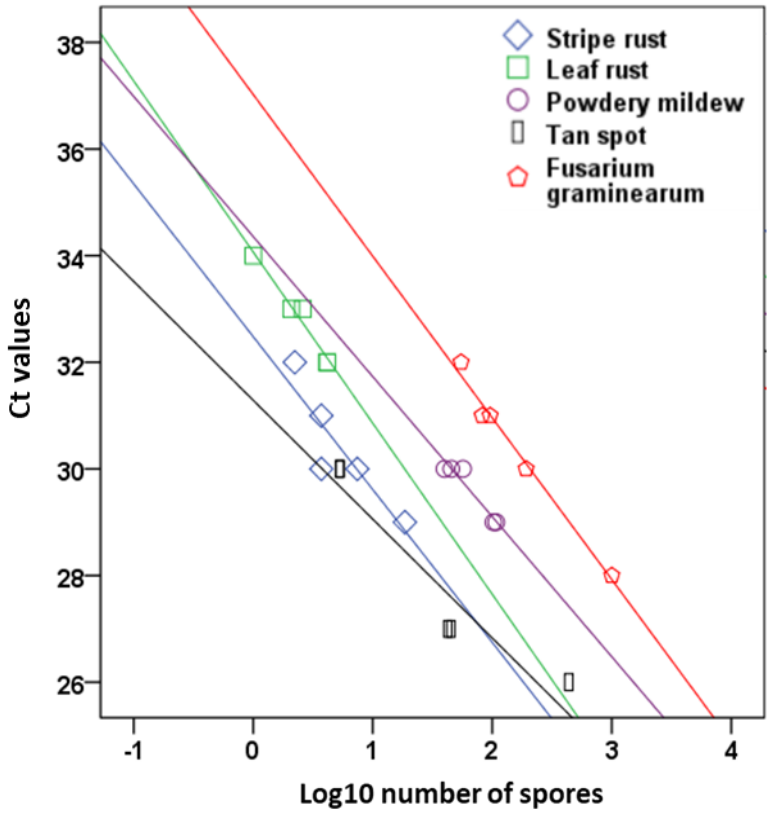

Target	Linear regression equations
Pst	Y = -2.87x + 32.48, R^2 = 0.80
Pt	Y = -3.21x + 34.10, R^2 = 0.97
Pgt	N/A
Bgt	Y = -2.63x + 34.36, R^2 = 0.92
Ptr	Y = -2.23x + 31.29, R^2 = 0.90
Fg	Y = -3.03x + 37.02, R^2 = 0.99

Appendix 16 - Linear relationship between log number of spores collected at the Enchant location in 2016 and Ct values in qPCR assays. The darker points represent results that overlapped.

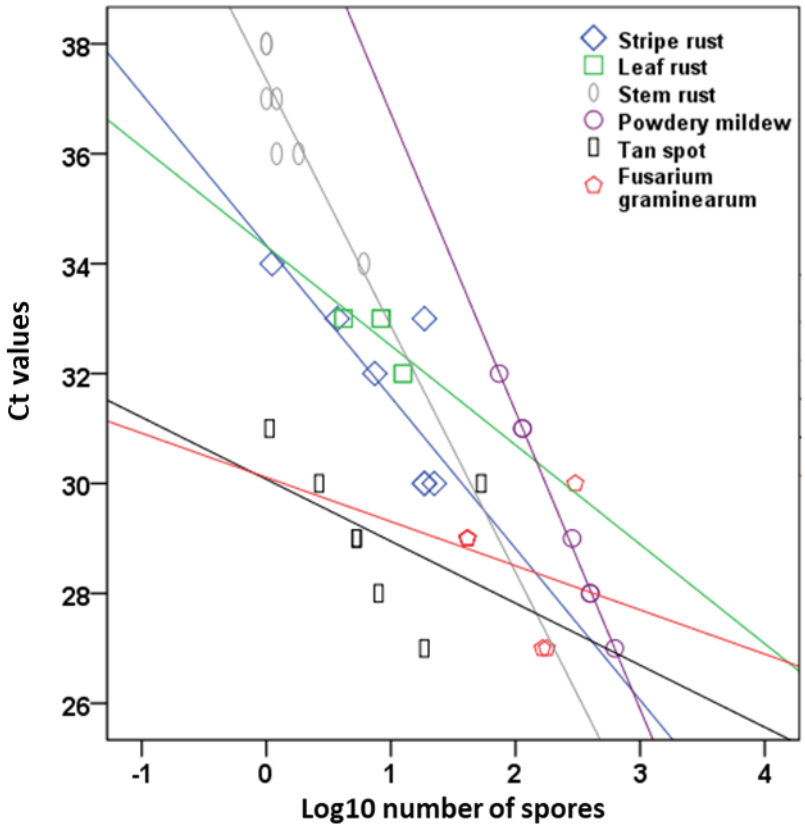

Target	Linear regression equations
Pst	$Y = -2.88x + 34.47$, $R^2 = 0.78$
Pt	$Y = -2.78x + 35.29$, $R^2 = 0.66$
Pgt	$Y = -4.48x + 37.35$, $R^2 = 0.83$
Bgt	$Y = -5.29x + 41.93$, $R^2 = 0.99$
Ptr	$Y = -2.19x + 31.24$, $R^2 = 0.54$
Fg	$Y = -1.17x + 30.70$, $R^2 = 0.13$

Appendix 17 - Linear relationship between log number of spores collected at the Enchant location in 2017 and Ct values in qPCR assays. The darker points represent results that overlapped.

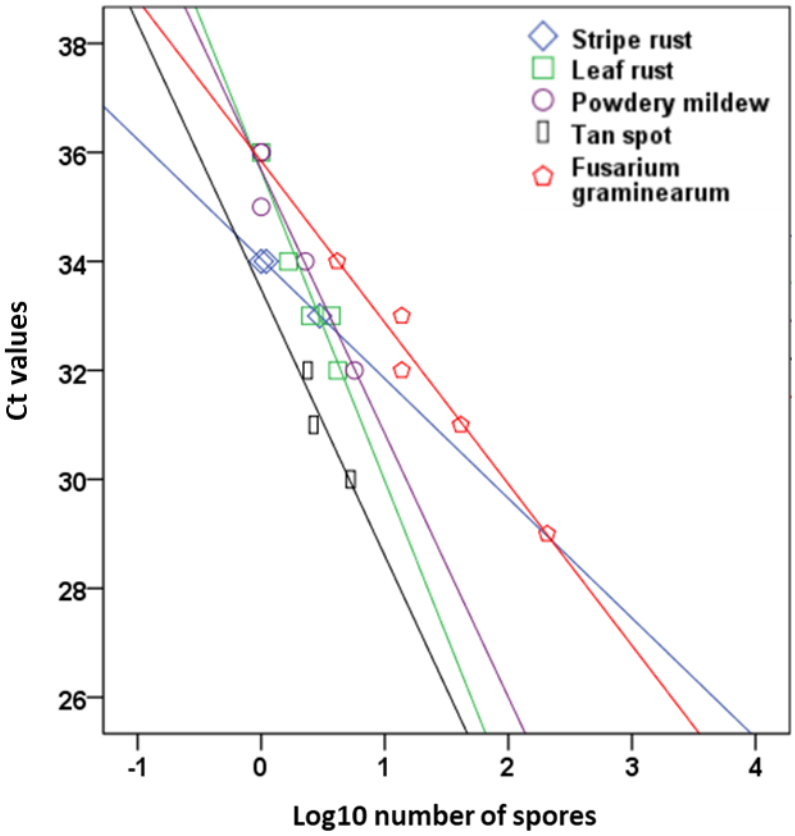

Target	Linear regression equations
Pst	Y = -2.20x + 34.04, R^2 = 0.99
Pt	Y = -5.68x + 35.65, R^2 = 0.91
Pgt	N/A
Bgt	Y = -4.84x + 35.68, R^2 = 0.94
Ptr	Y = -4.88x + 33.48, R^2 = 0.85
Fg	Y = -2.96x + 35.84, R^2 = 0.97

Appendix 18 - Linear relationship between log number of spores collected at the Milk River location in 2017 and Ct values in qPCR assays. The darker points represent results that overlapped.

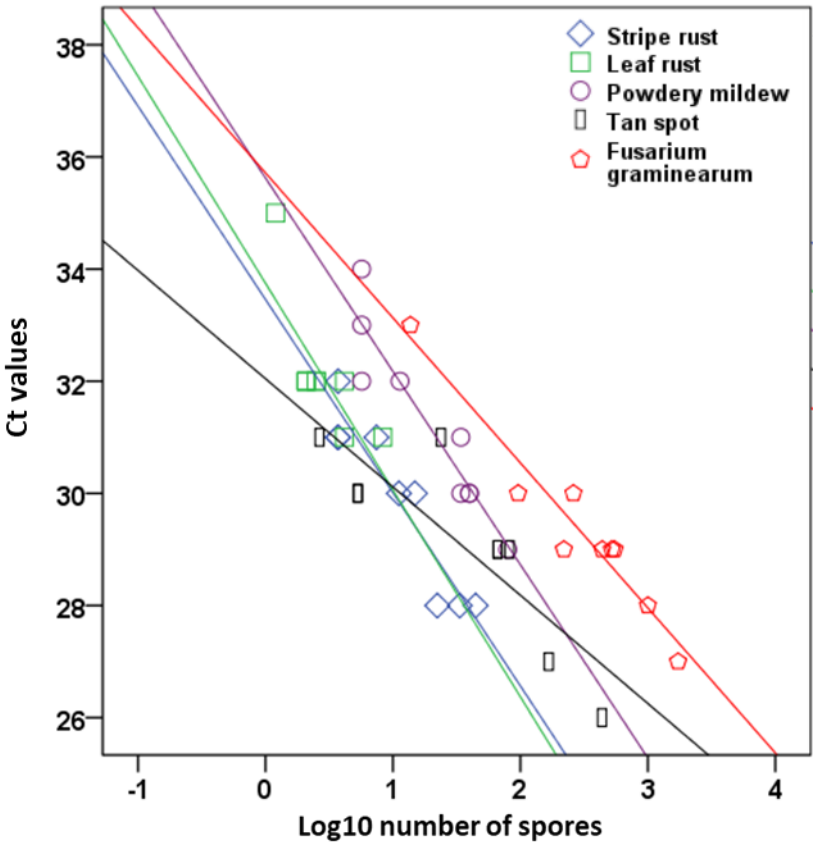

Target	Linear regression equations
Pst	Y = -3.49x + 33.50, R^2 = 0.94
Pt	Y = -3.69x + 33.75, R^2 = 0.60
Pgt	N/A
Bgt	Y = -3.91x + 36.45, R^2 = 0.83
Ptr	Y = -2.94x + 33.94, R^2 = 0.73
Fg	Y = -2.40x + 35.23, R^2 = 0.97

Appendix 19 - Linear relationship between log number of spores collected at the LeRDC Fairfield in 2017 and Ct values in qPCR assays. The darker points represent results that overlapped.

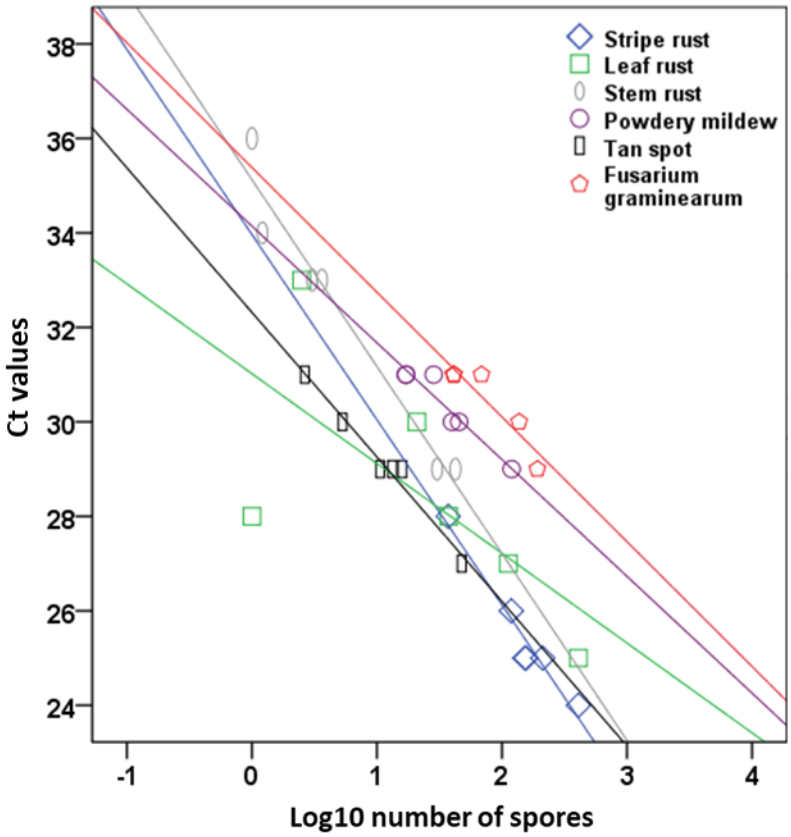

Target	Linear regression equations
Pst	Y = -3.54x + 33.13, R^2 = 0.99
Pt	Y = -2.26x + 32.10, R^2 = 0.50
Pgt	Y = -4.14x + 35.36, R^2 = 0.96
Bgt	Y = -2.89x + 34.90, R^2 = 0.85
Ptr	Y = -3.05x + 32.30, R^2 = 0.98
Fg	Y = -2.56x + 35.31, R^2 = 0.83